EVALUATION AND DEVELOPMENT OF BIO-OPTICAL ALGORITHMS FOR CHLOROPHYLL RETRIEVAL IN WESTERN PUERTO RICO

by

Marcos A. Rosado-Torres

A thesis submitted in partial fulfillment of the requirements for the degree of

DOCTOR OF PHILOSOPHY
in
MARINE SCIENCES
(Biological Oceanography)

UNIVERSITY OF PUERTO RICO
MAYAGÜEZ CAMPUS
2008

Approved by:

_____	_____
Jorge R. García Sais, Ph. D. Member, Graduate Committee	Date
_____	_____
Fernando Gilbes-Santaella, Ph. D. Member, Graduate Committee	Date
_____	_____
Nazario D. Ramírez-Beltrán, Ph. D. Member, Graduate Committee	Date
_____	_____
Roy A. Armstrong, Ph. D. President, Graduate Committee	Date
_____	_____
Raúl Macchiavelli, Ph. D. Representative of Graduate Studies	Date
_____	_____
Nilda E. Aponte, Ph. D. Chairperson of the Department	Date

ABSTRACT

A series of cruises were carried out in Mayagüez Bay from January, 1997, to January, 2004, with the purpose of studying phytoplankton dynamics, optically active water components and ultimately developing bio-optical algorithms for the estimation of chlorophyll *a* (Chl *a*). Fourth derivative spectroscopic analyses were applied to phytoplankton absorption spectra in order to determine phytoplankton pigments that could be identified as chemotaxonomic markers and to quantify Chl *a*. The spectral maxima found in the fourth derivative spectra were associated with chlorophylls a, c and carotenoid pigments, probably fucoxanthin. Good correlation was found between *in situ* Chl *a* concentration and the fourth derivative peaks associated to photosynthetic pigments. These results suggest that diatoms are the dominant phytoplankton group in Mayagüez Bay. Surface Rrs spectra were modeled with Hydrolight using a four component case 2 model with in situ data for input. The moderate agreement of the model for some of the data was attributed to the error associated with using TSS as a proxy for mineral concentrations. The effect of the bio-optical components concentration on the Rrs curve was then evaluated using Hydrolight. It was determined that for the range of Chl *a* values normally observed in Mayaguez Bay (0.1 to 1 $\mu g\ l^{-1}$), mineral values over 5 $mg\ l^{-1}$ were sufficient to mask the Chl *a* signal. These results were used to tentatively set a TSS threshold of 5 $mg\ l^{-1}$ over which Chl *a* concentrations cannot be derived from the Rrs spectra. Three empirical algorithms were developed for Mayagüez Bay. When tested with a data set different that the one used for their development, the fourth order polynomial and the red band ratio algorithms produced a 120.15 and 79.00 mean percent error in Chl *a* estimation respectively. The quasi-analytical algorithm (QAA) from Lee *et al*. (2002) was also evaluated with Mayagüez Bay data. The QAA performed poorly when the derived inherent optical properties were compared to measured data. The poor performance of the QAA was attributed to its inadequacy in the modeling of the spectral particle backscattering coefficients for Mayagüez Bay.

RESUMEN

Una serie de cruceros se llevaron a cabo en la Bahía de Mayagüez desde enero de 1997 hasta enero de 2004 con el propósito de estudiar la dinámica de fitoplancton, los componentes ópticamente activos y finalmente desarrollar algoritmos bio-ópticos para estimar clorofila *a* (Chl *a*). Análisis espectroscópico de cuarta derivada fueron aplicados a los espectros de absorción de fitoplancton para determinar pigmentos fitoplanctónicos que pudiesen ser identificados como marcadores quimiotaxonómicos. Los máximos espectrales encontrados en las curvas de cuarta derivada fueron asociados con clorofila *a*, *c* y pigmentos carotenoides, probablemente fucoxantina. Se encontró una buena correlación entre la concentración de Chl *a* *in situ* y los máximos de cuarta derivada asociados con pigmentos fotosintéticos. Estos resultados sugieren que las diatomeas son el grupo fitoplanctónico dominante en la Bahía de Mayagüez. Espectros de superficie de Rrs fueron modelados con Hydrolight usando un modelo caso 2 de cuatro componentes con datos *in situ* como insumo. El ajuste moderado del modelo para algunos de los datos fue atribuido al error asociado con usar TSS como estimador de concentración de minerales. El efecto de estos componentes en la curva de reflectancia fue evaluado usando Hydrolight. Se determinó que para el intervalo de valores de Chl *a* observados normalmente en la Bahía de Mayagüez (0.1 to 1 µg l^{-1}), concentraciones de minerales mayores de 5 mg l^{-1} fueron suficientes para enmascarar la señal de Chl *a*. Estos resultados fueron usados para fijar un umbral de TSS de 5 mg l^{-1} sobre el cual la señal de Chl *a* no se puede extraer de la curva de Rrs. Tres algoritmos empíricos fueron desarrollados con los datos de la Bahía de Mayagüez. Dos de ellos produjeron un por ciento de error promedio de 120.15 y 79.00 respectivamente. El algoritmo cuasi-analítico (QAA) de Lee *et al.* (2002) también fue evaluado con datos de Mayagüez. El algoritmo QAA se desempeñó pobremente cuando las propiedades ópticas derivadas fueron comparadas con las medidas de campo. El pobre desempeño del QAA se atribuyó a su incapacidad para modelar los coeficientes espectrales de retrodispersión de partículas en la Bahía de Mayagüez.

I dedicate my dissertation work to the following people:

- My parents, Gloria and Rafael who gave me strength and hope through this long journey.
- My friends Alexandra, Jesús, José, Julio, Patrick, and Ramón. Your counsel, patience and friendship helped me endure the hardships of graduate school.

ACKNOWLEDGEMENTS

Many people helped me through this journey, which sometimes I believed would not come to its conclusion. My love and warmth goes to my family, especially to my parents; this accomplishment is yours too! I would like to thank my graduate committee, Dr, Roy A. Armstrong, Dr. Fernando Gilbes-Santaella, Dr. Nazario D. Ramírez-Beltrán and Dr. Jorge R. García-Sais, for their leadership, support and understanding. Special thanks to Dr. Carlos Del Castillo; I hope you are still fishing every chance you have! I would also like to acknowledge Captain Dennis Corales; his wise suggestions and valuable help made the difference in the field. My gratitude goes to the faculty, personnel and peers of the Department of Marine Sciences. My doctoral studies were made possible by NASA Graduate Student Researchers Program grant NGT 13-52746. This research was funded in part by NASA grants NAG13-99029, NAG13-54, and NCC5-518. Data Collection and processing was also supported by the NOAA Cooperative Remote Sensing Science and Technology Center (CREST) program under grant number NA06OAR4810162.

TABLE OF CONTENTS

LIST OF TABLES

LIST OF FIGURES

INTRODUCTION

Coastal zones are important boundaries between land masses and the oceans (Oubelkheir *et al.*, 2006). Although coastal waters only constitute 7% of the global ocean, they account for about 20% of the world's annual primary productivity (Wollast, 1998). Quantitative assessment of the primary production and its role in the global carbon cycle is a critical environmental issue. This knowledge is necessary to calculate new primary production, to derive the effect of biological processes on the partial pressure of CO_2 and therefore to understand how phytoplankton carbon fixation affects the net CO_2 flux across the air-sea interface (Gross *et al.*, 2000).

Furthermore, roughly 50% to 60% of the Earth's human population lives within 60 km of the coast (Hinrichsen, 1998). Consequently coastal areas are more immediately affected by anthropogenic activities than any other part of the ocean. Coastal ecosystems are very dynamic and complex and the effect of land-sea boundaries on circulation, river runoff, tidal currents and human activities such as industrialization and agriculture all contribute to this intricacy (Millero, 2006). The effects of these factors on the coastal ocean are not always clear but inland and coastal waters are more prone to eutrophication as the result of human activities. The need for research and monitoring of the coastal zones is evident if proper management of this valuable resource is the goal.

Due to the importance of coastal areas in understanding the ocean as a whole, great effort is being put in their study. Traditional monitoring such as oceanographic cruises and moorings are an important part of this effort but have several shortcomings, the principal being their limited area of coverage. Ocean color remote sensing has demonstrated a great potential for studying coastal ecosystems. In this technique, the remote sensing reflectance [$Rrs(\lambda)$], an apparent optical property (AOP) is used to quantify the ocean color. Ocean color depends on the geometry of the light field and on the inherent optical properties (IOPs) of the body of water (Kirk, 1994). The IOPs are defined by the optically active constituents of the body of water that absorb and scatter light, mainly the water itself, inorganic and organic suspended particles, colored dissolved organic matter (CDOM) and phytoplankton (Ruddick et al., 2001; Oubelkheir *et al*., 2006). The rationale behind ocean color remote sensing is that changes in the

characteristics of the optically active constituents of the water body affect IOPs and ultimately AOPs. As a result, AOPs such as water leaving radiance [Lw (λ)] and Rrs(λ), provide important information about the composition of a water mass. In order for ocean color remote sensing to be effective, quantitative relationships between the optically active constituents of interest, the IOPs and the AOPs must be acquired.

Morel and Prieur (1977) classified the global ocean in two optical types, Case I and Case II waters. Case I waters are those in which the optical properties are dominated by phytoplankton. In Case II waters, others substances that do not co-vary with phytoplankton pigments dominate the optical properties. Such substances are CDOM, suspended sediments, bacteria and detritus (Carder *et al.*, 1999).

Of the various hydrologic parameters which can be measured using ocean color remote sensing, one of the more important is chlorophyll-*a* (Chl *a*). Chlorophyll *a* is a photosynthetic pigment present in most groups of phytoplankton (Kirk, 1994). Taking advantage of this characteristic, Chl *a* is generally used as an index of phytoplankton biomass (Falkowski *et al.*, 1998). Since Chl *a* is the main photosynthetic pigment, it has also been used extensively as a proxy of primary production (Gross *et al.*, 2000; Chami and Robilliard, 2002). Chl *a* absorbs strongly in the blue (~443 nm) and the red part (~670 nm) of the visible spectrum, reflecting and transmitting green light (~555 nm) (Kirk, 1994). This spectral signature is the basis for optical remote sensing of Chl *a* and most bio-optical algorithms exploit this phenomenon in one way or another.

A great deal of effort has been made to accurately measure Chl *a* in the ocean. Several algorithms have been successfully developed to assess Chl *a* concentration in Case I waters with an acceptable level of error (less than 35% mean percent error). However, no satisfactory algorithm has been developed for Case II waters (Ruddick *et al.*, 2001). For example for the Coastal Zone Color Scanner (CZCS), Gordon *et al.* (1983) reported ± 40% of error in Chl *a* retrieval for Case I waters. In contrast up to 133% of error in Chl *a* estimation was reported for the same data set in Case II waters. Due to the important contribution of Case II waters to global phytoplankton biomass, and the implication on the Earth's carbon budget, the development of accurate algorithms for Chl *a* retrieval in coastal waters is a top priority for the remote sensing community.

There are various approaches for the remote sensing of Chl-*a* concentration in the ocean. Empirical and semi-analytical algorithms have been proposed and employed with a varying degree of success. A more recent procedure involves the use of Neural Network Techniques (NNT) for Chl *a* retrieval. Other methods have been suggested for Chl *a* estimation but they have not been widely implemented at this time.

Empirical algorithms use statistically derived relationships between AOPs and Chl *a*. The most common type of empirical algorithm is the band ratio algorithm. These algorithms usually use ratios of bands in the blue and green regions of the visible spectrum to estimate Chl *a* concentration by means of a polynomial regression. The majority of band ratio algorithms use ratios of Rrs (443)/Rrs (555) and Rrs (490)/Rrs (555) as established in Gross *et al.*, (2000). These algorithms are widely used because their ease of computation, allowing fast processing of remotely sensed data sets. However, noise due to CDOM and detritus absorption in the 400 – 500 nm region of the spectrum is very high in Case II waters. A novel approach for implementing band ratio algorithms in turbid waters is the use of selected red and near infrared bands. This technique circumvents the problem of non algal absorption by CDOM and detritus in the blue region of the spectrum (Ruddick *et al.*, 2001). The rationale of this type of band ratio algorithm is to exploit the 670 nm Chl *a* absorption feature. Despite the theoretical plausibility of this approach, it also has several limitations, one of them being the applicability of such algorithms to humid geographical regions where the atmosphere absorbs most of the infrared radiation. The biggest shortcoming of empirical algorithms as a whole is that their implementation is normally limited to the waters in which they were developed (Salinas *et al.*, 2007).

Semi-analytical (SA) algorithms are derived from solutions to the radiative transfer theory. This makes them inherently more accurate than empirical algorithms (Lee *et al.*, 2002). SA algorithms are dependent on the precise knowledge of the absorption and scattering profiles of the different water constituents. They do not retrieve biogeochemical parameters directly but fortunately these can be modeled from the IOPs once they are known. However, semi-analytical models need to be coupled to an appropriate optimization method in order to retrieve IOPs from AOPs. This can be complicated and time consuming, especially for large data sets such as satellite images. Hence empirical algorithms are almost always preferred for these purposes. Most semi-analytical and quasi-analytical algorithms use empirical methods to estimate the

spectral shape of the IOPs. This method has been shown to be inadequate for turbid coastal waters due to the optical complexity of these systems (Chang *et al.*, 2006). Another drawback of semi-analytical algorithms is that multiple combinations of IOPs could result in identical reflectance values. This problem is referred to as the ambiguity of the ocean color inversion (Sydor *et al.*, 2004). The error ascribed to this ambiguity is especially large in highly absorbing water masses (Defoin-Platel and Chami, 2007).

Recently, neural networks have been used to retrieve ocean composition variables from remotely sensed data. Neural networks provide a family of functions that can approximate a wide range of nonlinear continuous functions (Gross *et al.*, 2000). There are several types of neural networks, each performing better for particular applications. For the bio-optical remote sensing of Chl *a*, multi-layered perceptrons and genetic programming algorithms are being actively researched. The accuracy of these techniques has been reported as low as < 33% for Case II waters (Chami and Robilliard, 2002). Their main drawback is that the calculations are complex and require lots of computational resources.

In practice, the ideal ocean color algorithm is the one capable of estimating Chl *a* concentrations accurately in a wide variety of ocean conditions. Generally sampling waters with a wide range of bio-optical parameters in order to develop such algorithms requires plenty of resources and logistics. Coastal and inland waters are convenient for bio-optical studies for a number of reasons. They provide accessible areas where to collect data and offer a diverse array of bio-optical conditions in relatively small geographical areas.

Western Puerto Rico offers a convenient location for the development of coastal ocean color algorithms. In particular, Mayagüez Bay is well suited for this purpose. Mayagüez Bay is a semi-enclosed bay, located on latitude 18° 12.00', longitude 67° 10.00'. It has an extension of about 47 km^2 out of a total of 100 km^2 if the entire Mayaguez - Añasco Bay complex is considered (Ludeña, 2007). Mayagüez Bay is subjected to a diversity of biogeophysical features that result in a complex bio-optical environment.

Mayagüez Bay has a relatively narrow shelf and is deeper on the northern part and becomes shallower to the south. Its outer boundary have some coral reefs reportedly with less than 10% of living coral cover (Morelock *et al.*, 2001). The sparse coral cover is attributed to high nutrient input and suspended sediment precipitation on the reef (Morelock *et al.*, 2001).

The Mayagüez-Añasco basin receives an average annual precipitation of approximately 220 cm (Pérez *et al*., 2005). Most of this rain falls during the island rainy season, which extends roughly from August to November. The rainy season is characterized by high river discharge and associated terrigenous input (Gilbes *et al.*, 1996). During the dry season, changes in local wind patterns produce a high energy environment in the bay. The increase in wave activity encourages heavy sediment resuspension during most of the dry season (Miller *et al.*, 1994). The sediment resuspension is particularly evident on the southern part of the bay. This event has been associated with high backscattering and CDOM absorption values in the shallower regions of the bay during the winter months (Gilbes, personal communication).

Three major rivers (Añasco, Yagüez and Guanajibo Rivers) discharge in the bay, supplying a large load of suspended sediments and dissolved organic matter which explain, in part, the optical variability of the bay (Rosado-Torres, 2000; Rodríguez, 2004). Smaller water bodies and tributaries also discharge sporadically into the bay. The high river discharge during the rainy season, and the associated reduction in salinity, has been implicated with biological succession of cyanobacterial and fungal populations (Ruiz-Suárez, 2004; Ludeña, 2007).

Añasco River is the largest of the three and the longest river in Puerto Rico (PUTPR, 2006). Although intensively used for agriculture in the past, nowadays the most part of the river basin is heavily populated. The absence of tree cover in much of the river basin promotes erosion and supplies large loads of inorganic particles in the rainy season. The mean annual discharge for Añasco River, considered from March 1963 to October 2002 was 9.1 m^3/s (Warne *et al.*, 2005).

Yagüez River originates in the mountains east of Mayagüez and crosses the city from east to west. This river is probably the one more directly influenced by anthropogenic activities due to large part of its basin being in the urban area of Mayagüez. Due to the lack of an USGS gauge station in this river, no river discharge data are available.

Guanajibo River discharges in the south margin of Mayagüez Bay and is the smallest in caudal of the three rivers (PUTPR, 2006). Its basin was historically devoted to sugar cane cultivation but has not been used for this purpose for more than a decade. During the dry season, Guanajibo River has little discharge values but during the wet season, its discharge becomes as large as Añasco River (Rosado-Torres, 2000). The mean annual discharge of this river for the period between January 1973 and October 2000 was 5.5 m^3/s (Warne *et al.*, 2005).

Beside the rivers, various other water bodies discharge in Mayagüez Bay, especially during events of high precipitation. Some of these are Caño La Boquilla, Quebrada Majagual and Caño Corazones. Although these are small compared to the principal rivers, they are surrounded by mangrove stands and their waters are very rich in CDOM. The extent of the impact of these smaller water bodies on the bio-optical properties of Mayagüez Bay is unknown.

The shoreline of Mayagüez Bay is heavily populated and some portions are industrialized. The Puerto Rico Waters Authority discharges effluent from a secondary sewage treatment plant in the bay through a T-shaped diffuser tube located between the Añasco River and the Mayagüez Port (Alfaro, 2002; Ruiz-Suárez, 2004). The tuna processing industry used to release by-products of their manufacturing operations in the bay, but this practice ceased several years ago and most of the tuna packaging operation has moved elsewhere (Gilbes et al., 1996; Alfaro, 2002).

The complex ecosystem that Mayagüez Bay represents provides a variety of optical provinces in a relatively small area (Rosado-Torres, 2000). This makes Mayagüez Bay an ideal laboratory for the development of coastal ocean color algorithms.

OBJECTIVES

The general objective of this work is to develop a set of ocean color algorithms capable of accurately estimating Chl *a* in the regional area of Mayagüez Bay. The acceptable error proposed for this set of algorithms is equal or less than 35%. This level of error is the one reported in literature for Case I waters. The specific objectives are the following:

1. To study phytoplankton dynamics and seasonality in Mayagüez Bay
2. To assess the effect of the various components of coastal sea water (CDOM, minerals and phytoplankton) typically found in Mayagüez Bay on the remote sensing reflectance curve.
3. To assess the performance of several ocean color algorithms for Mayagüez Bay.
4. To develop a regional set of algorithms to estimate Chl *a* in turbid coastal areas using several approaches.
5. To validate the bio-optical algorithms developed in the bay with coastal data of western Puerto Rico.

Hyperspectral Derivative Analysis of Phytoplankton Dynamics and Seasonality in Mayagüez Bay

Introduction

Although variations in the optical properties of ocean water are almost exclusively attributed to absorption by a single pigment in phytoplankton, Chlorophyll *a*, the process is far more complex (Bigidare et al., 1989). Accessory pigments play an important role in the optical characteristics of most natural waters, especially in the 460 – 640 nm spectral region. In addition, certain accessory pigments are found exclusively in certain phytoplankton groups (Millie et al., 1995; Suzuki et al., 1997) and could be used as markers, in order to optically study phytoplankton seasonality in natural waters. Accessory pigments usually used as chemotaxonomic markers are fucoxanthin in diatoms, prymnesiophytes, raphidophytes and chrysophytes (Wright and Jeffrey, 1987; Ansotegui *et al*., 2001) and peridinin in dinoflagellates (Wright and Jeffrey, 1987; Suzuki et al., 1997) among others. In many studies dealing with estuaries, where pigment composition has been analyzed by HPLC, fucoxanthin has generally been found the dominant auxiliary pigment and can be attributed to diatoms as revealed by the microscopic examination of samples (Laza-Martínez, 2007). However, other classes of phytoplankton containing fucoxanthin have been occasionally observed in estuarine waters and may cause blooms in some instances.

The study of phytoplankton dynamics is essential for the understanding of the trophic levels and their influence in the bio-optical properties of aquatic ecosystems (Ludeña, 2007; Tapia-Larios, 2007). Traditional methods for the study of phytoplankton population dynamics include plankton net trawls and microscopic examinations of the samples. More modern methods include molecular biology assays for phytoplankton group discrimination (Lee-Borges, 2003). Both methods have their drawbacks, the first being tedious and time consuming and the second being work intensive. Another problem is that certain phytoplankton groups are not easily collected in plankton trawls (e.g. crytophyceans). A novel approach for studying phytoplankton dynamics is fourth derivative spectroscopy.

Derivative spectroscopy is a powerful tool that is commonly used in the analyses of hyperspectral remote sensing data (Louchard et al., 2002). Spectral derivative analysis has been applied successfully to optical data as a mean to produce wave crests at wavelengths where

shoulders and peaks occur in spectroscopy curves (Millie at al., 1995). These wave crests, when derivative analysis is applied to phytoplankton absorption curves, correspond to the absorption peaks of accessory pigments. The advantages of this method over solvent extraction and HPLC are that natural samples are processed rapidly with a high degree of precision, no extraction of pigments is needed, several pigments are determined at the same time, and errors due to pigment loss in extraction methods are minimized (Faust and Norris, 1985).

Although second derivative spectroscopic analysis is the more commonly used method, fourth derivative analysis has several advantages. In fourth derivative analysis, a maximum in the original spectrum corresponds with a maximum in the fourth derivative, instead of a minimum as in the second derivative. The fourth derivative is also more selective to narrow bands than the second derivative (Lange and Balny, 2002).

The main objective of this work, is to obtain some insight about phytoplankton dynamics and seasonality in Mayagüez Bay using hyperspectral derivative analyses of the Chlorophyll *a* mass-specific phytoplankton absorption coefficients ($a_\varphi^*(\lambda)$) curves measured during a series of cruises spanning from February, 1997, to January, 1998. This information may compare with taxonomical findings by other researchers (Lee-Borges, 2003; Ludeña, 2007; Tapia-Larios, 2007) and help choose spectral regions for Chl *a* estimation where interference by accessory pigments is minimal.

A secondary objective is to assess the feasibility of quantifying Chl *a* retained in glass fiber filters using spectral fourth derivative analysis of the $a_\varphi(\lambda)$ curves. If a strong correlation between the fourth derivative of $a_\varphi(\lambda)$ and Chl *a* concentration is found, fluorometric measurements of the pigments extracted would be unnecessary, implicating savings in processing time and money.

This study will also evaluate the efficiency of the hot methanol extraction method first proposed by Kishino *et al.* (1985) in sediment rich environments. The methanol extraction method is widely used for the measurement of particle absorption and related optical quantities. However, not many works have assessed the efficacy of the procedure, especially in waters with high content of suspended clay. Clays are known to adsorb organic matter and other electrically charged particles (Tietjen *et al*., 2005). Chlorophylls are known to be polar molecules (Campbell *et al*., 2008) and adsorption to clay surfaces during extraction could be possible, resulting in the

underestimation of the chlorophyll measured in the methanol extract. This occurrence would adversely affect the chlorophyll values used for algorithm development.

Materials and Methods

Field Work

Water samples were collected in a series of cruises carried out monthly from February, 1997, to January, 1998 in Mayagüez Bay. Water samples and ancillary data were taken from six oceanographic stations strategically located across the bay (Figure 1). Of the six stations sampled, the data of three of them were used for the derivative analysis. The stations selected were Oceánica, an offshore station, Añasco, located close to the Añasco River mouth and Rodríguez, a station located close to the Rodríguez Reef. These stations were selected because they represent three distinct environments (offshore, river mouth and reef) in the bay and are well spaced from each other. The remaining stations were located next to anthropogenic pollution sources that were not operating after 1998 (Atuneras) or very close to sewage discharges (Acueductos) and are not representative of the rest of the bay.

Laboratory Work and Data Analysis

Water samples were transported in an ice chest to the laboratory and filtered using the filter pad technique proposed by Mitchell and Kieffer (1984). The samples were collected on 25 mm Whatman GF/F filters. These filters were kept at 0°C until absorption measurements were done. The absorption spectra between 375 and 800 nm was measured using a GER 1500 portable spectroradiometer attached to a Li-Cor integrating sphere by a fiber optic cable. A blank filter was made by filtering a volume of 200 ml of distilled water. The absorption of the blank was also measured and the difference between the sample and the blank spectra was taken as the particulate absorption spectrum (a_p). Following this measure, hot methanol was passed through the filter (Kishino *et al.*, 1985), and the measurement procedure repeated. These spectra were taken as absorption by non-methanol extractable detrital matter (a_d). The difference between a_p and a_d represents the phytoplankton absorption (a_φ). This value, divided by the Chl *a* concentration corresponds to the Chlorophyll-a specific absorption coefficient (a_φ^*). All spectra were normalized to zero absorbance at 750 nm and corrected for path length amplification using the β factor from Bricaud and Stramski (1990). Chl *a* concentration extracted in methanol was measured with a Turner Designs Model 10-AU fluorometer using the method developed by Welschmeyer (1994). This procedure provides the capacity of measuring the Chl *a* concentration

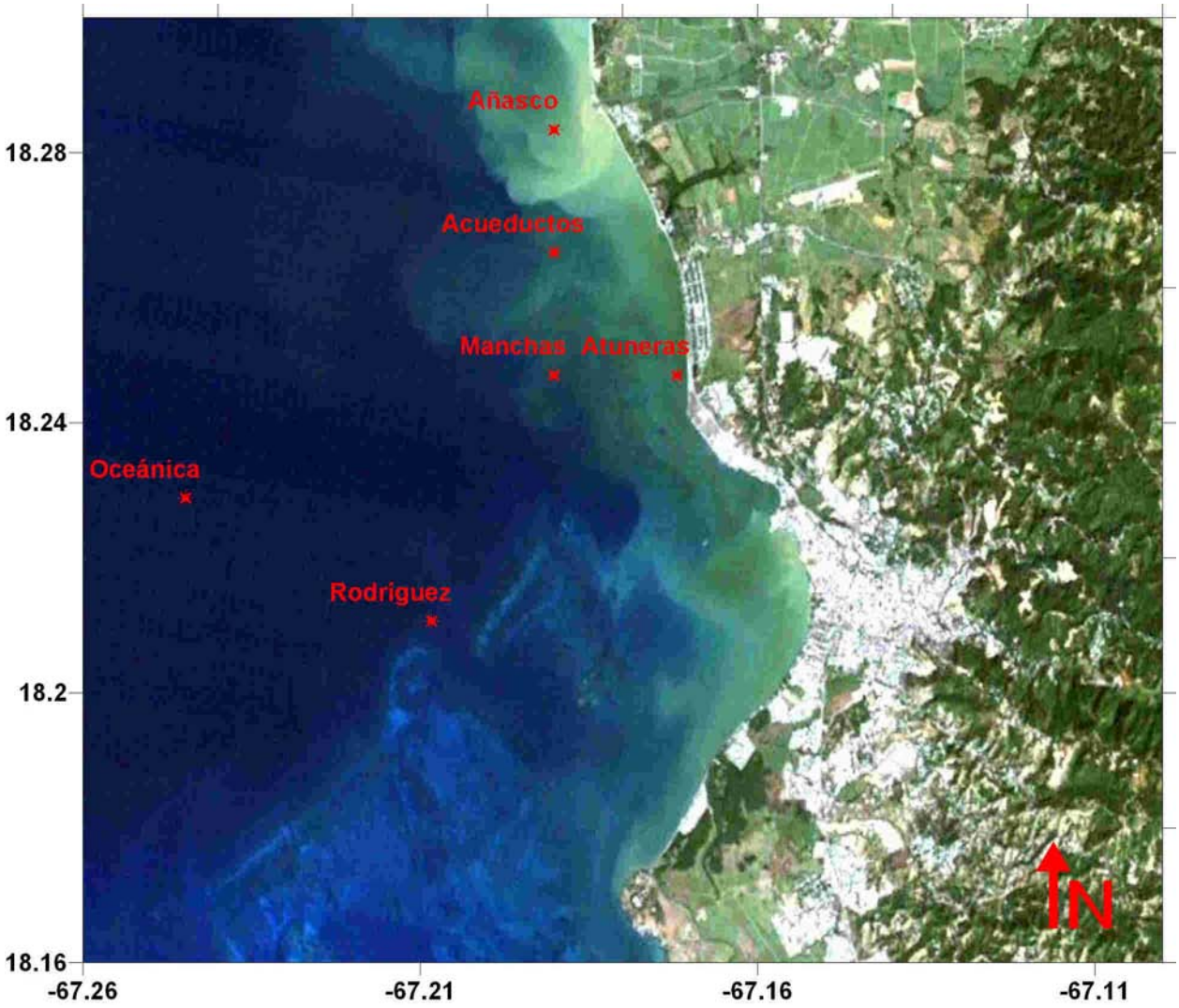

Figure 1. *Oceanographic stations occupied during the 1997 – 1998 series of cruises.*

directly, without acidification of the sample. The fluorometer was calibrated regularly using Chl *a* from the alga *Anacystis nidulans*.

The fourth derivative of the $a_\varphi^*(\lambda)$ and the $ad(\lambda)$ curves was calculated by applying a 41 point fourth degree polynomial smoothing and then differentiating using the Savitzky-Golay method (Savitzky and Golay, 1964). The polynomial smoothing was applied because differentiation tends to amplify the effects of high frequency noise in the spectra (Aguirre-Gómez *et al*., 2001). The procedure was carried out using Microcal Origin 7.0 Scientific Analysis Software. Peaks in the fourth derivative curves were selected using the peak finder tool found in Origin 7.0.

Derivative peaks positions were compared to data published (Bigidare *et al*., 1988; Millie *et al*., 1995; Aguirre-Gómez *et al.*, 2001; Louchard *et al.*, 2002) on natural populations of phytoplankton and to HPLC of pigments standards. When analyzing absorption curves using the fourth derivative procedure, positive peaks represent accessory pigment absorption maxima.

Results

The a_φ* curves from the three stations considered have the typical spectral shape and magnitude of curves reported in the literature (Bricaud and Stramski, 1990; Lee and Carder, 2004). The most notable features are the Chl *a* absorption peaks at 439 and 674 nm respectively (Figure 2). Shoulders and bumps in the curves, corresponding to phytoplankton accessory pigments, are evident, but are not easy to identify and absorption peaks cannot be isolated.

The fourth derivative analysis enhance and amplify the absorption peaks in the a_φ* curves. The most obvious peaks were those corresponding to Chl *a,* found at 440 and 675 nm. A number of peaks were found, namely at 468, 492, 546, 589 and 639 nm. According to Bigidare (1989) and Millie at al. (1995) those peaks correspond to Chlorophyll *c* and fucoxanthin/carotenoids. The a_φ* curves and their fourth derivatives of the Oceánica, Añasco and Rodríguez stations for the 1997-1998 data set are shown in Figure 2.

Figures 3, 4 and 5 presents a_φ* curves and their fourth derivatives for March, July and November of 1997, respectively. The fourth derivative analysis of Mayagüez Bay revealed similar accessory pigment peaks through the year. However, the peaks at 546 and 591 nm were more pronounced in November, suggesting an abundance of phytoplankton groups containing carotenoids or fucoxanthin pigments (Millie *et al.*, 1995; Louchard *et al*., 2002). In addition, Añasco Station in March 1997 shows different peaks that the rest of the curves, namely at 530, 550 and 580 nm.

The Pearson's correlation coefficient (r) between the $a_\varphi(\lambda)$ fourth derivative and Chl *a* concentration was calculated for each nanometer of the spectral range from 400 to 700 nm. The intention was to determine if the fourth derivative is useful for the Chl *a* concentration estimation of filter retained particles. Strong correlations were found between these parameters at several wavelengths, Figure 6 shows the results of the correlation analysis. Notice that the highest coefficient was found at 667 nm (r = 0.93). A linear regression between the fourth derivative of a_φ(675 nm) and Chl *a* yielded a high regression coefficient (r of 0.93, Fig. 7). Figure 8 presents the results of the fourth derivative of $a_d(\lambda)$ of the Oceánica, Añasco and Rodríguez stations for the 1997 – 1998 data set. Positive peaks were found at 430, 475, 540, 620 and 670 consistent with the presence of Chl *a*, Chl *c* and carotenoid pigments in the filter after the hot methanol extraction. These findings suggest an incomplete removal of the photosynthetic pigments by the procedure.

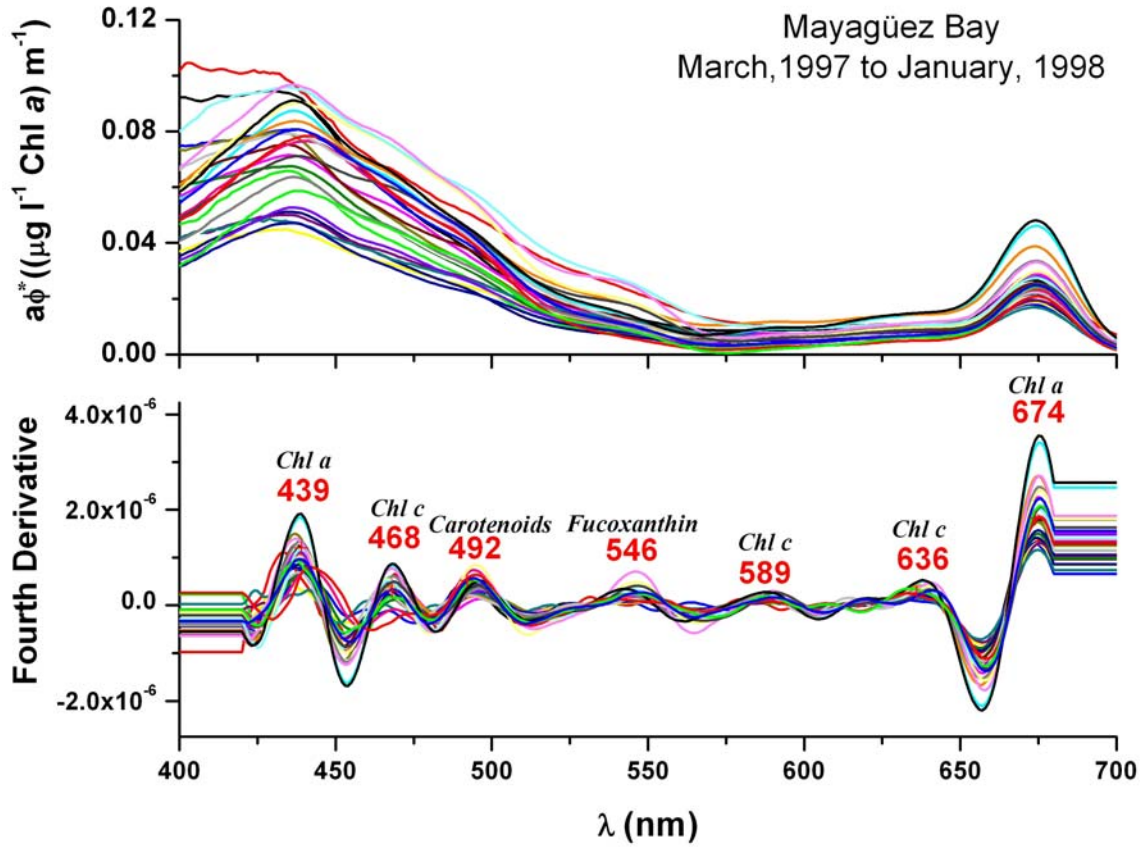

Figure 2. *Spectral specific phytoplankton absorption (aφ*(λ)) and their fourth derivatives for Oceánica, Añasco and Rodríguez stations in Mayagüez Bay, March 1997 to January 1998.*

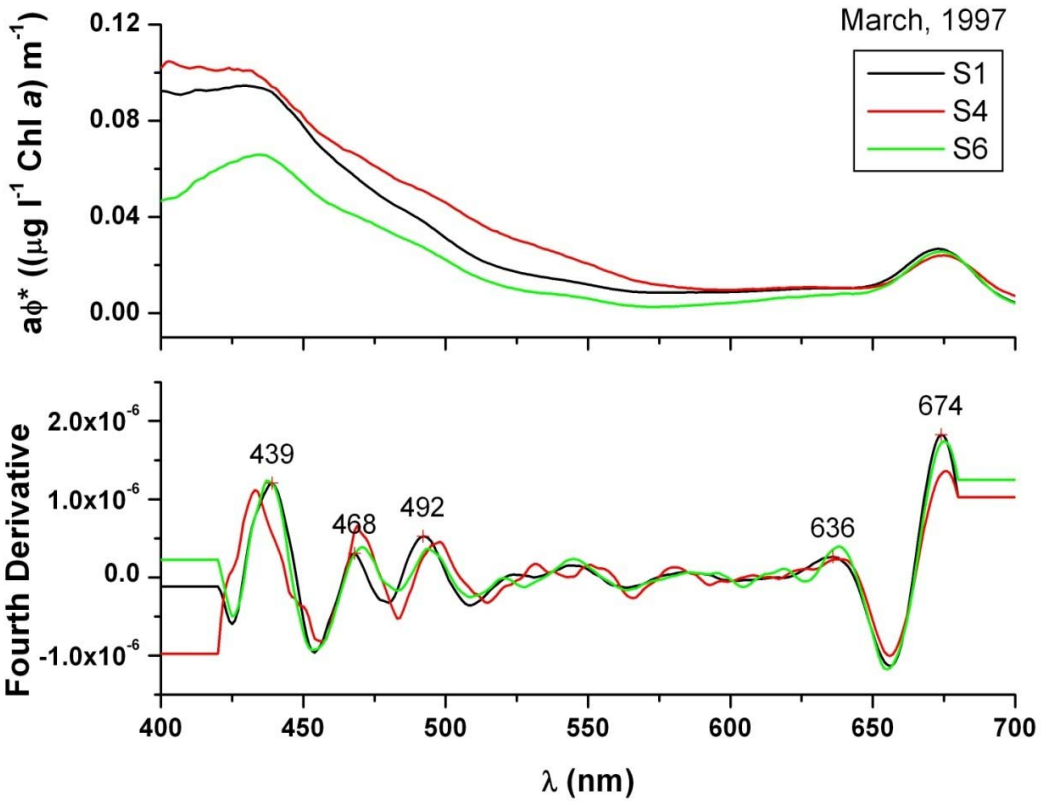

Figure 3. *Spectral specific phytoplankton absorption (aφ*(λ)) and their fourth derivatives for Oceánica (S1), Añasco (S4) and Rodríguez (S6) stations for March, 1997*

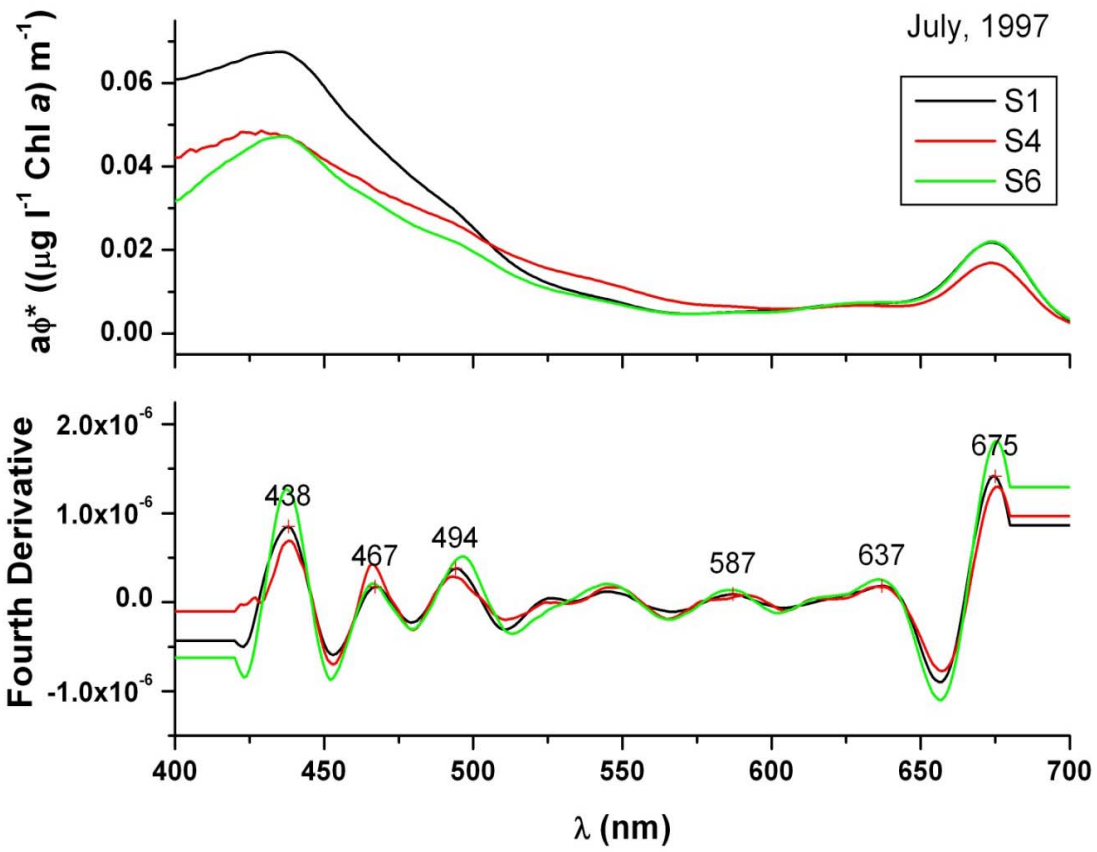

Figure 4. *Spectral specific phytoplankton absorption (aφ*(λ)) and their fourth derivatives for Oceánica (S1), Añasco (S4) and Rodríguez (S6) stations for July, 1997.*

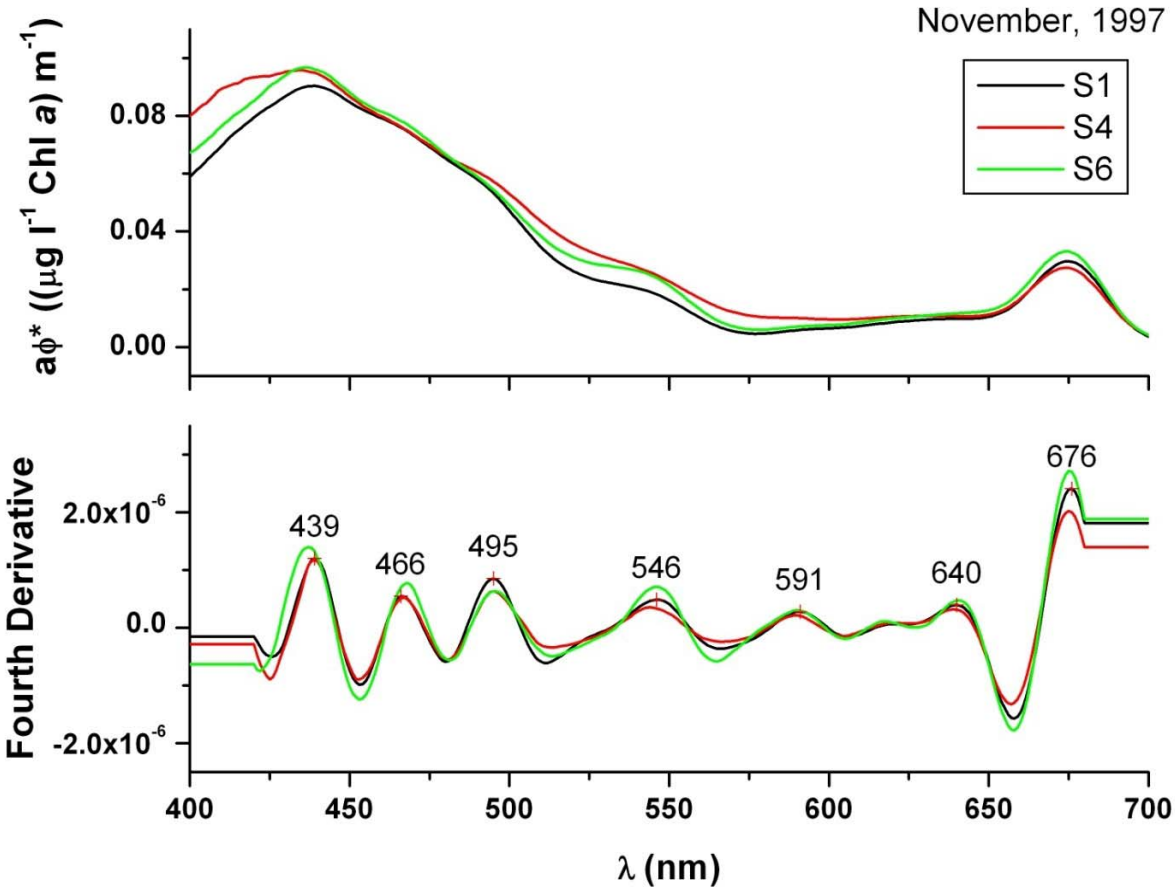

Figure 5. *Spectral specific phytoplankton absorption (aφ*(λ)) and their fourth derivatives for Oceánica (S1), Añasco (S4) and Rodríguez (S6) stations for November, 1997.*

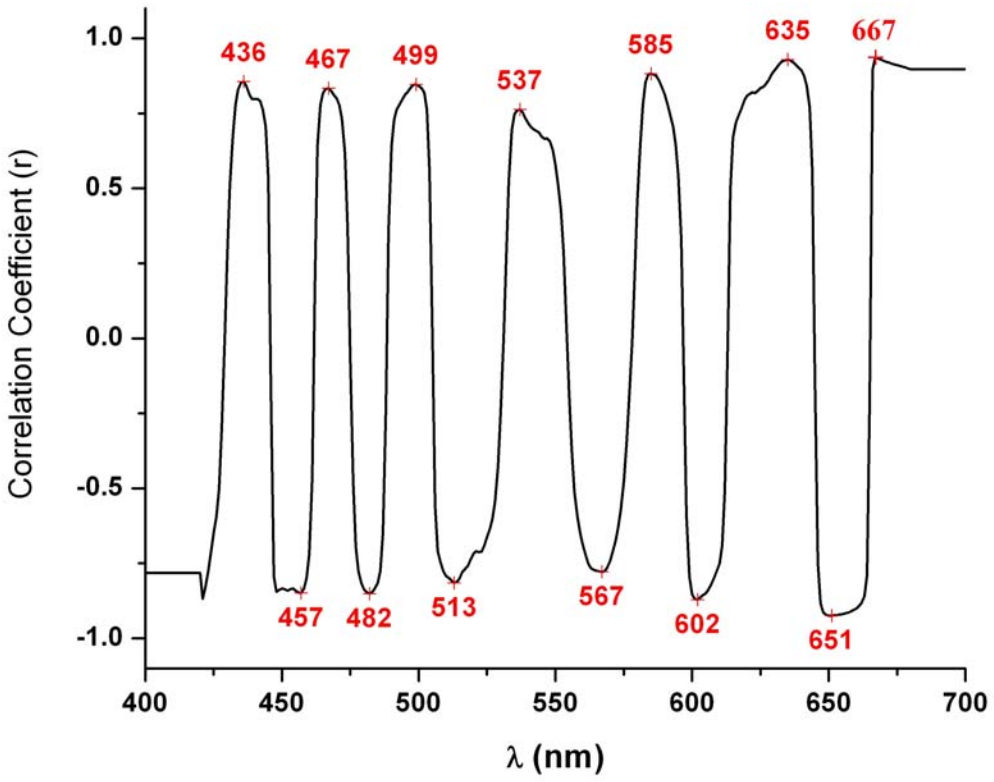

Figure 6. *Results from the spectral correlation coefficient (r) analysis between Chl a concentration and the $a_{\varphi}(\lambda)$ 4^{th} derivative for the March 1997 to January 1998 data set (n = 28).*

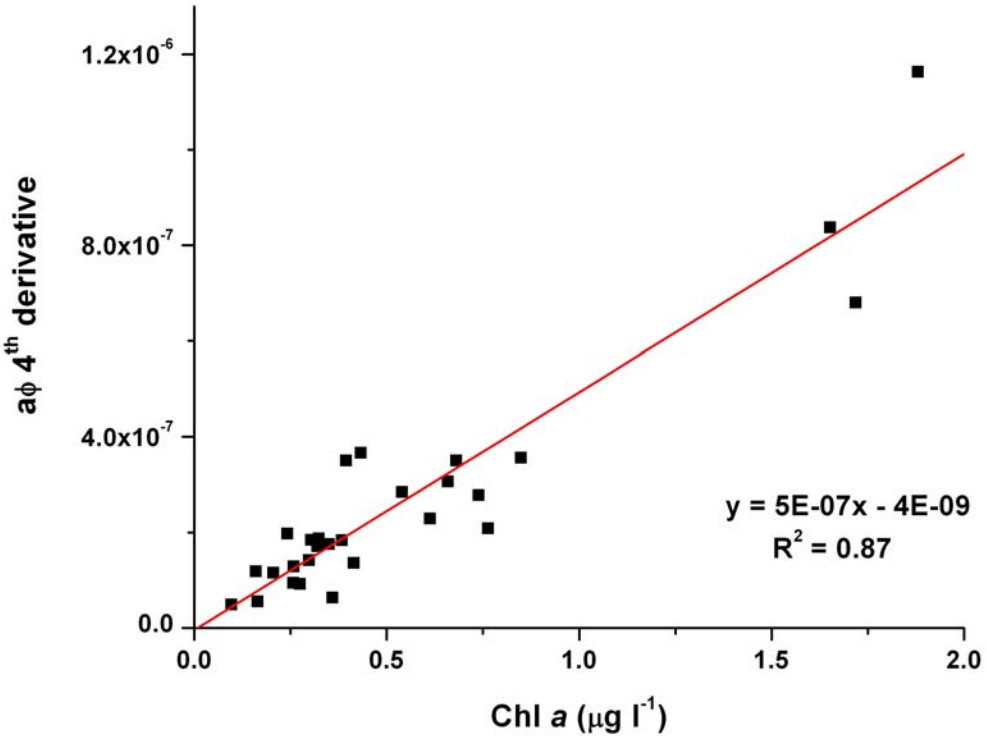

Figure 7. *Results from the linear regression analysis between Chl a concentration and the 4th derivative of a_{φ}(675 nm) for the March 1997 to January 1998 data set (n = 28).*

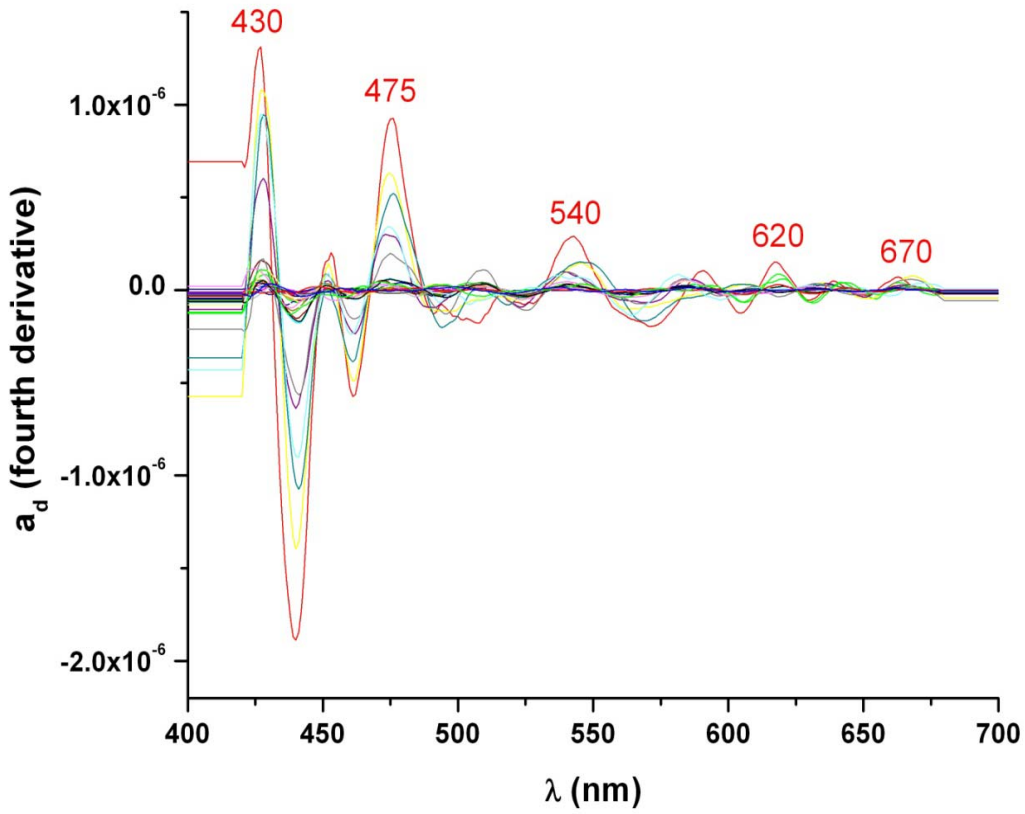

Figure 8. *Spectral detritus absorption ($a_d(\lambda)$) and their fourth derivatives for Oceánica, Añasco and Rodríguez Stations, March 1997 to January 1998.*

Discussion

The spectral shape and magnitude of the phytoplankton absorption curve reflects the pigment composition and concentration found in the natural assemblage from where the sample was collected (Lee-Borges, 2003). Each species has its unique pigment signature and therefore contributes to the shape of the absorption spectrum.

The accessory chlorophylls and carotenoid pigments have their absorption peaks in the 450 – 550 nm region (Lee-Borges, 2003). Since Chl *a* is the most abundant pigment found in phytoplankton and its absorption maxima are around the 440 and 670 nm wavelengths, the accessory pigments absorption peaks are relatively easy to identify in the 450 - 550 nm spectral region with fourth derivative analysis.

Several works have identified the position of the absorption peaks of phytoplankton pigments either with fourth derivative analysis, HPLC or a combination of these tools. Bigidare *et al*. (1989) reported absorption peaks for Chlorophyll *a* at 675 nm and Chlorophyll *c* at 467 nm. Absorptions peaks at 438 and 677 nm were reported for Chlorophyll *a* and at 466, 589 and 639 nm for Chlorophyll *c* by Millie *et al*. (1995). Carotenoids, especially fucoxanthin, diadinoxanthin and β-carotene, have peaks reported at 495 and in the case of fucoxanthin, at 550 – 555 nm (Millie *et al*., 1995: Louchard *et al*., 2002).

Based on the literature, the peaks found at Mayagüez Bay with the fourth derivative analysis are consistent of Chlorophyll *a* (439 and 674 nm), Chlorophyll *c* (468, 589 and 636 nm) and carotenoid pigments, probably fucoxanthin (492 and 546 nm). It is recommended for future studies of the phytoplankton dynamics of Mayagüez Bay that HPLC analysis of the accessory pigments is performed in order to validate these results.

Chlorophyll *a* is the principal photosynthetic pigment of phytoplankton and is common to all species (Kirk, 1994). Chlorophyll *c* is a very common photosynthetic pigment, found in diatoms, dinoflagellates and other groups. Fucoxanthin and diadinoxanthin in the other hand are carotenoid pigments found in diatoms, prymnesiophytes, raphidophytes and chrysophytes (Hsiu-Ping *et al.*, 2002). The absorption peaks identified in Mayaguez Bay are consistent with the dominance of these groups in the phytoplankton community.

Ludeña (2007) found that diatoms dominated the phytoplankton community in Mayagüez Bay especially in the stations closer to the rivers. Her work was based on microscopic and molecular identification of phytoplankton groups. These findings agree with the results of the

$a_{\varphi}(\lambda)$ fourth derivative analysis and suggest that fourth derivative analysis may be an efficient tool for the monitoring of chemotaxonomic markers in phytoplankton assemblages.

Some minor variations in the magnitude of the fourth derivative peaks and the appearance of new peaks, especially in Station 4 during March, 1997, suggest that there might be occurring minor seasonal changes in phytoplankton species composition, especially at the river mouths of the bay. Ludeña (2007) found that diatom abundance was especially high in the proximity of river mouths. In general, the fourth derivative analysis suggests that the relative composition of the phytoplankton community is very stable throughout the year.

Bigidare *et al*. (1989) reported a good correlation (r = 0.89) between the fourth derivative of $a\varphi(\lambda)$ at 467, 650 and 675 nm and Chl *a* concentration in the Sargasso Sea. The spectral correlation analysis between the fourth derivative of $a_{\varphi}(\lambda)$ and Chl *a* verifies their results. High correlation coefficients were also found for all the wavelengths associated with carotenoid accessory pigments. This suggests the possibility that the concentration of these pigments co-vary with Chl *a* in the Mayagüez Bay. Ludeña (2007) reported a strong correlation between Chl *a* concentration and diatom abundance in Mayagüez Bay. Tapia-Larios (2007) found, with the aid of microscopic techniques, that diatoms were the dominant taxonomic group in Mayagüez Bay both in the dry and the rainy season. Since diatoms possess all the photosynthetic pigments identified in this study, this hypothesis is worth investigating in more detail. In summary, the fourth derivative of $a\varphi(\lambda)$ appears to be a valuable alternative method for the quantification of Chl *a* in Mayagüez Bay. Considering the ease of performing the fourth derivative analysis, the routine validation of Chl *a* concentrations obtained by fluorometric analysis is suggested.

A fourth derivative analysis of the $a_d(\lambda)$ curves detected peaks consistent with the presence of Chl *a*, Chl *c* and possibly carotenoid pigments (Figure 8). These findings suggest that the methanol extraction was not complete and that some pigments were retained in the filter. The presence of high concentrations of iron rich red clays in some stations, especially during the rainy season, may in part explain the incomplete extraction. The chlorophylls and some carotenoid pigments (e.g. fucoxanthin) are polar molecules which may be attracted to the electrically charged surface of the red clays and thus remained in the filter after the extraction. Activated red clays are used in vegetable oil manufacture to adsorb chlorophyll and other pigments in order to produce clearer oil (Güler and Tunc, 1992; Adhikari *et al.*, 1997). Theoretically, the pigments responsible for the $a_{\varphi}(\lambda)$ curve are not recovered entirely in the

methanol extraction process and the Chl *a* concentration underestimated as a result. The loss of Chl *a* would be proportional to the inorganic sediment content of the sample. Since this value is assumed to vary from sample to sample, the loss of Chl *a* would not be uniform across the data set and consequently a low correlation was found. This possible source of error should be explored in more detail as it affects the accuracy of Chl *a* measurements made using the hot methanol extraction procedure.

The results obtained support that diatoms are the dominant phytoplankton group in Mayagüez Bay. It is also evident that phytoplankton communities are stable through the year, with the offshore stations showing the most variability during the dry season. Fourth derivative analysis appears to be an efficient tool for the estimation of Chl *a* concentration of phytoplankton retained on filters and very useful for the monitoring of phytoplankton dynamics using chemotaxonomic marker pigments.

Hydrolight Simulations: The Effect of Optically Active Constituents on the Remote Sensing Reflectance Curve

Introduction

Coastal waters are characterized by their bio-optical complexity. While in oceanic waters, phytoplankton and the water itself define the bio-optical properties, in coastal waters both CDOM and detritus contribute a significant portion to the ocean color. The fact that CDOM and detritus does not co-vary with phytoplankton pigments in case-2 waters makes the estimation of pigment concentration from ocean color challenging.

Although the nature of the optically active components of coastal waters is well known (Kirk, 1994; D'Sa and Miller, 2005), most works trying to understand the interactions between the optical constituents of case-2 waters and the remote sensing reflectance focus on *in vitro* experiments (e.g. Karabulut and Ceylan, 2005). While these experiments provide valuable insight into the bio-optical interactions in case-2 waters, most results are limited to the specific constituents used in the experimental setup and hence are limited to the specific geographic regions where those particular components occur. Another drawback of *in vitro* experiments is that because of the large quantity of materials necessary in order to recreate the artificial conditions to be measured, most experiments only report limited concentrations of one or two optical constituents (e.g. chlorophyll or total suspended solids).

Another alternative to the *in vitro* approach is to use numerical models in order to study the remote sensing reflectance curves resulting from different concentrations of optically active substances. If the concentration values of optically active constituents are selected using the known variability of those components in the natural water body of interest, then a large synthetic data set representative of the water body could be produced. Such a data set could be used to better understand the interactions between chlorophyll, CDOM and minerals in the study area.

Hydrolight is a commercial software package created by Curtis D. Mobley that uses numerical models to compute the radiance distributions and derived quantities for natural waters (Mobley and Sundman, 2001). The model provides solutions to the time-independent radiative transfer equation to obtain the radiance distribution within and leaving plane-parallel water bodies. Hydrolight uses as input the absorbing and scattering properties of the water body, the

nature of the wind-blown sea-surface, the sun and sky incident radiation on the water body and the nature of the bottom of the water column (Mobley and Sundman, 2001). The output is arranged in order to simplify analysis using spreadsheet and graphical software.

Hydrolight has been widely used by the bio-optical community for different purposes from simulating the optical properties of natural water bodies (Albert and Mobley, 2003) to creating synthetic data sets in order to validate ocean color algorithms (Lee *et al.*, 2007).

The aim of this chapter is to validate Hydrolight 4.2 as a tool for modeling Rrs curves under the conditions found in Mayagüez Bay and to generate a data set of Rrs curves representing the various permutations of concentrations of chlorophyll, CDOM and minerals found in Mayagüez Bay. This information should help to understand the relative contribution of each constituent to the bio-optics of Mayagüez Bay and serve as a guide for the development of novel methodologies for the estimation of Chl *a* in coastal waters.

Materials and Methods

Field Work

Oceanographic cruises were undertaken in Mayagüez Bay from February, 1997, to January, 2004. The cruises differed in the sampling design, sampling frequency and data collected. Chl *a* and radiometric quantities were measured in the majority of the cases and form the basis of the data set. The study design and samples collected are described below.

The data collection began with monthly cruises carried out from February, 1997, to January, 1998. Six oceanographic stations were sampled each month, selected because of their proximity to nutrient sources or critical habitats of the bay. The stations considered where Añasco, close to the Añasco River mouth, Oceánica, 4 miles offshore, Acueductos, near the Mayagüez municipal sewage plant diffuser tubes, Atuneras, near the tuna processing plants, Manchas, near the Manchas reef, and Rodríguez, close to the Rodríguez reef (Figure 9). Table 1 presents a summary of the stations and their geographic location. Water samples for absorption measurements, downwelling irradiance, water radiance, sky radiance and ancillary data were collected at each station.

Another oceanographic cruise was performed in July, 1998. The same stations described above were sampled. A data set similar to the one described above was collected at each station during this cruise.

An additional set of two cruises to Mayagüez Bay were completed in October 1999. The cruises consisted of a total of eleven stations aligned to the Yagüez River and Guanajibo River mouths (Figure 10). Water samples, radiance, irradiance, and ancillary data were collected in the cruises. Geographic coordinates for the October, 1999, stations are presented in Table 2.

The remaining part of the data set consists of a total of seven cruises conducted from April, 2001, to January, 2004, at irregular intervals. Each cruise comprised twenty four stations divided among six transects, covering the majority of Mayagüez Bay (Figure 11). The geographic location for each station is presented in Table 3. Stations were located one kilometer apart. In twelve of the stations water samples, radiometric measurements, and ancillary data were collected. In the remaining twelve stations, profiling instruments were deployed and the data collected are not being considered in this work.

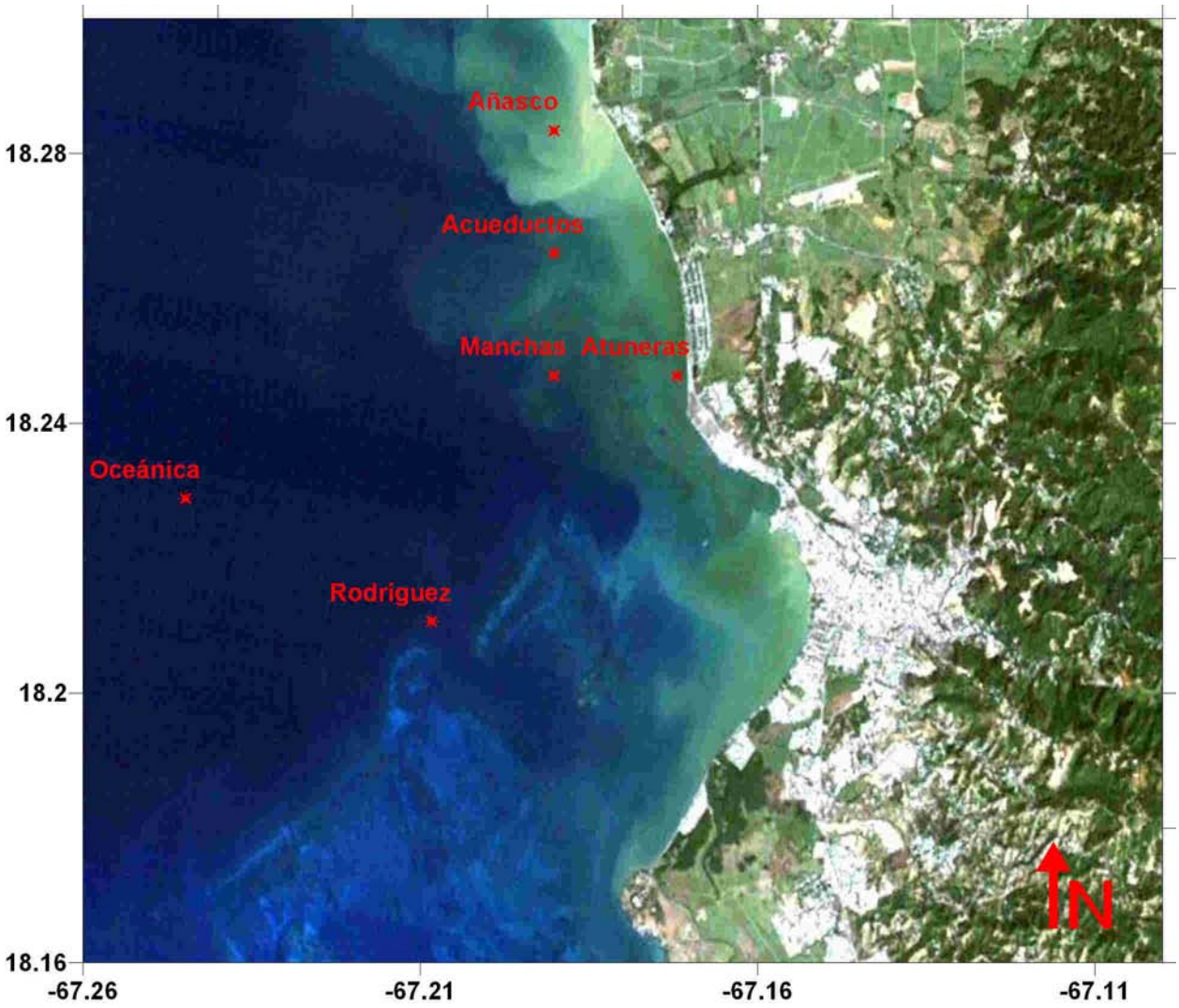

Figure 9. *Oceanographic stations occupied during the 1997 – 1998 series of cruises.*

Station	*Longitude (°W)*	*Latitude (°N)*	*Depth (m)*
Oceánica	-67.233	18.200	> 500
Manchas	-67.183	18.217	120
Atuneras	-67.167	18.217	10
Añasco	-67.183	18.250	5
Acueductos	-67.183	18.233	11
Rodríguez	-67.200	18.183	8.5

Table 1. *Geographical coordinates for the 1997 – 1998 Mayagüez Bay cruises.*

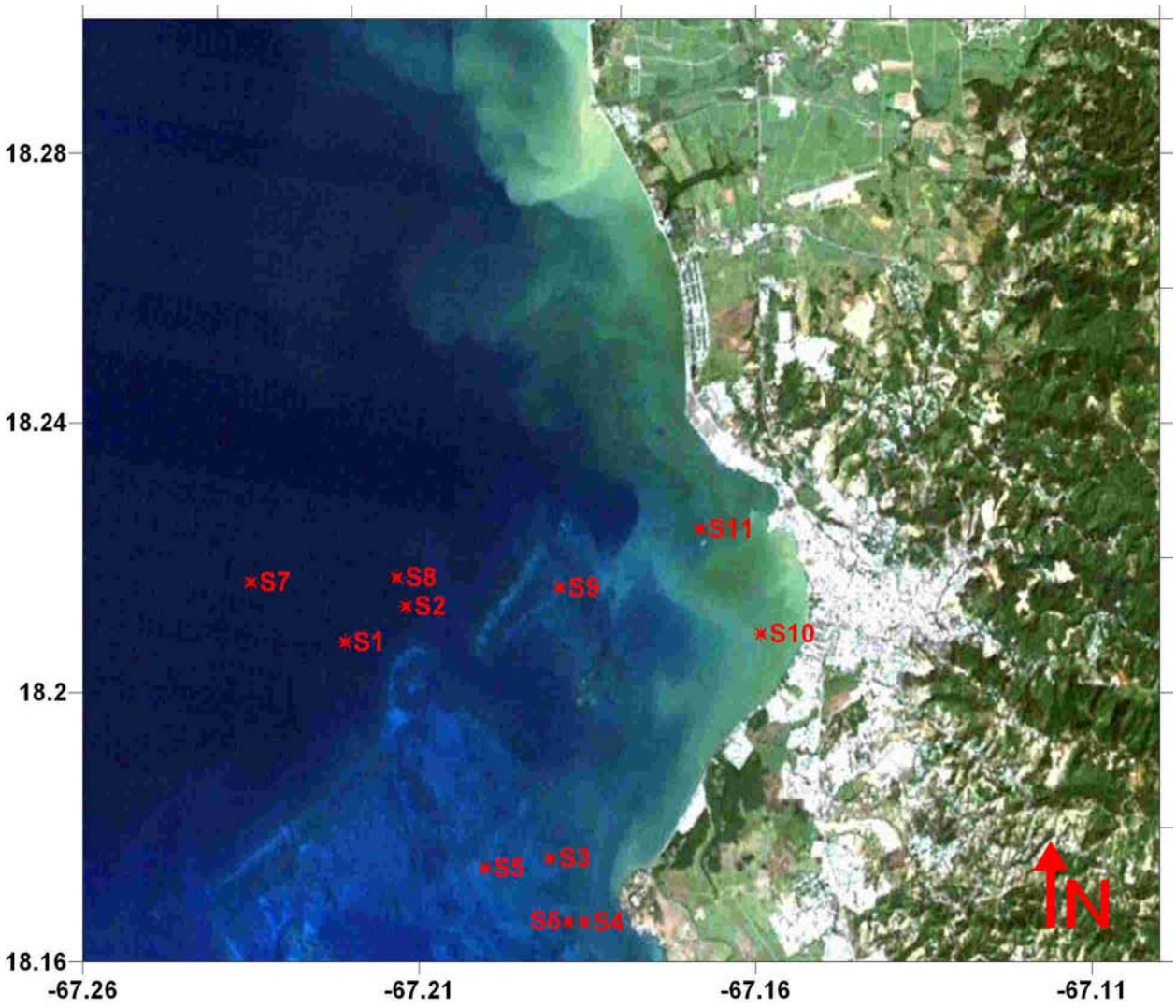

Figure 10. *Oceanographic stations sampled in the October 1999 cruise to Mayagüez Bay.*

Station	*Longitude (°W)*	*Latitude (°N)*	*Depth (m)*
S1	-67.216	18.204	38.7
S2	-67.208	18.209	19.3
S3	-67.189	18.177	4.6
S4	-67.185	18.168	4.6
S5	-67.198	18.175	3.6
S6	-67.187	18.168	5.9
S7	-67.228	18.212	153
S8	-67.209	18.213	52
S9	-67.188	18.211	17
S10	-67.162	18.206	5
S11	-67.170	18.219	9

Table 2. *Geographic coordinates for the stations sampled in the October 1999 cruise.*

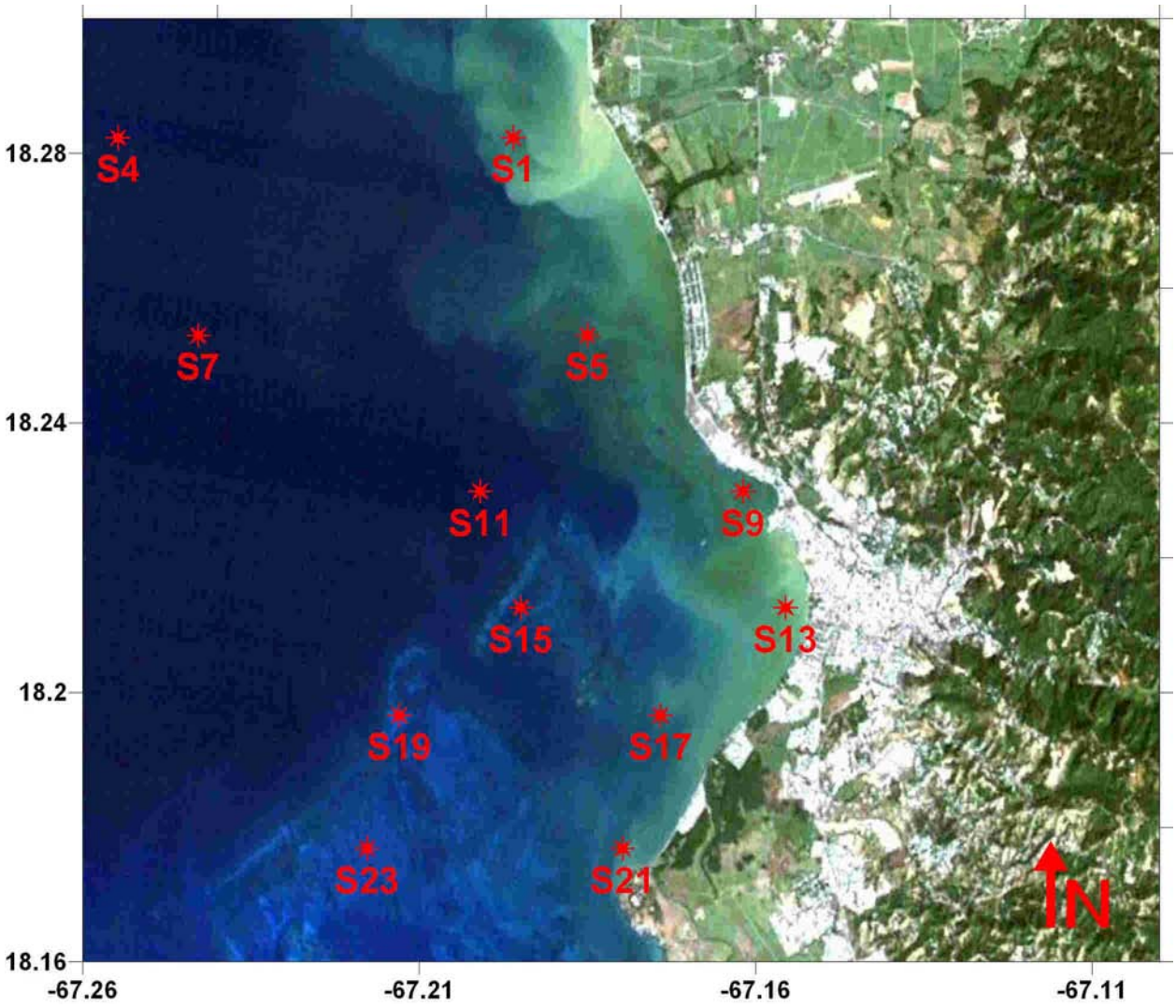

Figure 11. *Oceanographic stations sampled during the 2001 – 2004 series of cruises.*

Station	*Longitude (°W)*	*Latitude (°N)*	*Depth (m)*
S1	-67.200	18.267	5
S4	-67.253	18.267	>500
S5	-67.190	18.240	11
S7	-67.242	18.240	120
S9	-67.169	18.219	10
S11	-67.204	18.219	46
S13	-67.163	18.203	5.5
S15	-67.199	18.203	8
S17	-67.180	18.189	5.5
S19	-67.215	18.189	8.5
S21	-67.185	18.171	5
S23	-67.219	18.171	9

Table 3. *Geographical coordinates of the 2001 – 2004 oceanographic stations sampled in Mayagüez Bay.*

Laboratory work

Chl *a* was measured using a modification of the method proposed by Kishino *et al.* (1985). From each sample, two 200 ml replicates were filtered using 25 mm German GF/F glass fiber filters (0.7 µm nominal pore size) under low vacuum. The filters were placed in 15 ml centrifuge tubes and 10 ml of HPLC grade methanol was added to each tube. The centrifuge tubes were then covered with aluminum foil and refrigerated at 5°C for 24 hours.

After the extraction was performed, the concentration of Ch *a* was measured using the fluorometric technique proposed by Welschmayer (1994). Chlorophyll *a* concentration was measured directly using either a Turner 10-AU or a Turner Model TD-700 fluorometer. Both instruments were modified with optical filters that allowed direct measurement of Chl *a*, without acidification. The instruments were calibrated regularly with Chl *a* dilutions prepared from *Anacystis nidulans* Chl *a* standards obtained commercially.

Total suspended sediment concentrations were analyzed using a modification of the Standard Methods for the Examination of Water and Wastewater protocol 2540D. GF/F filters were dried in a laboratory oven at 60°C for 24 hours. The filters were removed from the oven one at a time and placed to cool in a dessicator for 3 minutes. After the cooling period, the filters were placed on the filtration funnel and a known volume of each sample was filtered. Once the filtration was complete, the funnel was rinsed two times with 10 ml of distilled water. Two replicates were obtained from each sample using the procedure described above. After the filtration process was finished, the filters were placed in aluminum plates and placed in an oven to dry for 24 hours at 60°C. After the drying was over, the filters were placed for 3 minutes in a dessicator and then weighted using a calibrated analytical balance. The TSS concentration was then calculated and reported in mg l^{-1}.

CDOM analysis was performed taking care that all sampling and analysis materials were clean and free from organic matter. Glass bottles, GF/F filters and the glass filtering rig were combusted in a muffle furnace at 300°C for at least 6 hours. All materials were cleaned with 1M HCl and 1 M NaOH and rinsed liberally with distilled water.

The CDOM samples were taken in 250 ml amber glass bottles and refrigerated at 5°C until analyzed. The water samples were filtered using GF/F filters and a glass funnel coupled with a glass filtration flask. The filtrate was then analyzed using a dual beam Pelkin Elmer Lambda 18 spectrophotometer using 10 cm quartz cells. A baseline correction was performed

and a distilled water blank was measured before analyzing the actual samples. Refer to Bricaud *et al.* (1981) for a more comprehensive description of this method.

Hydrolight Simulations

The effect of the optically active substances present in coastal waters on the Rrs curves was accomplished using the commercial software package called Hydrolight, version 4.2. This software is a collection of FORTRAN subroutines that provides numerical solution to the radiative transfer equations for natural water bodies (Mobley and Sundman, 2001).

The approach used in this work consisted of two parts. First, the Rrs curves produced by Hydrolight 4.2 using measured parameters as input were compared with Rrs curves measured *in situ* in order to validate Hydrolight 4.2 in Mayagüez Bay. Second, simulations were made using a four parameter optical model developed for case-2 waters. The parameters used in the model were selected from the observed range of those parameters in Mayagüez Bay.

For the validation of Hydrolight 4.2 in Mayagüez Bay, a total of two cruises were randomly selected from the 2001 – 2004 data. This data set was selected because most of the necessary parameters for the Hydrolight 4.2 simulations were measured during that period. The data set was divided between dry and rainy season (Gilbes *et al*., 1996; Rosado-Torres, 2000) and a cruise was randomly selected from each season. A total of six stations from each cruise, three inshore and three offshore were taken into account for the validation. The stations are evenly spaced through Mayagüez Bay and aligned with the major rivers in order to maximize the optical variability of the data set.

A four component model for case-2 waters was used in Hydrolight in order to model the Rrs curve for all 12 stations considered. The components considered in the model are water, chlorophyll bearing particles, colored dissolved organic matter (CDOM), and minerals.

The optical properties of pure water were taken from Smith and Baker (1981) and Pope and Fry (1997). There is no need to specify the water concentration for the model. The chlorophyll *a* concentration was specified to be constant with respect to depth. Chlorophyll bearing particles absorption was modeled using the following equation from Prieur and Sathyentranath (1981):

$$a(\lambda) = 0.06\, a_c^*(\lambda) C^{0.65}$$

where a_c* = specific absorption coefficient of chlorophyll bearing particles and C = chlorophyll concentration.

Chlorophyll bearing particles scattering was modeled using a power law with Loisel-Morel near surface parameters (Loisel and Morel, 1998):

$$b(\lambda) = b_0 x^n \left(\frac{\lambda_0}{\lambda} \right)^m$$

where $b_0 = 0.407$, x = chlorophyll concentration, $\lambda_0 = 660$, $n = 0.795$ and $m = 1$.

The CDOM absorption was assumed to be constant with depth at the reference wavelength. This simplification was made because no CDOM profiles were available. The wavelength dependence of the CDOM absorption was modeled using the following equation (Mobley, 1994):

$$a^*(\lambda) = a^*(\lambda_0) \exp\left[-\gamma\left(\lambda - \lambda_0\right)\right]$$

where $a^*(\lambda_0) = 1$, $\lambda_0 = 440$ and γ = spectral slope from 412 to 440 nm. CDOM is assumed to be non scattering.

Minerals were also specified as constant with respect to depth as no profiles were taken for this study. Since inorganic mineral concentrations were not measured directly, the total suspended sediments concentrations (TSS) were used as a proxy. The specific absorption and scattering coefficients where taken from the values published for red clays by Ahn (1990). The average mineral particles phase function, bb/b, was supplied by the Hydrolight database.

The different sources of inelastic scattering such as chlorophyll fluorescence, CDOM fluorescence and Raman scattering where included in the Hydrolight runs. The simulations included wavelengths from 400 to 700 nm uniformly spaced every 3 nm. In addition, geographic coordinates, wind speed, cloud cover and GMT time were included in each simulation. The direct and diffuse components of the irradiance were calculated using the RADTRAN model. The angular pattern of the sky radiance was calculated from a subroutine named hcnrad, supplied by Hydrolight. The water column was assumed to be infinitely deep, and the radiometric quantities were calculated for surface only.

The *in situ* Rrs curves were calculated using the following equation (Lee *et al.*, 1997):

$$Rrs(\lambda) = \frac{L_0(\lambda) - f\ (L_s(\lambda))}{E_d(0^+, \lambda)}$$

where L_o is the water radiance measured at a 45^o angle to the water, L_s is the sky radiance measured at a 45^o angle to the sky and f is Fresnel's number, the percent of sky radiance reflected back to the atmosphere. Fresnel's number has a value of 0.028 at a 45^o angle.

The goodness of fit between modeled and measured Rrs curves was estimated using both the root mean squared error (RMSE) in sr^{-1} and the Willmott's Index of Agreement, d (Legates and McCabe, 1999). The calculations were performed using Microsoft Excel.

The second part of this exercise consists of creating a database of Rrs curves for Mayagüez Bay. This was accomplished generating Rrs curves by varying the optically active constituents of the water column using Hydrolight 4.2. The components considered in the study are the three components whose concentrations can be defined in the Hydrolight four component case-2 model. These are chlorophyll bearing particles, CDOM and inorganic minerals. Each component was assigned five different concentrations, using published values (Rosado-Torres, 2000) as a guide, with the intention of covering the variability range observed in Mayagüez Bay for each component. Each combination of parameters was used to produce a single Rrs curve, representing the Rrs curve expected to be observed at the bay for that particular combination of parameters. The combinations produced a total of 125 Rrs curves. Table 4 gives a summary of the values assigned to each component during the simulations.

The various parameters used in the Hydrolight 4.2 simulations were identical to the ones explained in the preceding section. Date, time, geographic location, wind speed and cloud cover remained constant for all the Hydrolight runs in order to generate a data set where only the optically active constituents of the water column varied, The optical properties of red clays supplied with the software were used when defining the specific absorption and scattering coefficients of mineral particles. The ancillary parameters were selected in order to minimize noise cause by surface condition and cloud cover. The optical properties of red clay minerals were used in the simulations. Table 5 gives a summary of the different parameters used in the exercise. The Rrs curves produced by Hydrolight were plotted using Origin 6.0 Scientific Analysis Software (Microcal Inc.).

Optically Active Component	*Concentration Values Assigned*
Chlorophyll Bearing Particles	0.1, 0.5, 1, 5 and 10 µg/l
CDOM	0.05, 0.1, 0.15, 0.25 and 0.5 m^{-1}
Minerals	1, 5, 10, 25, and 50 mg/l

Table 4. *Summary of the concentration values assigned to each model component for the Hydrolight simulations.*

Parameter	*Value*
Date	July 1, 2001
Time	12:00 PM
Latitude	18.17°
Longitude	-67.18°
Cloud Cover	0%
Wind Speed	0 m/s
Mineral Type	Red Clay

Table 5. *Summary of the ancillary data used for the Hydrolight simulations.*

Results

Descriptive Statistics

Descriptive statistics for the Chl *a* and TSS values measured in Mayagüez Bay are shown in Table 6. The mean Chl *a* concentration for the complete data set was 0.65 µg/l (0.56, 0.76 µg/l). The majority of the samples (54.93%, n=78) had Chl *a* concentrations less than 0.65 µg/l. The smallest Chl *a* concentration measured in this data set was 0.09 µg/l for S7 in October, 2003. The largest Chl *a* concentration recorded during this study was 11.75 µg/l for S10 in October, 1999.

The mean TSS concentration for the Mayagüez Bay data set was 8.15 mg/l (7.10, 9.35 mg/l). In the case of TSS, 52.63% of the samples (n=50) have a TSS value greater than the mean. Station 21 had the largest concentrations of TSS measured during this study, 50.34 mg/l in October, 2003, followed by a value of 38.30 mg/l for February, 2002.

Figure 12 shows the variability observed in Rrs measurements for the Mayagüez Bay data set. Note that a variety of spectral shapes can be identified, suggesting a diverse set of bio-optical properties for Mayagüez Bay. The highest Rrs value recorded during this study was 0.11 sr^{-1} at 579 nm for Manchas Station in August, 1997. Averaging all Rrs curves results in Figure 13. The mean Rrs increases with wavelength from 400 nm. The curve features a peak approximately at 550 nm and then decreases sharply up to 600 nm and then shows a gradual decrease up to 700 nm.

CDOM absorption (a_g) variability can be appreciated in Figure 14. CDOM absorption coefficients ranged from 0.02 m^{-1} to 0.65 m^{-1} at 443 nm. The CDOM absorption curves show the typical exponential shape. Station 10 in October, 1999 had the highest absorption coefficients measured for the data set, with an a_g of 0.65 m^{-1} at 443 nm. The mean and 95% confidence intervals results for $a_g(\lambda)$ are shown in Figure 15. CDOM absorption at 443 nm has a mean value of 0.087 m^{-1} with 95% confidence intervals of (0.075, 0.10 m^{-1}). Note the presence of an atypical hump on the mean CDOM absorption curve around 550 nm.

The results of correlation analysis between several optically active water components are shown in Table 7. Weak positive correlations were found between TSS and Rrs 555 (r = 0.63) and Rrs 670 (r = 0.62). A strong correlation was found between Chl *a* and a_g 443 (r = 0.83).

Parameter	*Count (n)*	*Mean*	*Standard Deviation (s)*	*Confidence Interval (95%)*
Chl a (µg/l)	142	0.65	2.46	(0.56, 0.76)
TSS (mg/l)	95	8.15	1.98	(7.10, 9.35)

Table 6. *Descriptive statistics for Chl a and TSS values measured in Mayagüez Bay.*

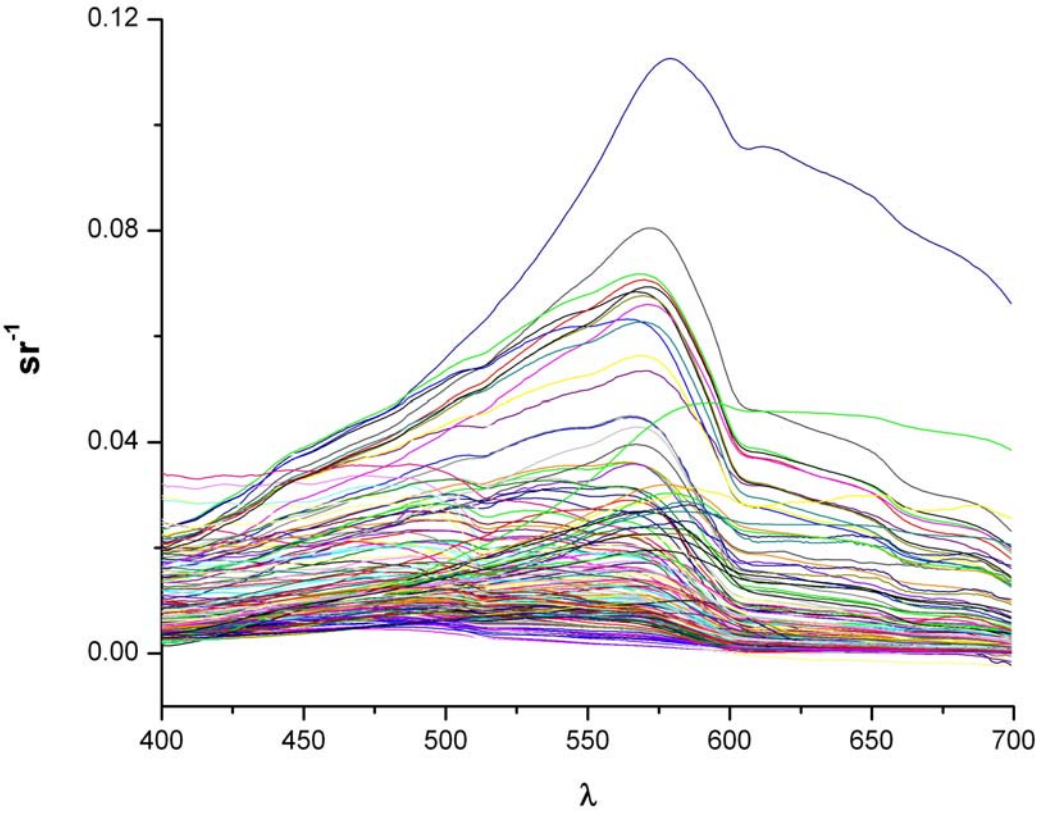

Figure 12. *Complete set of Rrs curves calculated for Mayagüez Bay (n = 142).*

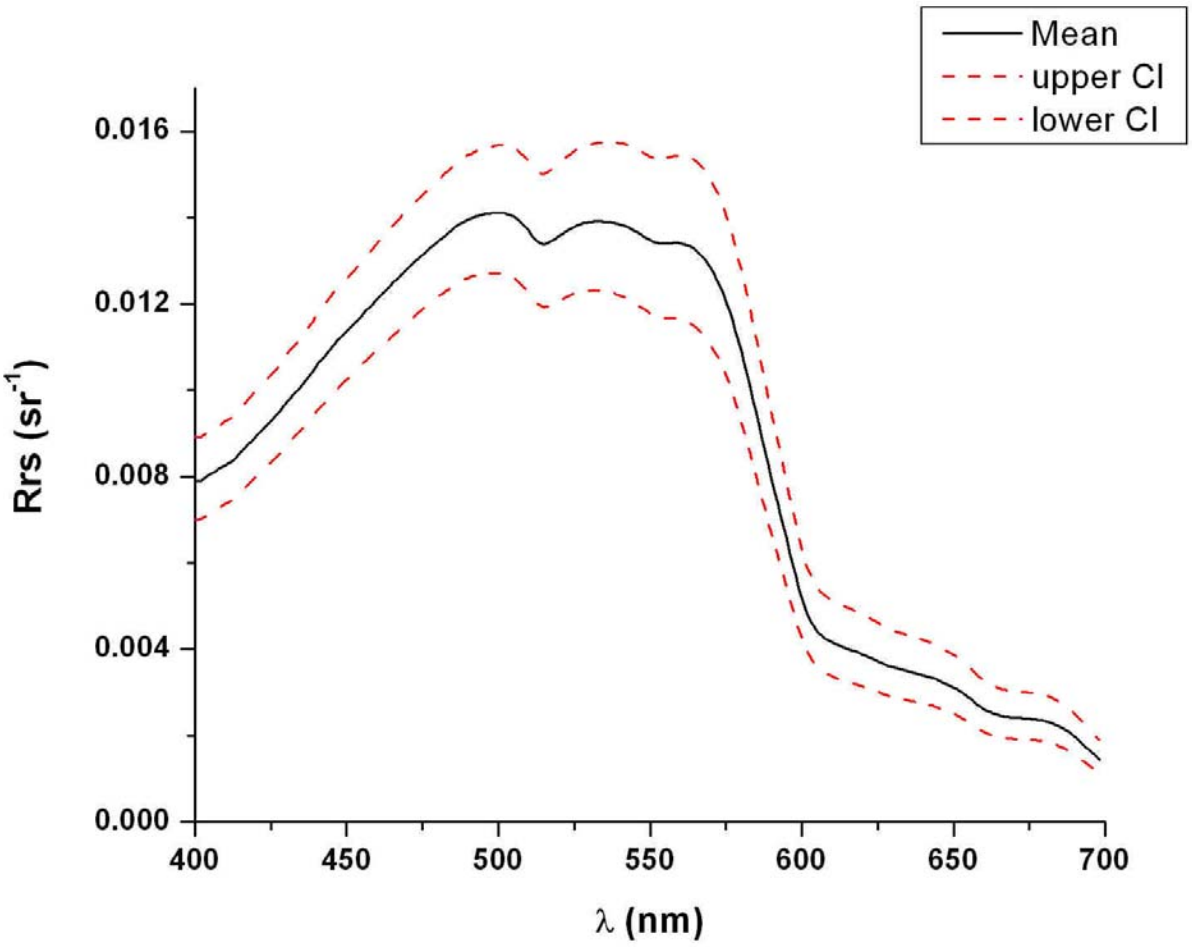

Figure 13. *Mean and 95% confidence intervals (CI) of the Rrs curves for Mayaguez Bay (n = 142).*

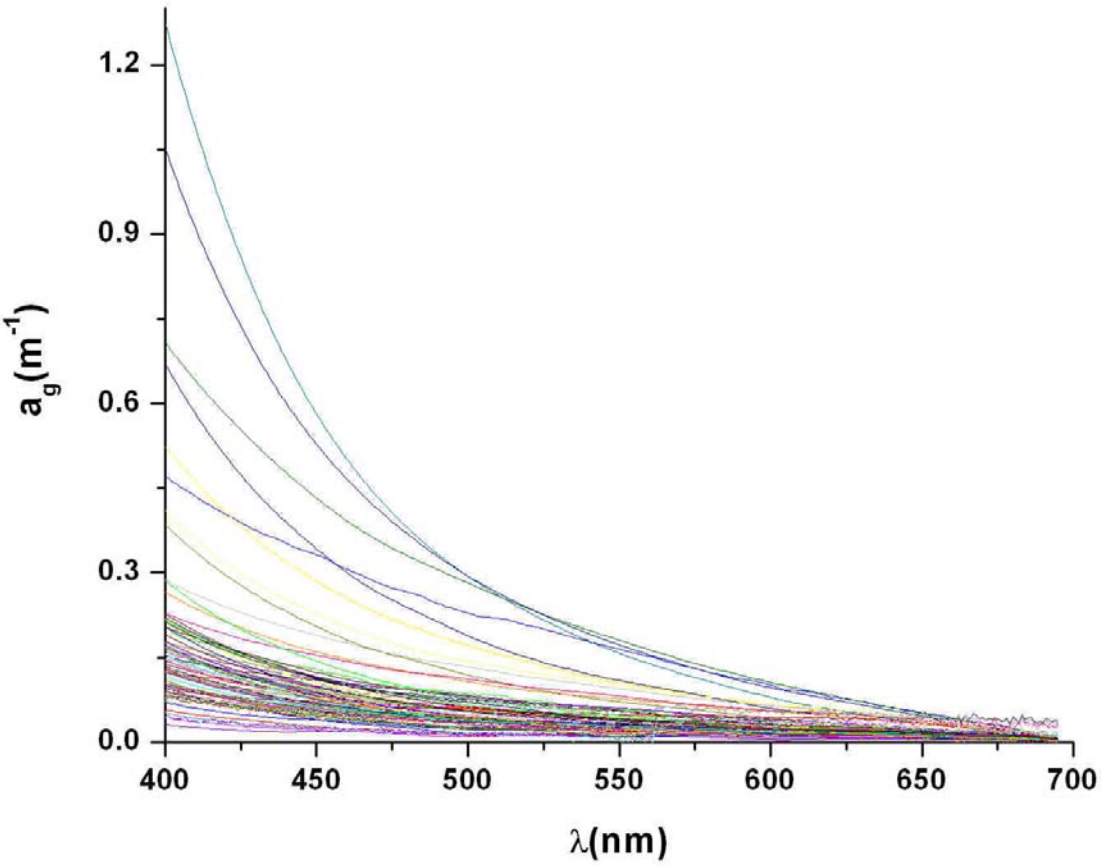

Figure 14. *CDOM absorption curves variability for Mayagüez Bay.*

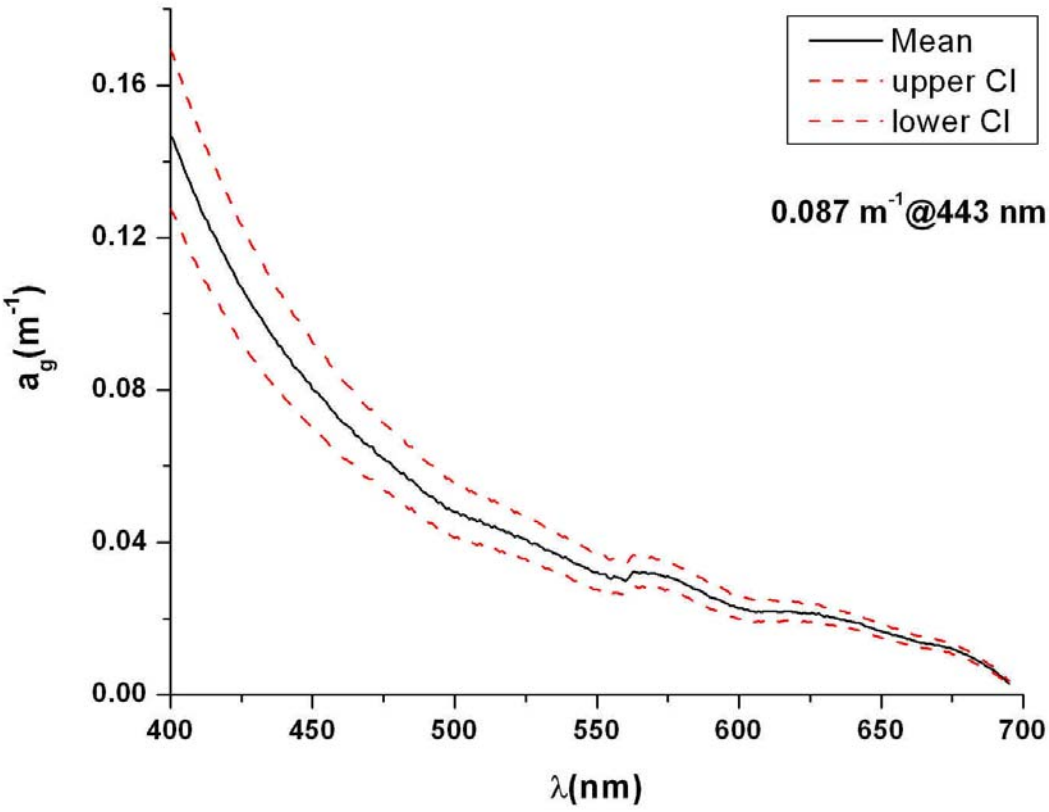

Figure 15. *Mean and 95% confidence intervals (CI) for the CDOM curves (n = 84) measured in Mayagüez Bay.*

Parameters	***n***	***Pearson's Correlation Coefficient (r)***
TSS vs. Chl *a*	95	0.37
TSS vs. Rrs 412	95	-0.14
TSS vs. Rrs 443	95	0.10
TSS vs. Rrs 555	95	0.63
TSS vs. Rrs 670	95	0.62
Chl *a* vs. Rrs 412	146	-0.06
Chl *a* vs. Rrs 443	146	0.01
Chl *a* vs. Rrs 555	146	0.25
Chl *a* vs. Rrs 670	146	0.31
Chl *a* vs. a_g 412	84	0.83
TSS vs. a_g 412	78	0.19

Table 7. *Pearson's Correlation Coefficients (r) for various combinations of optically active components measured in Mayagüez Bay.*

Hydrolight Validation

A reasonably good agreement was found between the measured Rrs curves and those modeled by Hydrolight 4.2 for October 2001. Root mean square error (RMSE) values where generally low (RMSE < 0.009) and Pearson correlation coefficients ranging from weak (r = 0.433) to very strong (r = 0.99) were obtained for all stations. Willmott's Index of Agreement (d) was greater than 0.526 for all stations. The Hydrolight fit was especially good from 400 to 500 nm for stations S1, S13, S21 and S23. This fact is important because most band ratio algorithms use wavelengths in this range for Chl *a* estimation. The results of the October 2001 Hydrolight simulations are shown in Figure 16.

Results for the February 2003 simulations are shown in Figure 17. Although the model fit estimators are somewhat lower than the ones for October 2001 ($0.383 \leq d \leq 0.821$), spectral shapes generally agree. A closer examination reveals departure from the measured Rrs curves mostly in the red portion of the visible spectrum.

A comparison between the October 2001 (rainy season) and February 2003 (dry season) simulations revealed that model fit estimators tended to be lower for the dry season. Note that TSS concentrations where used in place of inorganic mineral concentrations for the Hydrolight simulations because of the lack of mineral data during this study.

Hydrolight Simulations

Figure 18 shows the results for the Hydrolight simulation with CDOM absorption of 0.05 m^{-1}. As the mineral concentrations approaches 5 mg/l the Rrs curves become much closer, most notably when Chl *a* = 0.1 to 1 µg/l. At higher mineral concentrations (mineral concentration > 25 mg/l), it becomes almost impossible to differentiate among Rrs curves based on their Chl *a* concentration.

The same phenomenon is observed at higher CDOM absorption values (0.10, 0.15, 0.25 and 0.50 m^{-1}) as shown in Figures 19, 20, 21, and 22. It is evident that when mineral concentration is greater than 5 mg/l, both CDOM absorption and Chl *a* concentration have moderate effect on the spectral shape and the magnitude of the Rrs curve.

An interesting feature of the Rrs curves measured *in situ* in Mayagüez Bay is that the reflectance values are not close to zero near 700 nm. This phenomenon was also observed in Rrs data modeled with Hydrolight 4.2. As the inorganic minerals concentration increases, the Rrs curve moves away from the abscissa in the red region of the visible spectrum.

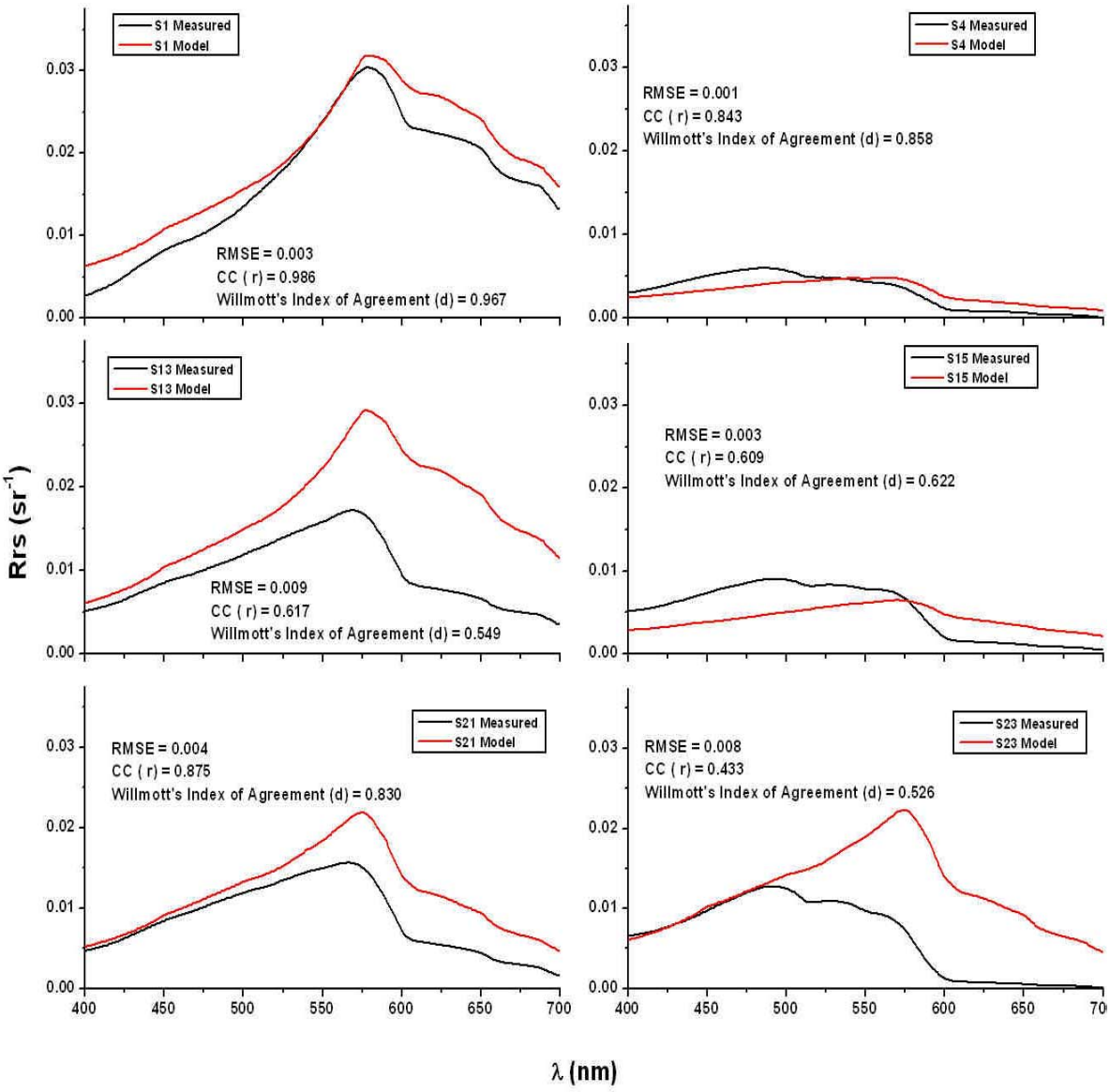

Figure 16. *October 2001 Hydrolight Rrs (0+, λ) validation results for selected stations in Mayagüez Bay.*

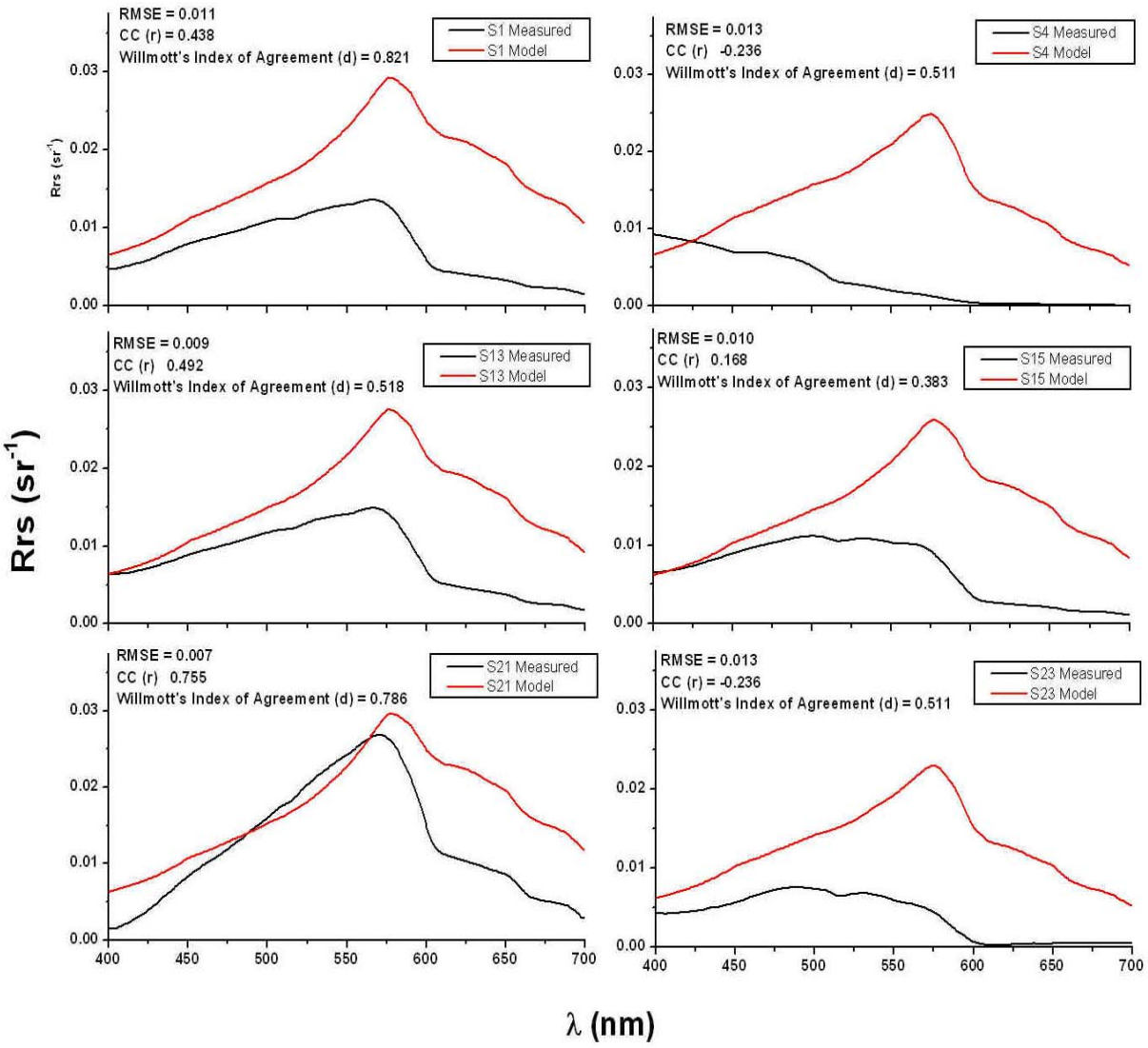

Figure 17. *February 2003 Hydrolight Rrs (0+, λ) validation results for selected stations in Mayagüez Bay.*

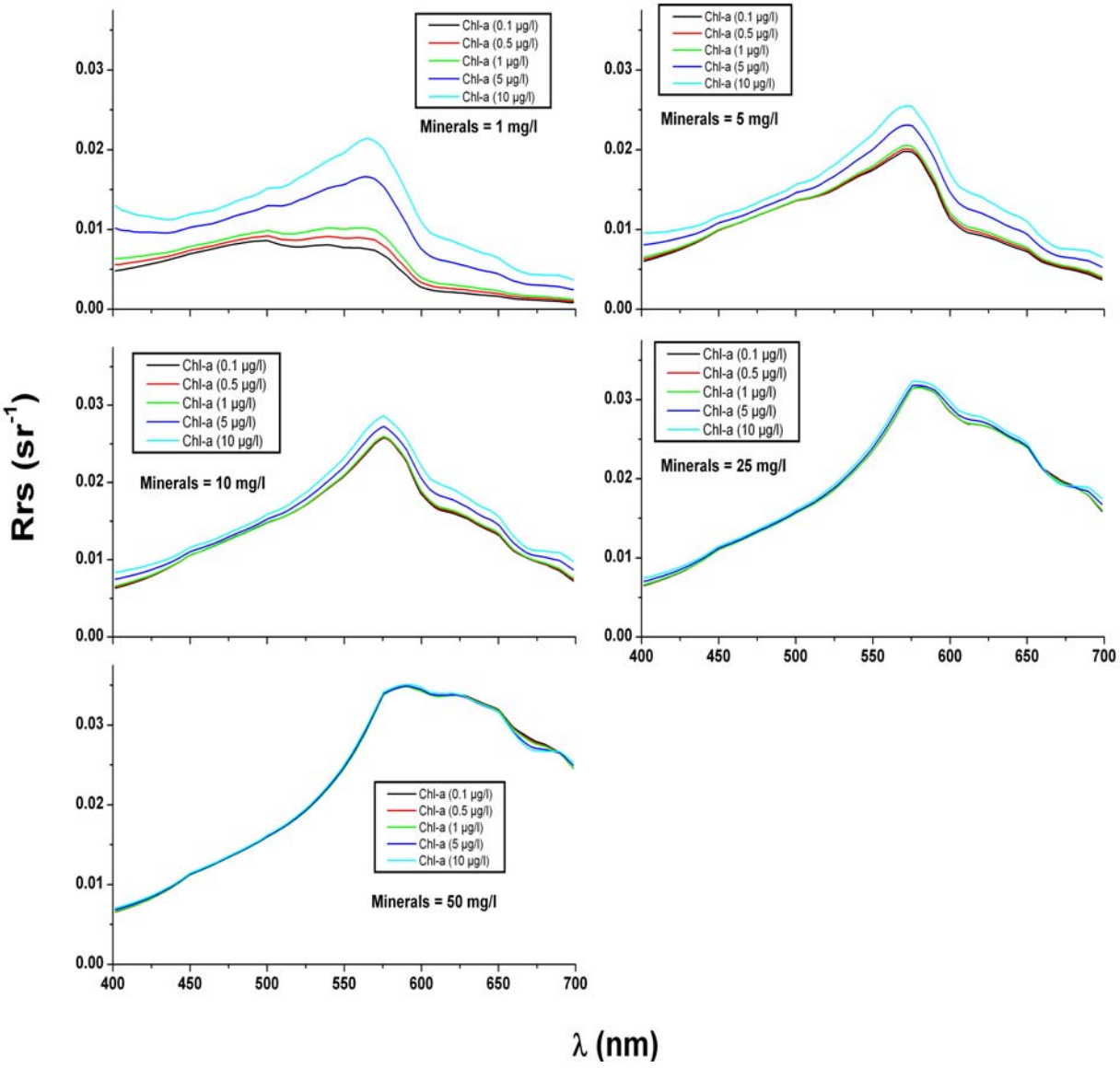

Figure 18. *Rrs curves modeled by Hydrolight when CDOM absorption was set at 0.05 m^{-1} at 443 nm. The graphs represent 1, 5, 10, 25 and 50 mg/l of red clay minerals.*

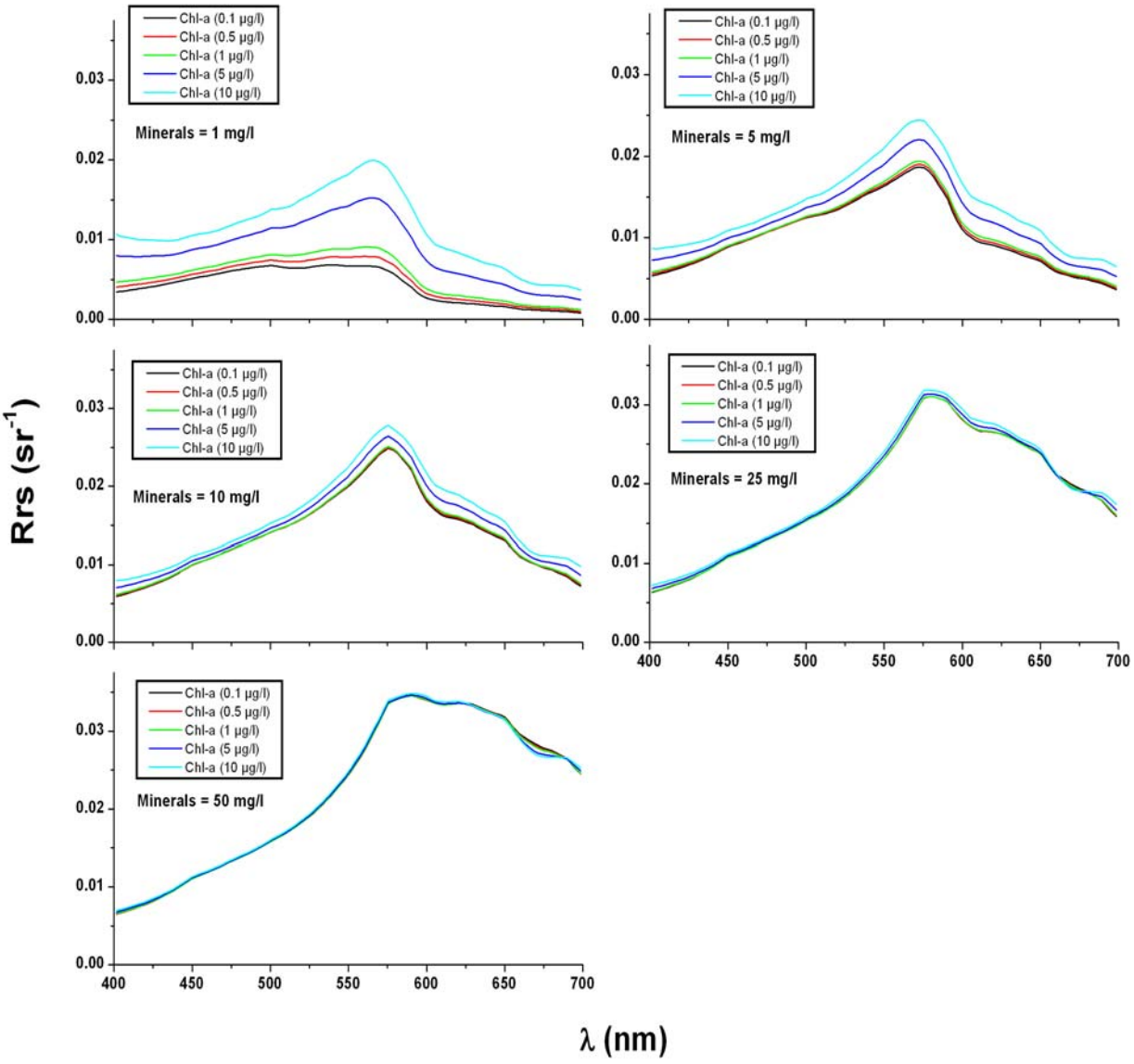

Figure 19. *Rrs curves modeled by Hydrolight when CDOM absorption was set at 0.10 m^{-1} at 443 nm. The graphs represent 1, 5, 10, 25 and 50 mg/l of red clay minerals.*

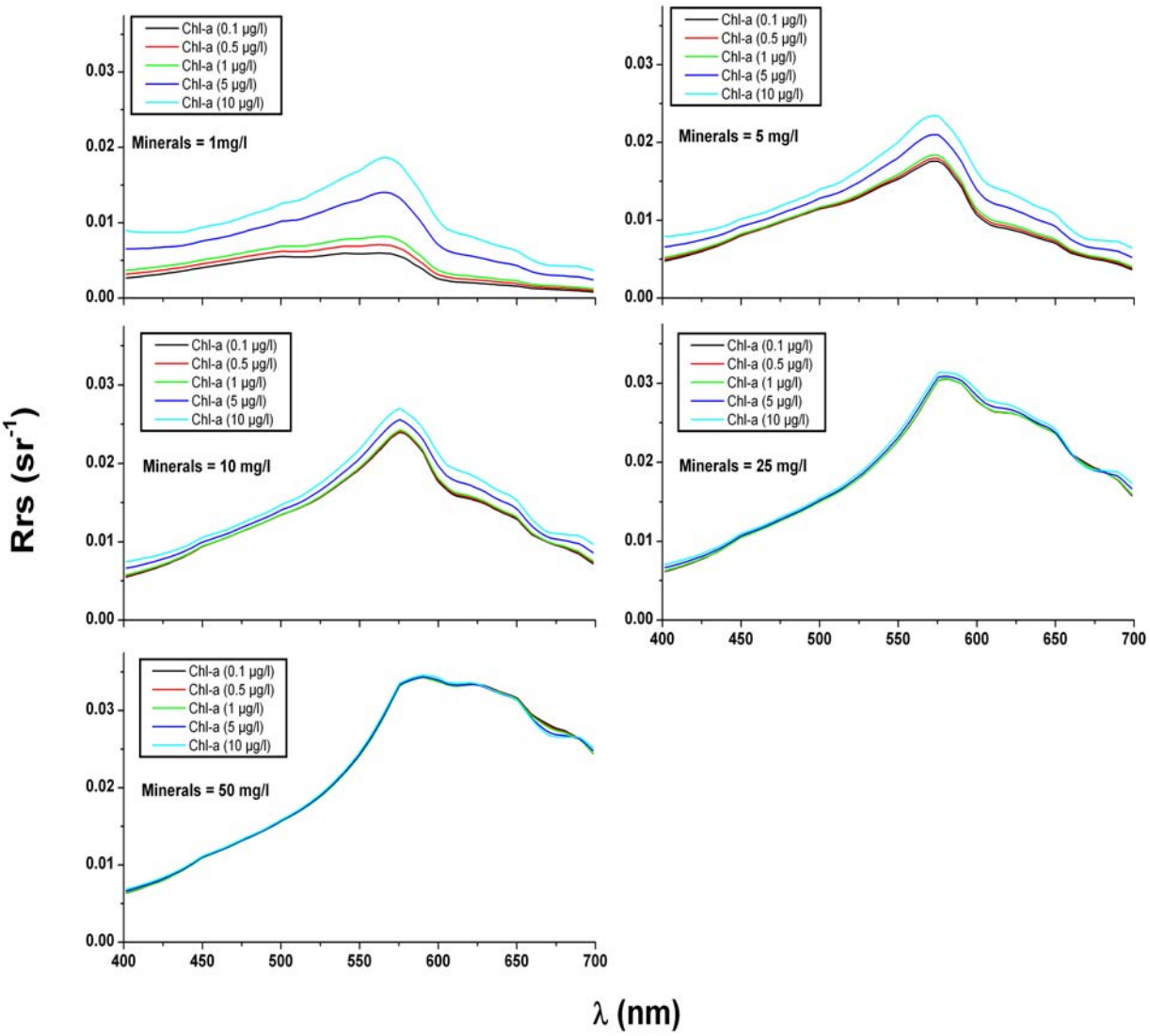

Figure 20. *Rrs curves modeled by Hydrolight when CDOM absorption was set at 0.15 m^{-1} at 443 nm. The graphs represent 1, 5, 10, 25 and 50 mg/l of red clay minerals.*

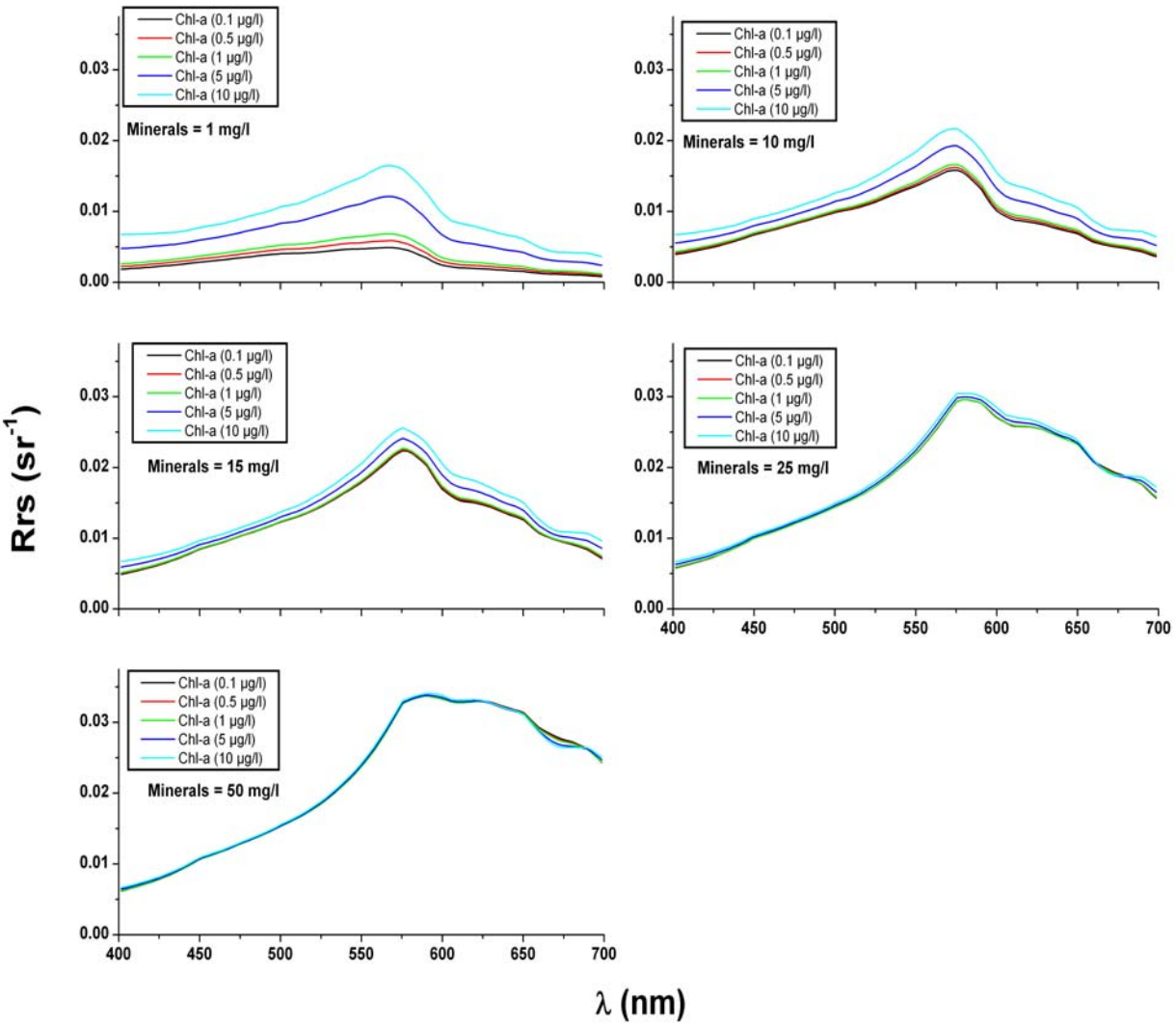

Figure 21. *Rrs curves modeled by Hydrolight when CDOM absorption was set at 0.25 m^{-1} at 443 nm. The graphs represent 1, 5, 10, 25 and 50 mg/l of red clay minerals.*

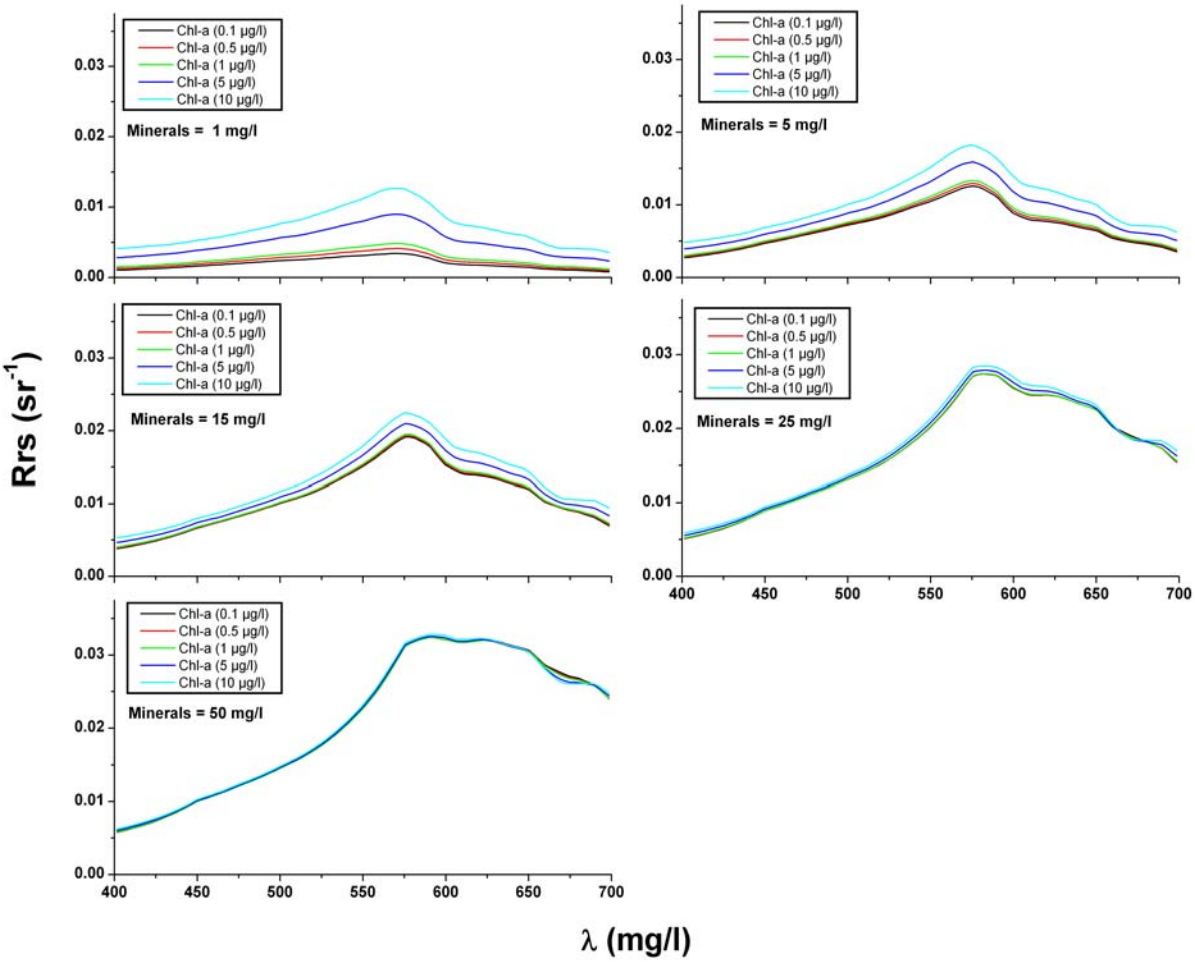

Figure 22. *Rrs curves modeled by Hydrolight when CDOM absorption was set at 0.50 m^{-1} at 443 nm. The graphs represent 1, 5, 10, 25 and 50 mg/l of red clay minerals.*

Discussion

Bio-optical Description

In order to understand the bio-optical relationships in Mayagüez Bay, a look into the variability of the optical constituents is warranted. As it is shown in this and previous works (Gilbes *et al.*, 1996; Rosado-Torres, 2000; Lee-Borges, 2003; Ludeña, 2007), Mayagüez Bay have the characteristics of a mesotrophic coastal bay.

Chl *a* concentrations in Mayagüez Bay are within the values reported for coastal and inland waters around the world. Bowers *et al*. (2004) reported Chl *a* values ranging from 0.73 to 9.9 µ l^{-1} in the Conwy Estuary, North Wales. Chl *a* concentrations from 0.4 to 3.8 mg m^{-3} were measured in the Gulf of Lions in the Mediterranean Sea by Ouillon and Petrenko (2005). A Chl *a* concentration range of 0.5 to 2.1 µg/l was reported for coastal waters of the northern Adriatic Sea by Zibordi *et al*. (2004). Chang *et al.* (2006) reported Chl *a* values ranging from 0.26 to 4.52 mg m^{-3} for the waters of the Santa Barbara Channel in the South California Bight.

TSS concentrations were also similar to those reported by other researchers in coastal systems. Mean concentrations of 12.55 mg l^{-1} were reported for the waters of the Conwy Estuary in North Wales by Bowers *et al*. (2004). Their TSS concentrations ranged from 4.4 to 57.0 mg l^{-1}. These values are in good agreement with the TSS concentrations measured in this study. TSS concentrations varying from 0.3 to 326.2 g m^{-3} were reported by Ouberkheir *et al.* (2006) for the Fitzroy Estuary-Keppel Bay system. Zibordi *et al.* (2004) reported TSS concentrations from 0.76 to 1.75 mg l^{-1}. Their range of TSS is much lower than that observed in Mayagüez Bay and reveals the great range of variability of this parameter among global coastal waters.

The Rrs curves measured in Mayagüez Bay are an assortment of those found in both oceanic and coastal waters. These findings were expected because of the large optical variability that characterizes the bay (Rosado-Torres, 2000). The mean Rrs curve shows low reflection in the blue wavelengths, high reflectance in the green wavelengths and relatively high reflectance in the red wavelengths. This result suggests that in average, the bay is dominated by high CDOM absorption, high Chl *a* concentrations and abnormally high reflection in the red, probably caused by the high concentrations of red clays found in the bay. These results are in good agreement with the variability of these parameters as reported in previous studies of Mayagüez Bay (Gilbes *et al.*,1994; Rosado-Torres, 2000; Lee-Borges, 2003 and Ludeña, 2007).

The range of a_g values measured in Mayagüez Bay is large compared to most data published for coastal waters. For example, Kirk (1994) published a_g data at 440 nm for various natural waters including oceanic, coastal and inland waters. Of all the measurements reported, only the Marseilles drainage outfall (0.07 to 0.65 m^{-1}) and the River Rhone mouth (0.09 to 0.57 m^{-1}) showed a range of a_g values similar to Mayagüez Bay. D'Sa *et al*. (2006) reported a_g 443 values from 0.073 to 0.277 m^{-1} for the Mississippi River Mouth before and after a cold front.

The large range of a_g observed is a function of the optical complexity of the bay. Del Castillo (2005) points out that in river dominated coastal environments; CDOM is a mixture of compounds of terrestrial and marine origins. Not only chemical composition varies between CDOM end-members from these sources, but also dilution with sea water affects the CDOM optical properties in estuarine waters. The formation of strong gradients in the chemical and optical properties of CDOM is the result of this process. Since in a relatively short distance (~ 4 km) there is a transition from river mouths to oceanic waters, large variability in a_g is expected in Mayagüez Bay. The occurrence of a hump around 550 nm in the mean CDOM curve may be explained by the contamination of CDOM samples by mineral particles. Bowers and Binding (2006) reported similar humps present in their mineral absorption data. They also noted that such feature never occurs in CDOM absorption curves.

The weak correlations found between TSS and Rrs 555 and Rrs 670 may be explained if we examine the TSS composition of Mayagüez Bay. Although the chemical nature of the TSS has not been studied yet in the bay, there is indirect evidence that red clay minerals comprise a large proportion of the TSS, especially during the rainy season. The evidence will be discussed in detail later in this section. Since red clay minerals reflect strongly in the green and red portions of the visible spectrum, their concentration may explain the correlation values found.

The strong correlation between Chl *a* and a*g* 443 is probably caused by the seasonality of the bay in terms of river discharge. The peak of the rainy season in western Puerto Rico is in October (Gilbes *et al.*, 1996; Rosado-Torres, 2000). October is also the month when higher Chl *a* values have been measured in the bay (Gilbes *et al.*, 1996; Rosado-Torres, 2000). It has been proposed by Gilbes *et al*.(1996) and Rosado-Torres (2000) that the input of nutrients resulting from the increase in river discharge is responsible for the high Chl *a* concentrations measured in the bay during the rainy season. High river discharge could also explain high CDOM

concentrations in Mayagüez Bay and the resulting large a_g values measured during the rainy season (Gilbes, unpublished data).

CDOM and Chl *a* concentrations do not co-vary in most coastal environments (Muller-Karger *et al.*, 2005; D'Sa and Miller, 2005). This seems not to be the case in Mayagüez. This attribute of Mayagüez Bay is worth examining because of its implications in the estimation of Chl *a* using remote sensing. Empirical algorithms typically rely on at least a band in the blue region of the Rrs curve for Chl *a* estimation (Ruddick *et al.*, 2001). Also, CDOM from terrestrial sources tends to absorb more at longer wavelengths (Del Castillo, 2005). Thus empirical algorithms, even the maximum ratio algorithms, should be negatively impacted by high a*g* values. A study of the CDOM dynamics in relation to the bio-optics of Mayagüez Bay is needed.

Hydrolight Validation

At first glance Hydrolight 4.2 is moderately capable of modeling the Rrs curve in Mayagüez Bay. A closer inspection reveals that the apparently limited predictive power of Hydrolight is probably more related to the nature of the data.

Although TSS concentrations were customarily measured for the stations considered in the simulations, Hydrolight routines use inorganic mineral concentrations for the bio-optical modeling. TSS is composed of both organic (detrital) and inorganic components. The temporal and spatial variability of these fractions is not known for Mayagüez Bay. Since red clays are the major mineral component of the suspended sediments and rivers are probably the main sources of red clays, it is plausible that during the rainy season red clays comprise a much larger fraction of the TSS, especially at inshore stations close to the river mouths. This hypothesis may explain why *in situ* and modeled Rrs data do not agree very well in the red portion of the spectrum in some stations. Although this assumption is supported by the modeled data, experimental data is needed in order to validate the suggestion.

To better illustrate the hypothesis suggested above, an iterative manipulation of the TSS values was performed for one of the stations where the modeled and measured Rrs curves deviated in the red part of the spectrum. Figure 23 shows the results of the Hydrolight Rrs modeling for station 13 on February, 2003, using TSS as equivalent of mineral concentration (TSS = Mineral concentration = 12.7 mg l^{-1}) and iteratively adjusting mineral concentration to 2 mg l^{-1}. Notice that Wilmott's Index of Agreement (d) increases from 0.57 to 0.95 indicating a

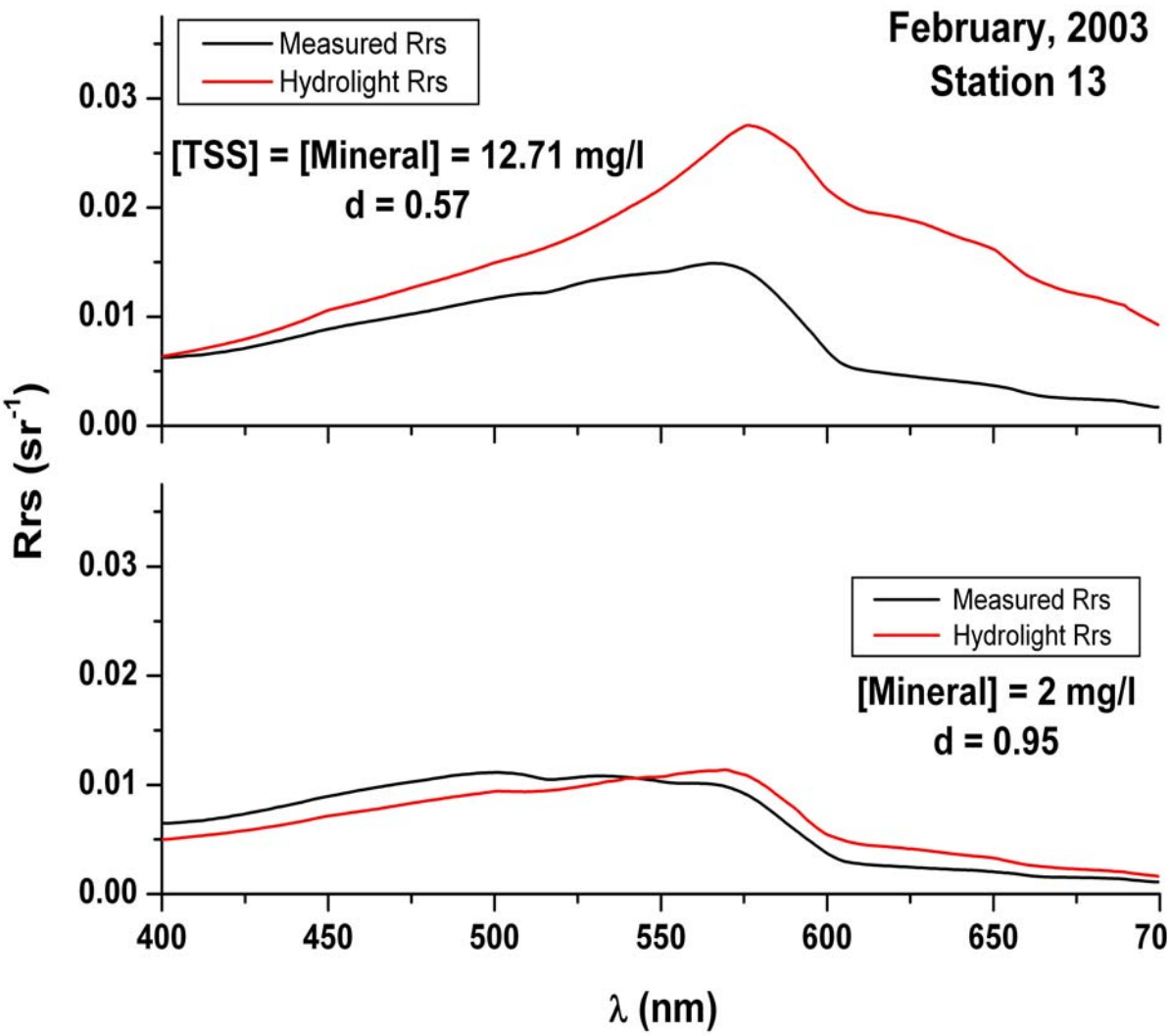

Figure 23. *Model fit when TSS was used to estimate mineral concentration (upper graph) and when mineral concentration was iteratively adjusted to 2 mg l^{-1}. The increase in Willmott's Index of Agreement suggests that the mineral fraction of the TSS was small (about 16%) for this particular sample.*

much better fit. Iterative manipulations of all the stations where the Rrs curve was overestimated in the red by the Hydrolight modeling yielded similar results.

A similar approach was undertaken with CDOM absorption. Although the CDOM absorption was carefully measured during this study, it is well documented that the sampling and quantifying process is prone to contamination (Del Castillo, 2005). Figure 24 shows the model results when CDOM concentration was iteratively decreased. Although the fit in the blue spectral region improves, Willmott's Index of Agreement improves only slightly.

These results suggest that although a small overestimation in CDOM absorption may be occurring, the largest impediment for improving the Hydrolight modeling of the Rrs curves for Mayagüez Bay is the lack of mineral concentration data. It is suggested that this parameter should be included in any future study of the bio-optics of the bay.

In conclusion, Hydrolight 4.2 is an excellent tool for modeling the bio-optical properties of coastal waters. A suggested future application of the Hydrolight software is the creation of a comprehensive virtual data set of bio-optical data based on the bio-optics of Mayagüez Bay. Such data set would prove invaluable for the development of neural network algorithms requiring huge data sets for their training and validation. It could, in theory, also be used for the development of look-up table algorithm that relates reflectance values at several wavelengths with optically active constituents.

This task will require the optical characterization of the inorganic minerals present in the bay. It is also important to understand the temporal and spatial optical variability of the inorganic suspended particles for the area. It is also suggested that future data sets take into account the three unknown components used for Hydrolight's bio-optical modeling of case-2 waters (Chl *a* bearing particles, CDOM and Minerals) in terms of supplying the software with the most in *situ data* possible in order to minimize the modeling of each component, especially if profiles of AOPs or IOPs are needed.

Hydrolight Simulations

It has been reported that in some coastal waters, CDOM absorption is the dominating optical feature (Hochman *et al.,* 1994; Carder *et al.,* 1989). Hydrolight simulations suggest that red clay minerals are the single most important optically active seawater constituent in Mayagüez Bay. It is clearly shown in the Hydrolight simulations that at all CDOM absorption levels considered,

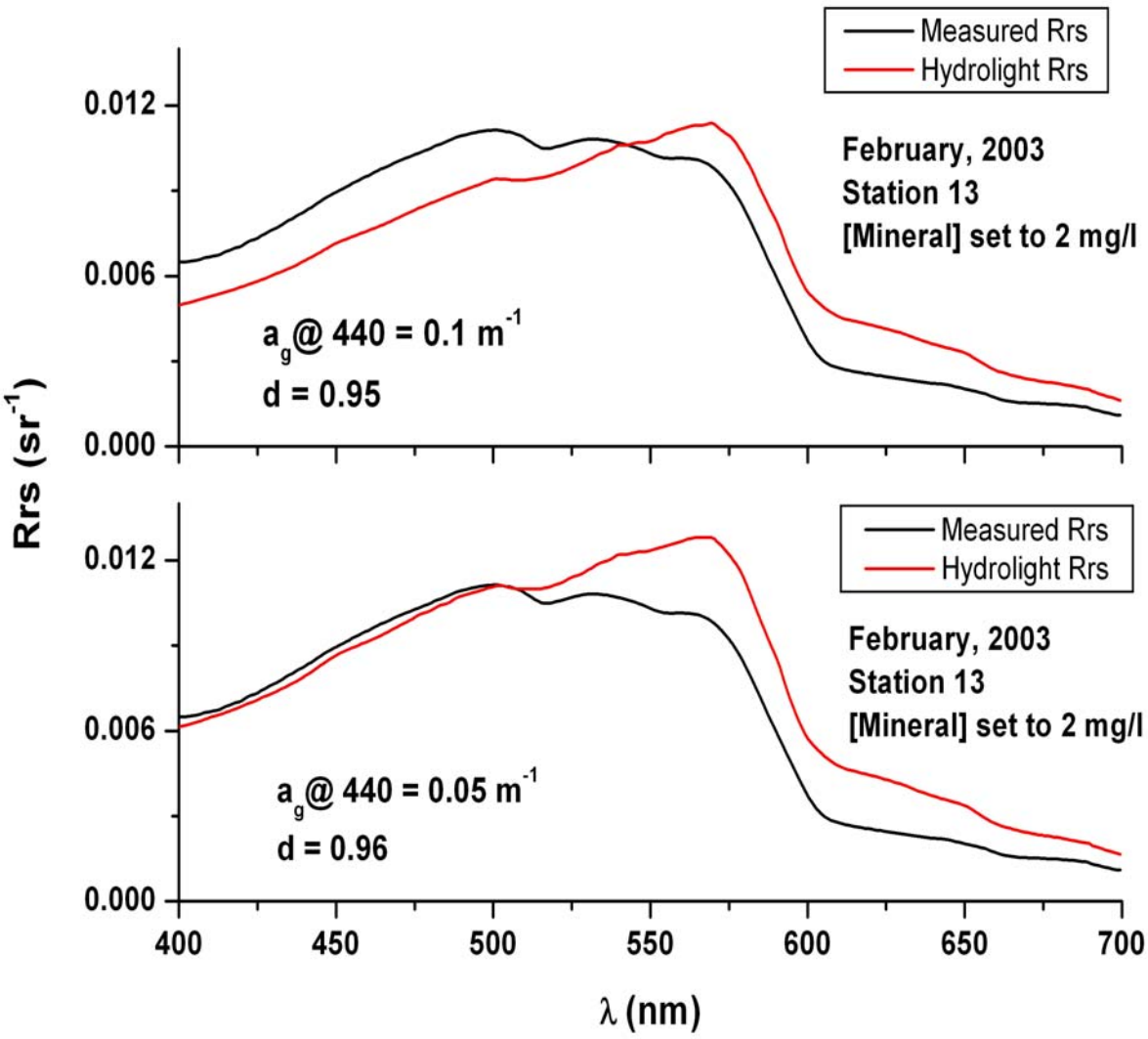

Figure 24. *The effect of decreasing CDOM absorption on the Hydrolight modeling of the Rrs curve. Note that decreasing CDOM absorption from 0.1 m^{-1} to 0.05 m^{-1} improves de Wilmott's Index of Agreement only slightly.*

there is a loss of dependence between Rrs and Chl *a* when mineral concentrations are greater than 5 mg l^{-1} and Chl a concentration is relatively low (0.10 to 1.0 µgl^{-1}).

This finding is very important and explains, in part, the poor performance of bio-optical algorithms for the estimation of Chl *a* in this region. Mayagüez Bay exhibits low Chl *a* concentrations (mean = 0.65 µg l^{-1}) and high TSS concentrations (mean = 8.15 mg l^{-1}) for most of the year. The reasons for the high TSS values found in Mayagüez Bay are thought to be the extremely high load of terrigenous sediments deposited in the bay during the rainy season and wave induced sediment resuspension during the dry season (Gilbes, personal communication). Based on the Hydrolight simulations, it may not be possible to estimate Chl *a* using Rrs at least in some stations during certain times of the year. To be able to establish a threshold value of inorganic suspended minerals that permits remote sensed estimations of Chl *a*, more information is required about mineral dynamics in Mayagüez Bay. Since suspended sediments are known to be present at high concentrations both during the dry season (wave induced resuspension) and the rainy season (river discharge), there is not a simple way to predict when or where to apply ocean color algorithms in Mayagüez Bay.

A practical application of the Hydrolight simulation data is the fragmentation of the Mayagüez Bay data set in two sub-sets. Since the data set in this study does not include mineral concentration, and TSS may include a large fraction of inorganic particles, especially, but not limited to, inshore stations during the rainy season, it was decided to use TSS = 5 mg l^{-1} as an arbitrary cut-off point for the data set. This assumption assures that the Rrs data used for algorithm development is dependent of Chl *a* concentration.

The importance of suspended inorganic particles is widely recognized in the bio-optical literature (Babin and Stramski, 2004). It is known that mineral particles are highly efficient scatterers (Bowers and Binding, 2006) and it has been demonstrated that iron rich minerals exhibit strong absorption in the blue-green spectral region (400 – 500 nm: Babin and Stramski, 2004). Thus, mineral particles, especially red clays have a profound effect in seawater IOP's and hence in the AOP's. In order to better understand the bio-optics of Mayagüez Bay, a deeper look into the mineral suspended particles is suggested.

Ocean Color Algorithms Performance Assessment and Development in Mayagüez Bay

Introduction

One of the main goals of ocean color remote sensing is the estimation of Chlorophyll *a* (Chl *a*). Accurate estimates of Chl *a* are of utmost importance for a better understanding of global, regional and local oceanographic processes. They could also be used to predict human impact on environmental and climate change and for the implementation of wise stewardship and management policies (Linton and Warner, 2003).

Most algorithms designed to estimate Chl *a* from remote sensing reflectance data fall in one of three categories: empirical, semi-analytic and neural network algorithms. Each of these approaches has its own advantages and disadvantages and examples abound in the literature.

Empirical ocean color algorithms, also known as band ratio algorithms, use statistically derived relationships between Rrs and Chl *a* concentration (O'Reilly *et al*., 1998). These types of algorithms are characterized for a lack of understanding of the underlying scientific theories that govern the relationships. Band ratio algorithms have been used extensively, especially in case-1 waters were their percent accuracy is about 30% (Gordon and Morel, 1983). In case-2 waters, they tend to overestimate Chl *a* by a far larger percentage (Carder *et al.*, 1991). The ease of calculation of the Chl *a* products when using band ratio algorithms and their reliability in case-1 waters make this class of algorithms the most used in ocean color remote sensing.

Semi-analytical algorithms are partially based on mathematical solutions to the radiative transfer equation (Carder *et al*., 1999; Lee *et al*., 2002). This approach usually yields a better estimate of Chl *a*, especially in case-1 waters, at the expense of computational resources. Recent literature suggests that inversion algorithms do not perform that well in case-2 waters because their mathematical foundation is not well posed. Semi-analytical algorithms are based in the relationship $Rrs = Q(b_b/a)$. It has been suggested that infinite combinations of b_b and a could produce exactly the same Rrs curve, and the possibility of that occurring is especially high in case-2 waters where CDOM and suspended sediments are found in high concentrations and does not co-vary with Chl *a*. In addition, semi-analytical algorithm must be optimized in order to accurately derive the inherent optical properties from the apparent optical properties. This optimization has to be done in a regional basis. Moreover; extensive computational resources are

needed in order to apply semi-analytical algorithms to large remote sensed data sets such as ocean color sensor images.

Artificial neural network (ANN) algorithms are a relatively new approach to ocean color estimation. ANN algorithms are widely used as continuous models to fit highly non-linear transfer functions and for inverting noisy data sets (Schiller and Doerffer, 1998, Gross *et al.*, 2000). ANN algorithms are complex, stable, and adaptative approximators, capable of minimizing the effects of measurement errors if properly trained (Gross *et al.*, 2000). They are usually better than empirical or semi-analytical algorithms at estimating Chl *a* from marine reflectance if properly trained (Gross *et al.*, 2000). One of the drawbacks of ANN algorithms is the difficulty of acquiring the large data sets (pairs of Rrs measurements and Chl *a* concentration) needed to properly educate the neural networks. This drawback is usually overcome by creating synthetic data sets. It is fundamental to incorporate the type of noise expected to be found in the waters where the ANN is to be applied because they do not cope well with noise that they were not trained with (Gross *et al.*, 2000).

Although many different versions of all major classes of ocean color algorithms have been published, the bio-optics community still has not reached consensus about what type of algorithm performs best in case-2 waters. Many researchers feel that the quest for a universal ocean color algorithm is futile and that the best approach is to develop site-specific algorithms.

The aim of this part is to assess the performance of several empirical and a quasi-analytical algorithm for the estimation of Chl *a* from Rrs in Mayagüez Bay. Due to the lack of sufficient, appropriate, *in situ* data, an ANN algorithm will not be considered.

Materials and Methods

Field Work

Several oceanographic cruises were carried out in Mayagüez Bay from February 1997 to January 2004. Water samples for Chl *a* and Rrs (λ) measurements were taken in all the cruises described hereafter.

The first series of cruises extended from February 1997 to January 1998 and consisted of a total of 6 oceanographic stations sampled on a monthly basis. The stations were selected taking into account the impact of the rivers and known sources of industrial and municipal effluents. Figure 25 shows the location and name of the stations. A more detailed description of the stations included in that series of cruises can be found in the first chapter of this document or in Rosado-Torres (2000).

Two additional cruises took place in October 1999. These two cruises sampled two transects, each of them aligned to the Guanajibo River and Yagüez River mouths respectively. A total of 11 eleven stations were occupied during the cruises. The sampling layout is shown in Figure 26. The October 1999 cruises are described in more detail in the first chapter of this document or in Rosado-Torres (2000).

A series of seven cruises were carried out in April 2001, October 2001, February 2002, August 2002, February 2003, October 2003 and January 2004. A total of 6 transects were sampled in each of those cruises, each transect comprised of four oceanographic stations. The stations where 1 km apart, the first station from each transect located as near as possible from the shore, limited by the bathymetry of the bay. During these cruises full water sampling and bio-optics measurements were only collected in selected stations, whereas a bio-optical package cast and Rrs (λ) measurements were taken in all stations (Figure 27).

Rrs(λ) was calculated following the methodology described in Rosado-Torres (2000). Water radiance, Lo(λ), sky radiance, Ls(λ), and the above surface downwelling irradiance, Ed(0+, λ) were measured using a GER 1500 field spectroradiometer. Lo(λ) was measured pointing the GER 1500 to the water surface in a 45° angle. The Ls(λ) was measured aiming the instrument 45° into the sky. In both cases, the measurements were taken with an azimuth 90° from the solar plane in order to minimize the sun glint. The Ed(0+, λ) was measured fitting the GER 1500 with a cosine collector and aiming the instrument at the zenith. The Rrs(λ) was then

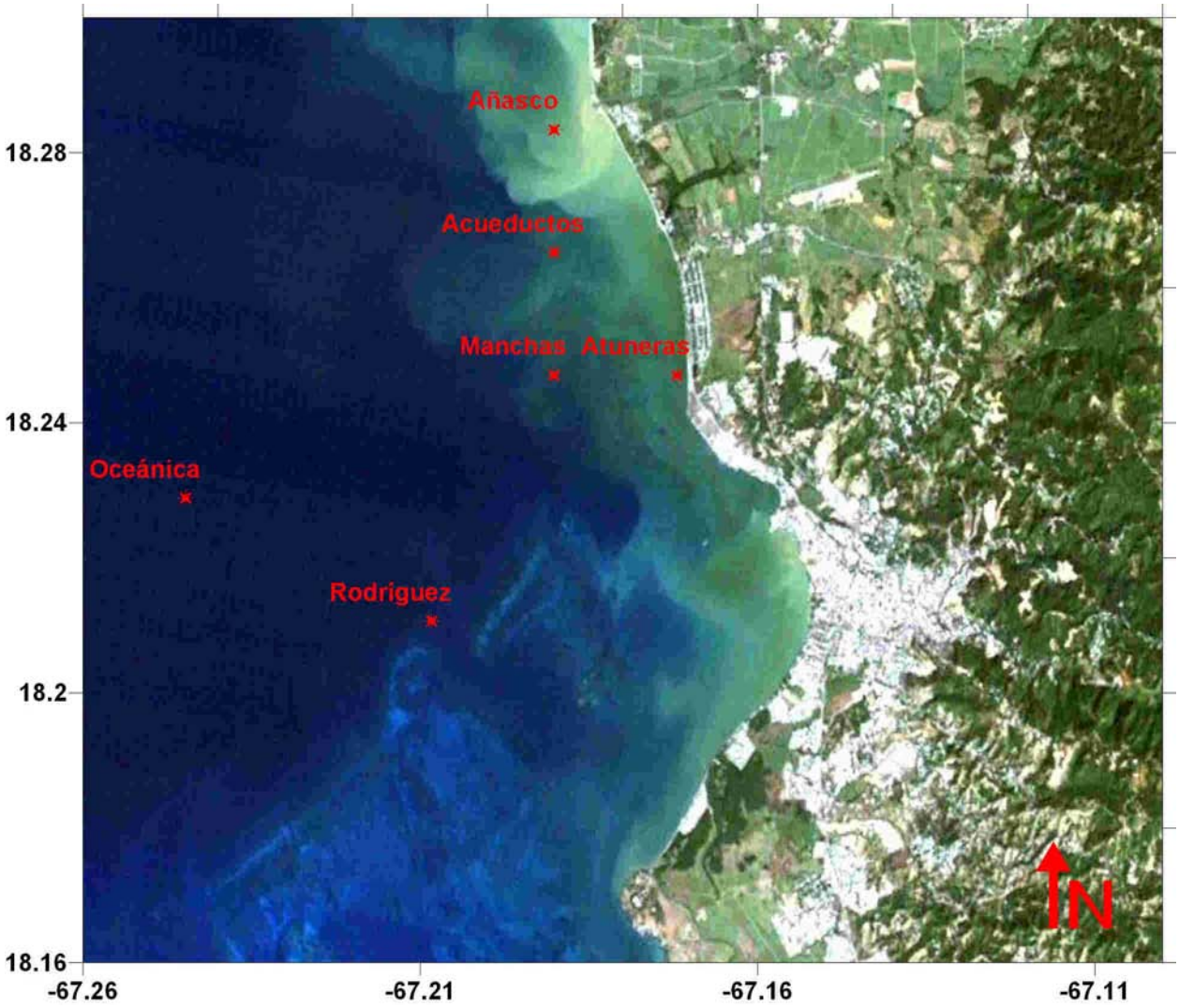

Figure 25. *A map showing the sampling pattern for the 1997-98 time series.*

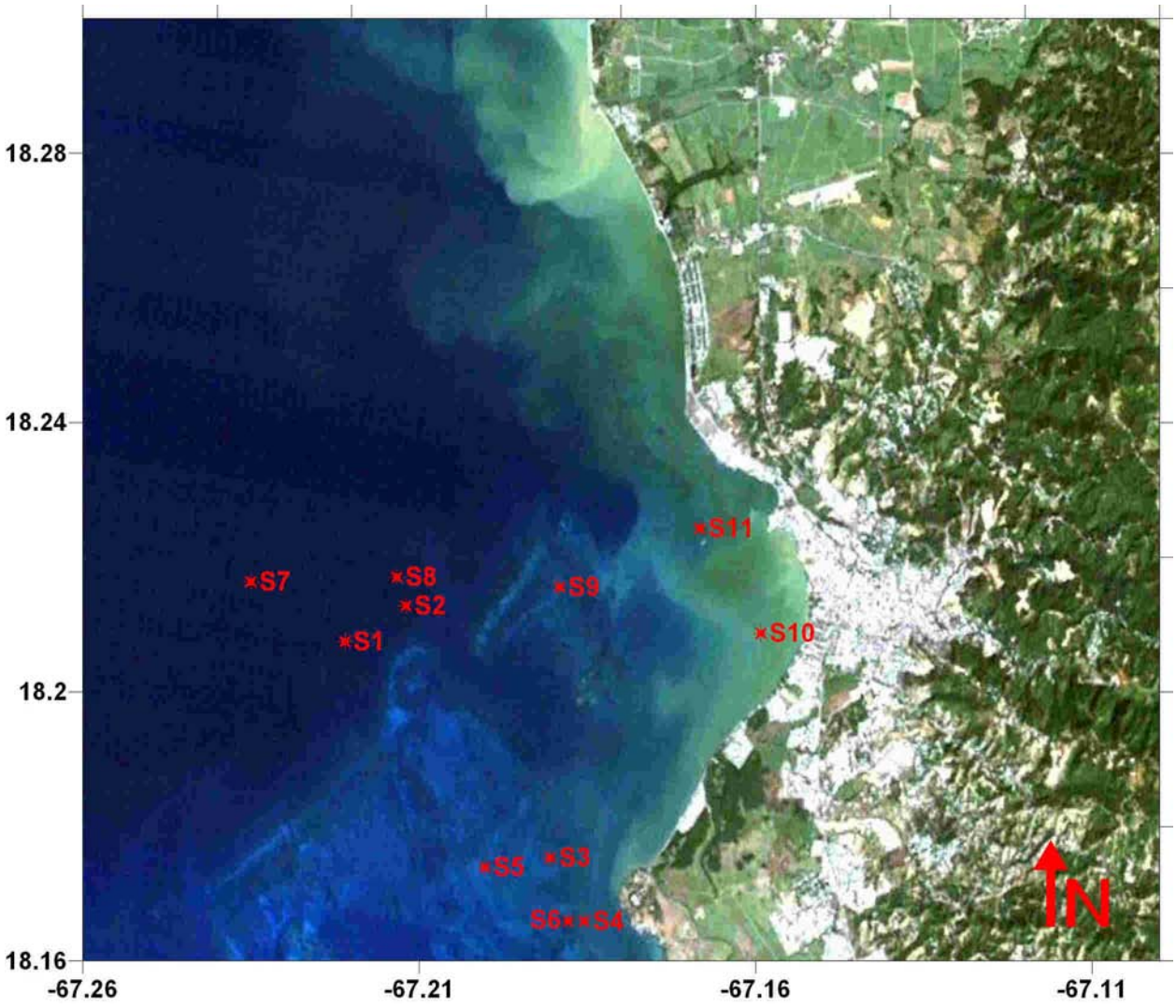

Figure 26. *A map showing the sampling pattern for the October 1999 cruises.*

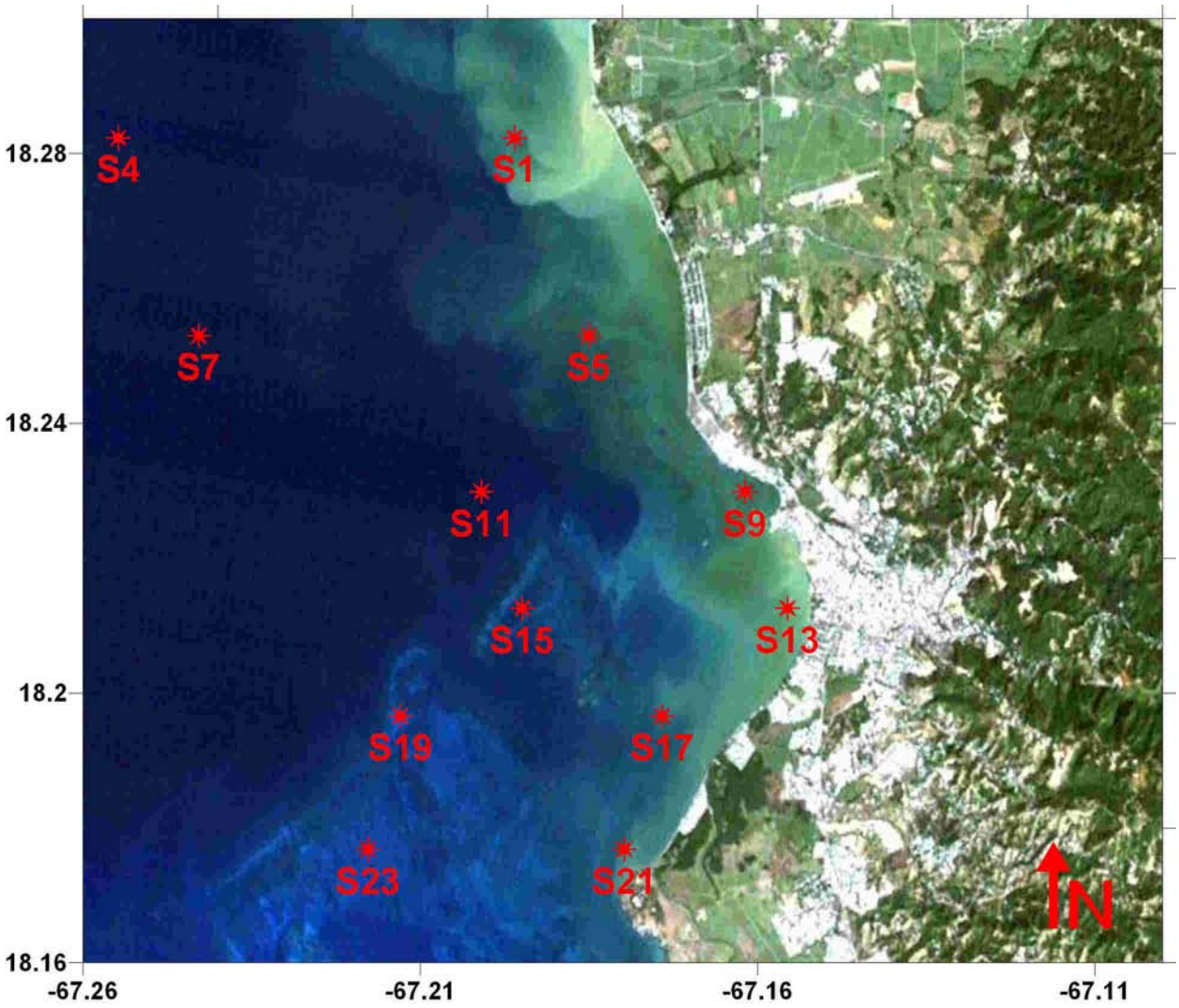

Figure 27. *Sampling pattern used in the April 2001 to January 2004 cruises. Only the stations where full water sampling was done are presented.*

calculated using the following equation:

$$Rrs = \frac{Lo(\lambda) - f[Ls(\lambda)]}{Ed(0+, \lambda)}$$

where f is Fresnel's number, the percent of sky radiance reflected back to the atmosphere. Fresnel's number has a value of 0.028 at a 45° angle. The Rrs curves were corrected for residual sky radiance by subtracting the Rrs value at 950 nm. If that value was found to be negative, the minimum Rrs value from the spectral range from 750 to 950 nm was then subtracted from each curve.

Samples were collected for Chl *a* and total suspended sediments (TSS) using either a horizontal sampling bottle or taken from the water surface directly in 1 liter dark Nalgene sampling bottles. The samples were refrigerated immediately and transported to the laboratory.

Laboratory work

For the 1997 – 1999 cruises, Chl *a* concentration was measured using a modification of the filter pad technique (Mitchell and Kiefer, 1984). The samples were filtered thru GF/F filters using a 200ml plastic filtration funnel connected to a Gast vacuum pump. The pigments were immediately extracted from the filters using the hot methanol extraction method proposed by Kishino *et al.* (1985). This method was used because particle, detritus and phytoplankton absorption were also being measured at the time.

For the rest of the cruises, Chl *a* was measured using the following methodology. Once the samples were filtered as above, replicate filters where placed in disposable plastic 15 ml centrifuge tubes, filled with 10ml of HPLC grade methanol and refrigerated for 24 hours at 5°C. Once the extraction was done, the Chl *a* concentration was measured in a calibrated Turner 10AU field fluorometer using the method proposed by Welschmeyer (1994).

In order to divide the data set according to a threshold value of mineral concentration, TSS data were collected. TSS was measured by filtering a known volume of water thru 0.45 µm Millipore membrane filters that were previously dried in an oven at 60°C for at least 24 hours and weighted using a Mettler analytical balance. The filters were dried again at 60°C for 24 hours and placed in a glass dessicator for cooling prior to weighing. The difference in weight for each filter (mg) was divided for the volume of water filtered (l) and the TSS concentration obtained in mg/l.

Data Analysis

The agreement between *in situ* Chl *a* and 14 empirical band ratio algorithms was estimated. The algorithms considered were CalCOFI P, CalCOFI C (Mitchell and Kahru, 1998), Morel 2, Morel 4 (Morel, 1988), OC1a, OC1b, OC1c, OC1d, OC2, OC2 v2, OC2c, OC2 v-4, OC4 v4 and OC3M (O'Reilly *et al.*, 1998; O'Reilly *et al.*, 2000). For this section, the Mayagüez Bay data set was considered both as a whole and for the data points where TSS < 5 mg/l. The reason was to evaluate the effect of high TSS values on algorithm performance. The algorithms were evaluated by calculating Root Mean Squared Error (RMSE) and Mean Percent Error (MPE). The MPE was calculated using the following formula:

$$MPE = \frac{100}{n}\sum_{1}^{n}\frac{\left|Chla_{measured} - Chla_{estimated}\right|}{Chla_{measured}}$$

Where $Chla_{\text{measured}}$ is the *in situ* Chl *a* concentration, and $Chla_{\text{estimated}}$ is the Chl *a* value obtained with a particular algorithm.

The calculations were done in MS Excel and the graphics were produced by Microcal Origin 6.0.

The performance of the Quasi-Analytical Algorithm (Lee *et al.*, 2002; Lee *et al.*, 2007) in Mayagüez Bay was also assessed. In this case, only data points with TSS ≤ 5 mg/l were considered. The following procedure was applied to the Rrs curves in order to estimate Chl *a*. First, the *in situ* Rrs (λ, 0^{+}) was converted in rrs (λ, 0^{-}) using the following equation (Lee *et al*., 2002):

$$rrs(\lambda) = Rrs(\lambda) \Big/ (0.52 + 1.7Rrs(\lambda))$$

Then, u (λ) was calculated using the following relationship (Lee *at al*. 2002):

$$u(\lambda) = \frac{-g_0 + [(g_0)^2 + 4g_1 rrs(\lambda)]^{1/2}}{2g_1}$$

Where $g_0 = 0.0895$, $g_1 = 0.1247$ for coastal waters.

The next step was to calculate total absorption at 640 nm, [a(640)]. This was achieved using the following relationship (Lee *et al*., 2002):

$$a(640) = 0.31 + 0.07\left[\frac{rrs(640)}{rrs(440}\right]^{1.1}$$

The particle backscattering at 640 nm [b_{bp} (640] was calculated as follows (Lee *et al*., 2002):

$$b_{b\,p}(640) = \frac{u(640)a(640)}{1-u(640)} - b_{bw}(640)$$

The particle backscattering curve was then modeled with the following power law relationship (Lee *et al*., 2002):

$$b_{b\,p}(\lambda) = b_{bp}(640)\left(\frac{640}{\lambda}\right)^{\mathrm{Y}}$$

Where Y was calculated from (Lee *et al*., 2002):

$$\mathrm{Y} = 2.2\left\{1 - 1.2\exp\left[-0.9\frac{rrs(440)}{rrs(555)}\right]\right\}$$

The total spectral absorption, a(λ) was then calculated from the following equation (Lee *et al*., 2002):

$$a(\lambda) = \frac{1-u(\lambda)\left[b_{bw}(\lambda) + b_{bp}(\lambda)\right]}{u(\lambda)}$$

The a(λ) must be partitioned into $a_{dg}(\lambda)$ and aφ(λ) for Chl *a* calculation. The partition was accomplished with the following pair of equations (Lee *et al*., 2002):

$$\zeta = a_{\phi}(410)/a_{\phi}(440) = 0.71 + \frac{0.06}{0.8 + rrs(440)/rrs(550)}$$

$$\xi = a_{g}(410)/a_{g}(440) = \exp S(440-410)$$

The ag(λ) spectral slope from 440 to 410 nm, (S(440-410)) was averaged for the TSS ≤ 5 mg/l data set.

The ratios above where then used to calculate the CDOM absorption at 440 nm as follows (Lee *et al*., 2002):

$$a_{g}(440) = \frac{\left[a410 - \zeta a(440)\right]}{\xi - \zeta} - \frac{\left[a_{w}(410) - \zeta a_{w}(440)\right]}{\xi - \zeta}$$

The a_g (λ) was the modeled using a_g (440) as reference, with the following relationship (Lee *et al*., 2002):

$$a_{g}(\lambda) = a_{g}(440)e^{-S(\lambda-440)}$$

The phytoplankton absorption was then obtained subtracting the CDOM absorption, $a_g(\lambda)$ and the water absorption, $a_w(\lambda)$ from the total absorption, $a(\lambda)$ as shown in the next equation (Lee *et al*., 2002):

$$a_\phi(\lambda) = a(\lambda) - a_g(\lambda) - a_w(\lambda)$$

The $a_w(\lambda)$ values were taken from Pope and Fry (1997) and the water backscattering coefficients were taken from Smith and Baker (1981) wherever they where used.

The Chl *a* concentration was finally estimated using the relationship proposed by Carder *et al*. (2003):

$$Chl\ a = 56.8\left(a_\phi(675)\right)^{1.03}$$

Results

Empirical algorithms

A summary of the performance of the empirical algorithms considered for the complete data set is shown in Table 8. The RMSE ranged from 2.49 µg l^{-1} for Morel 2 to 21.46 µg l^{-1} for Morel 4. The MPE varied from 298.28 % for OC2 v2 to 2096.52 % for Morel 4. In general, all empirical algorithms tended to overestimate Chl *a* in Mayagüez Bay. The performance of each algorithm can be better appreciated in Figures 28, 29, 30 and 31.

The empirical algorithms were also assessed for the samples where the TSS concentrations were less than 5mg/l. The RMSE ranged from 0.71 µg l^{-1} for OC2 v2 to 5.26 µg l^{-1} for Morel 4. The MPE varied from 142.99 % for OC2 to 1249.07 % for Morel 4. There was an overall reduction of roughly a factor of 3 for RMSE and a factor of 2 for MPE for all the algorithms evaluated. The results of the algorithms performance are shown in Table 9. The fit of estimated Chl *a* versus measured Chl *a* for each empirical algorithm is shown in Figures 32, 33, 34 and 35.

Based on the empirical algorithms performance results mentioned above, two band algorithms were developed for the TSS < 5mg/l data set. The first was based on the OC1d/OC2 family of algorithms and consisted of a third order polynomial regression. The second algorithm was based on the OC4 v4 algorithm and consisted of a fourth order polynomial regression. These algorithms were selected because they were among the best performers of all empirical algorithms tested in the case of OC1d/OC2, and because the most recent empirical algorithms in use by NASA (OC4 v4 and OC3M) are based on fourth order polynomials.

The cubic fitting of log (Chl *a*) versus log (Rrs 490/Rrs 455) is shown in Figure 36. Note that the R^2 for the model is 0.26. The high variability of the data points is typical when empirical ocean color algorithms are applied to coastal data. The performance of the cubic polynomial fit is shown in Figure 37. The RMSE and MPE are much lower than the tested empirical algorithms in the preceding section. The fourth order polynomial fit for the TSS < 5 mg/l data set is shown in Figure 38. The $R^2 = 0.33$ for the model, increasing slightly from the cubic polynomial fit. This was possibly the result of the capacity of higher order polynomials to better adjust to a complex non-linear curve.

Algorithm	*RMSE*	*Mean Percent Error (%)*
CalCOFI P	4.40	459.80
CalCOFI C	7.48	578.59
Morel 2	2.49	440.29
Morel 4	21.46	2096.52
OC1a	3.64	379.92
OC1b	3.30	359.33
OC1c	5.78	473.96
OC1d	5.60	424.90
OC2	5.88	430.21
OC2 v2	2.90	298.28
OC2c	7.88	518.05
OC2 v4	3.38	331.70
OC4 v4	3.08	329.21
OC3 M	4.06	355.35

Table 8. *Chl a estimated by published empirical algorithms versus Chl a measured in situ in Mayaguez Bay. These results comprise the Mayagüez Bay data set of Rrs and Chl a measurements collected for this work.*

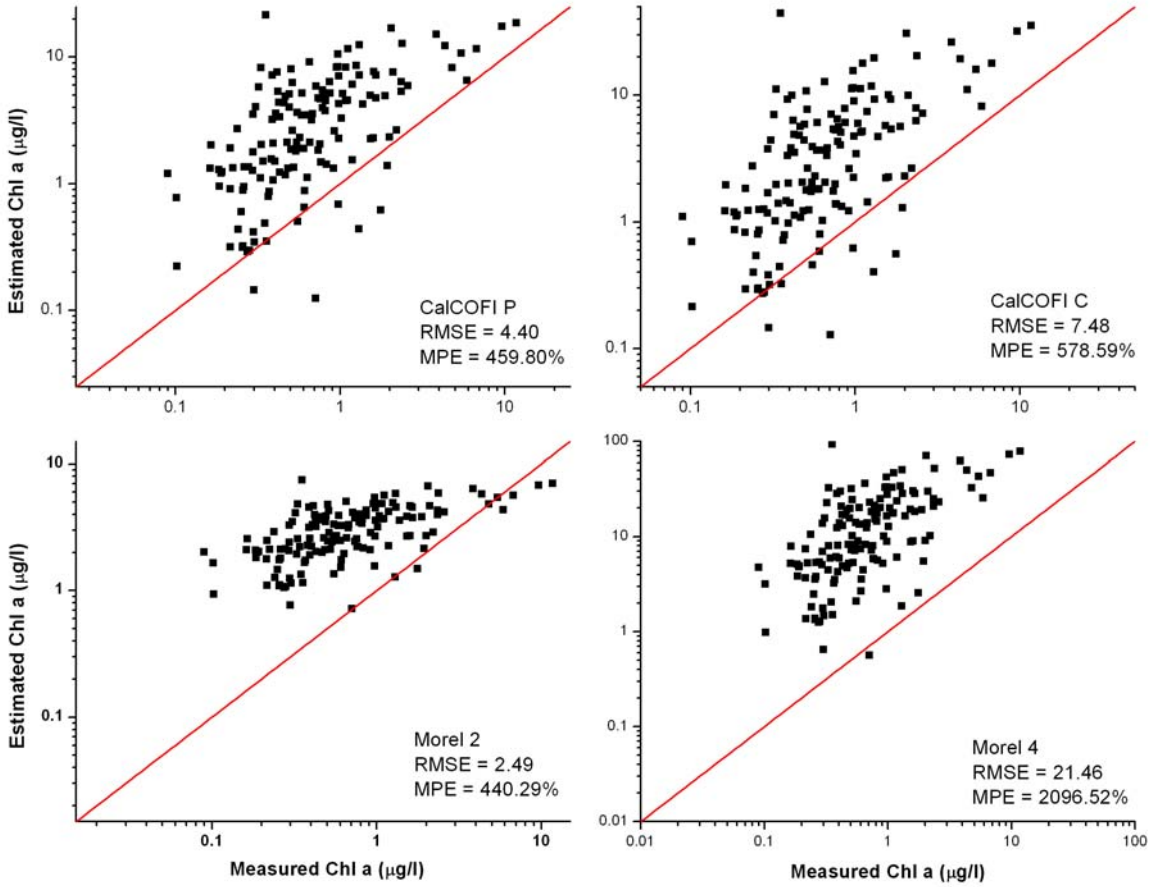

Figure 28. *Chl a estimated by CalCOFI P, CalCOFI C, Morel 2 and Morel 4 empirical algorithms versus measured Chl a for the Mayagüez Bay data set (RMSE in* µg l^{-1}).

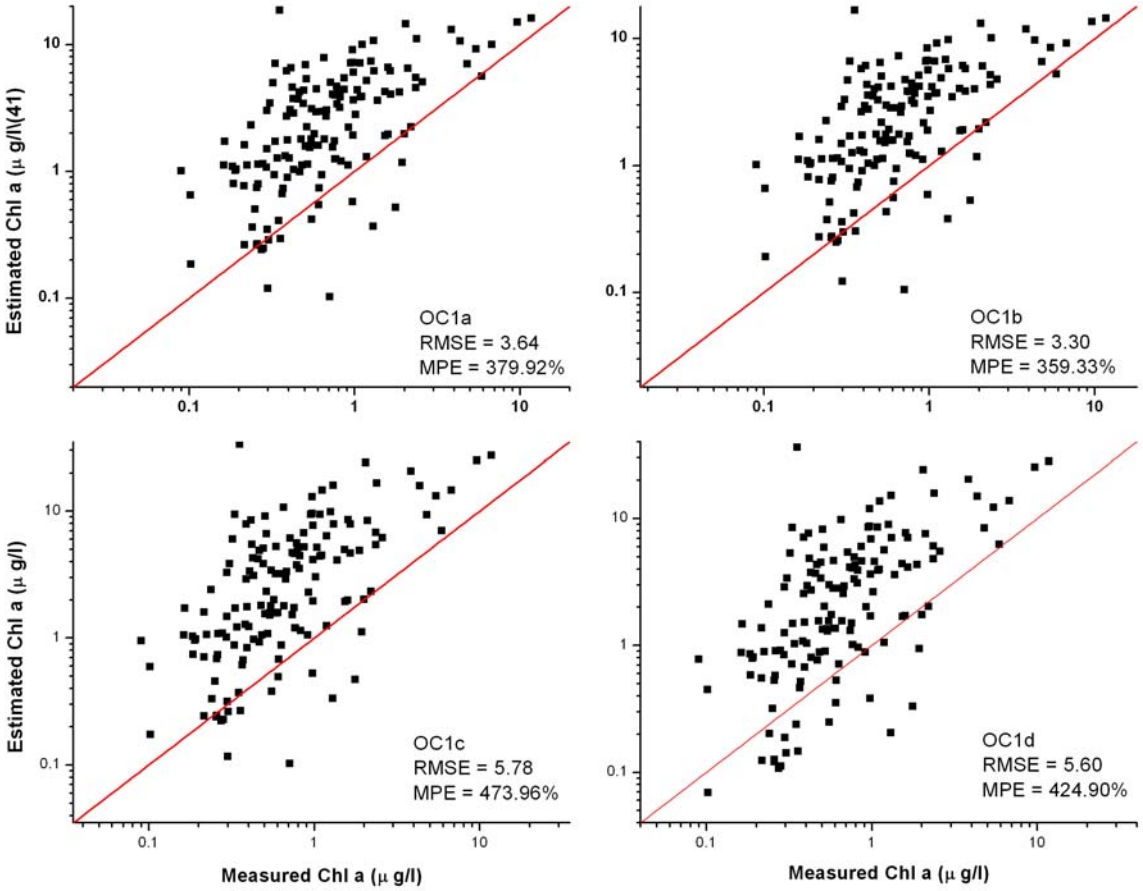

Figure 29. *Chl a estimated by OC1a, OC1b, OC1c and OC1d empirical algorithms versus measured Chl a for the Mayagüez Bay data set (RMSE in* μg l^{-1}).

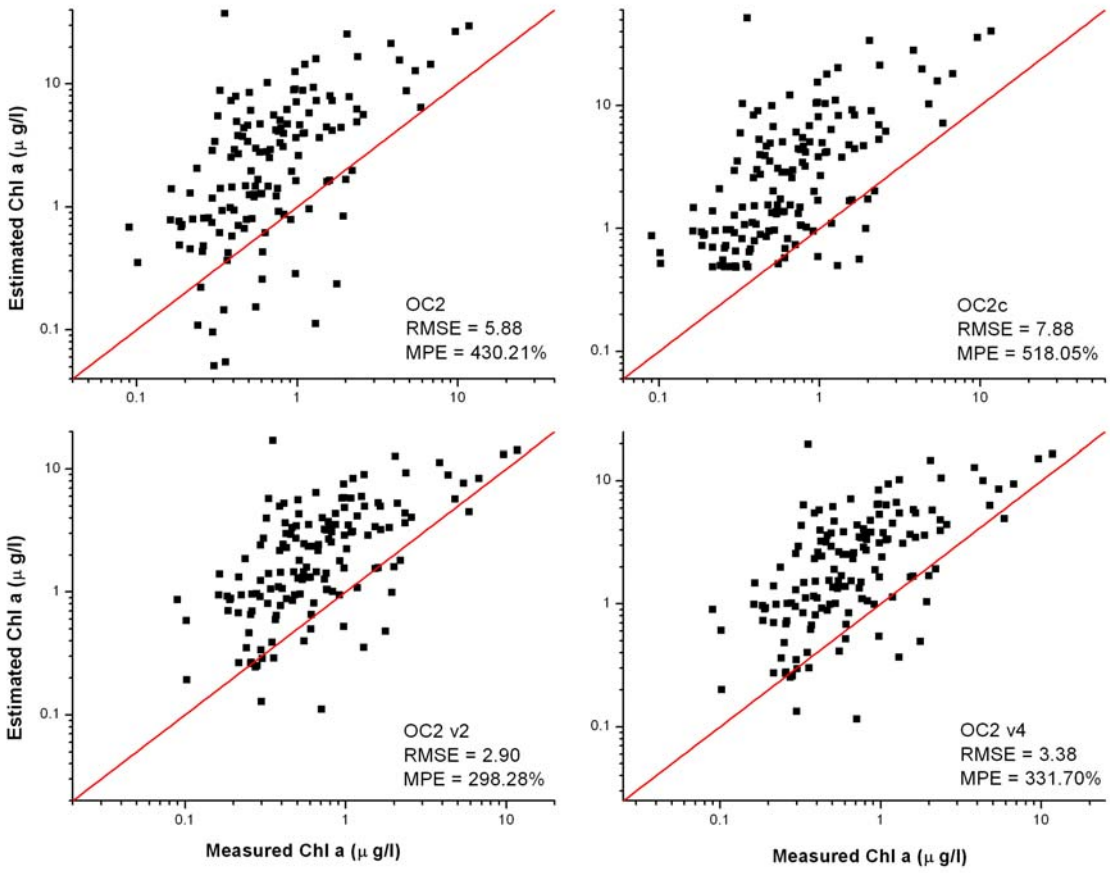

Figure 30. *Chl a estimated by OC2, OC2C, OC2 v2 and OC2 v4 empirical algorithms versus measured Chl a for the Mayagüez Bay data set (RMSE in* $\mu g\ l^{-1}$).

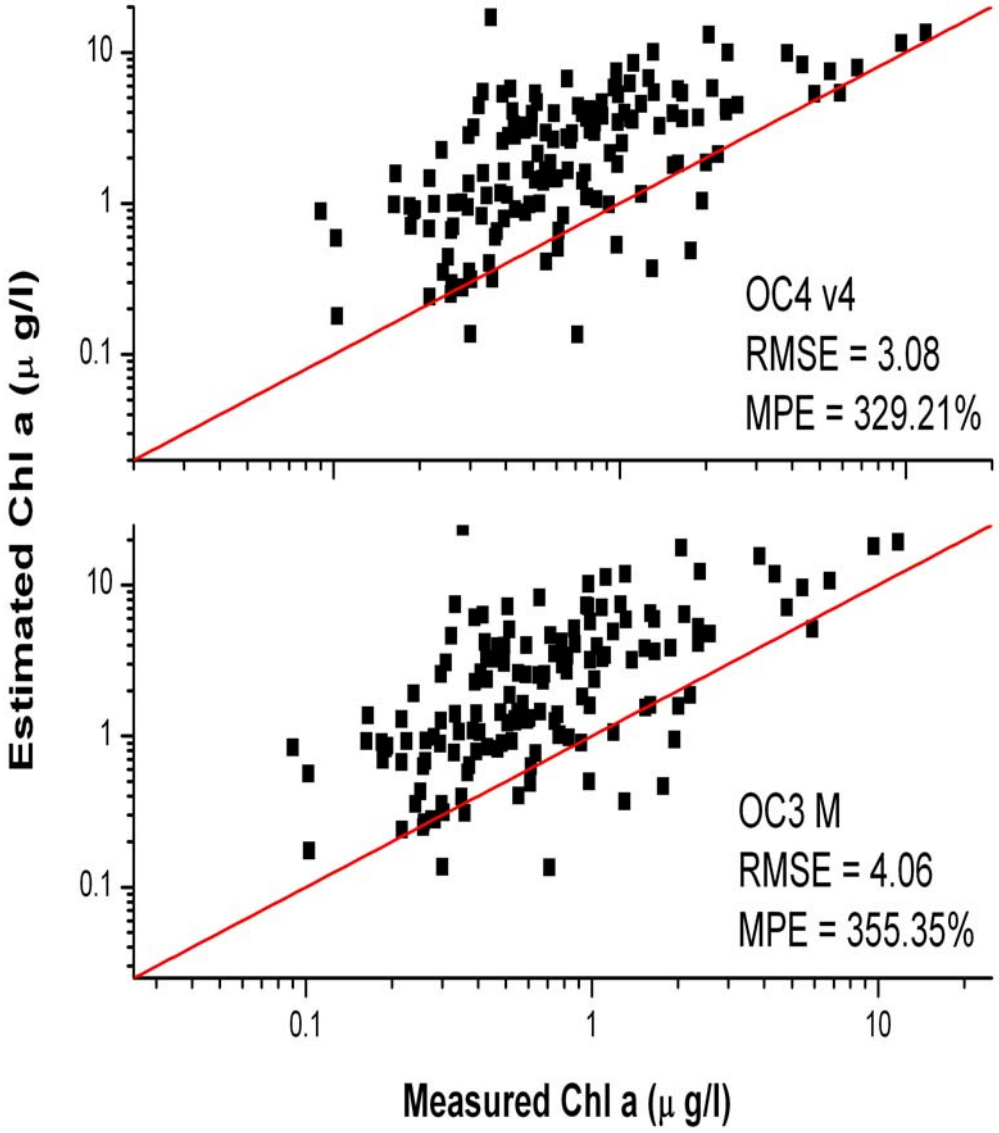

Figure 31. *Chl a estimated by OC4v4 and OC3M empirical algorithms versus measured Chl a for the Mayagüez Bay data set (RMSE in* μg l^{-1}*).*

Algorithm	*RMSE*	*Mean Percent Error (%)*
CalCOFI P	1.08	250.05
CalCOFI C	1.05	232.41
Morel 2	1.58	458.20
Morel 4	5.26	1249.07
OC1a	0.89	199.81
OC1b	0.87	198.79
OC1c	0.89	191.53
OC1d	0.77	153.68
OC2	0.74	142.99
OC2 v2	0.71	158.96
OC2c	0.78	187.75
OC2 v4	0.75	170.20
OC4 v4	0.81	174.06
OC3 M	0.72	155.66

Table 9. *Chl a estimated by published empirical algorithms versus Chl a measured in situ in Mayaguez Bay. These results comprise the subset of Rrs and Chl a measurements where the TSS where less than 5 mg/l.*

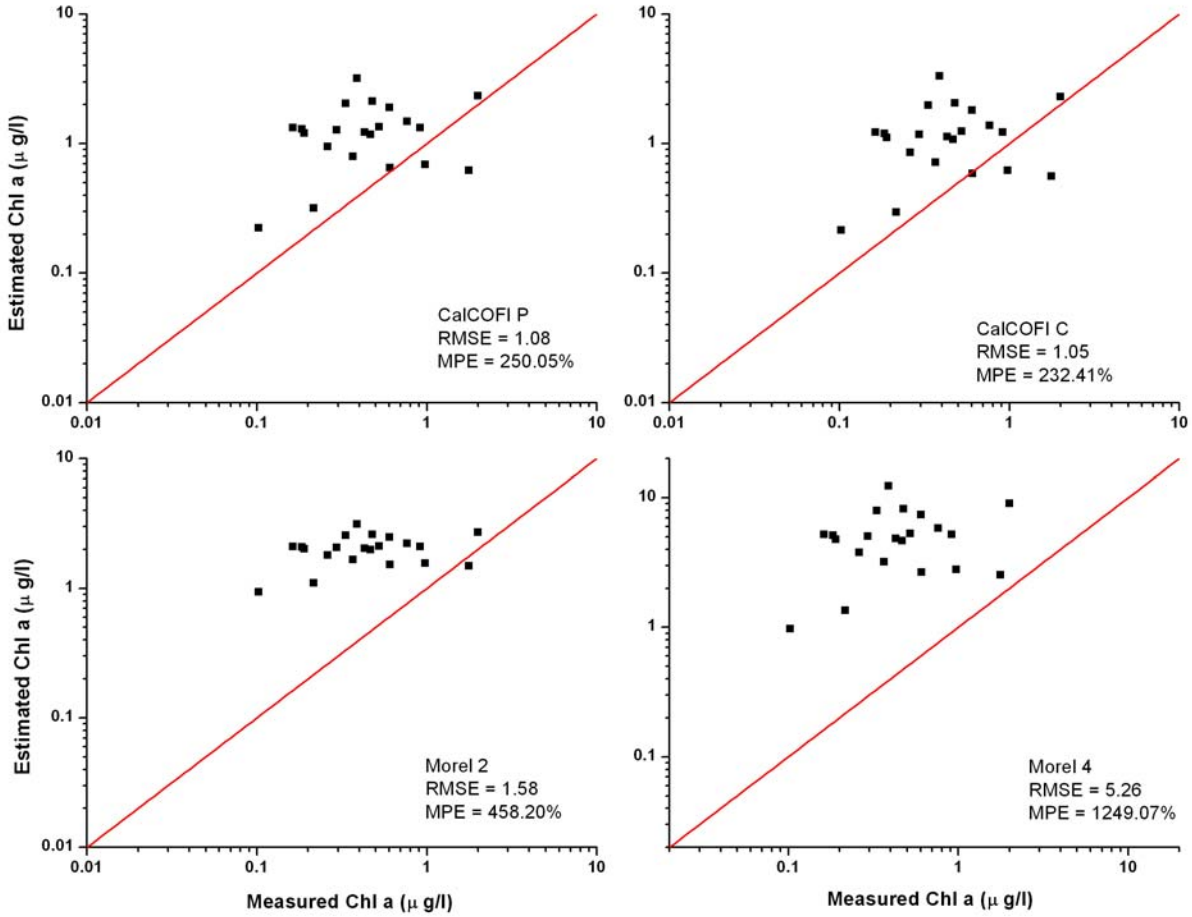

Figure 32. *Chl a estimated by CalCOFI P, CalCOFI C, Morel 2 and Morel 4 empirical algorithms versus measured Chl a for the data subset TSS < 5 mg/l (RMSE in* $\mu g\ l^{-1}$).

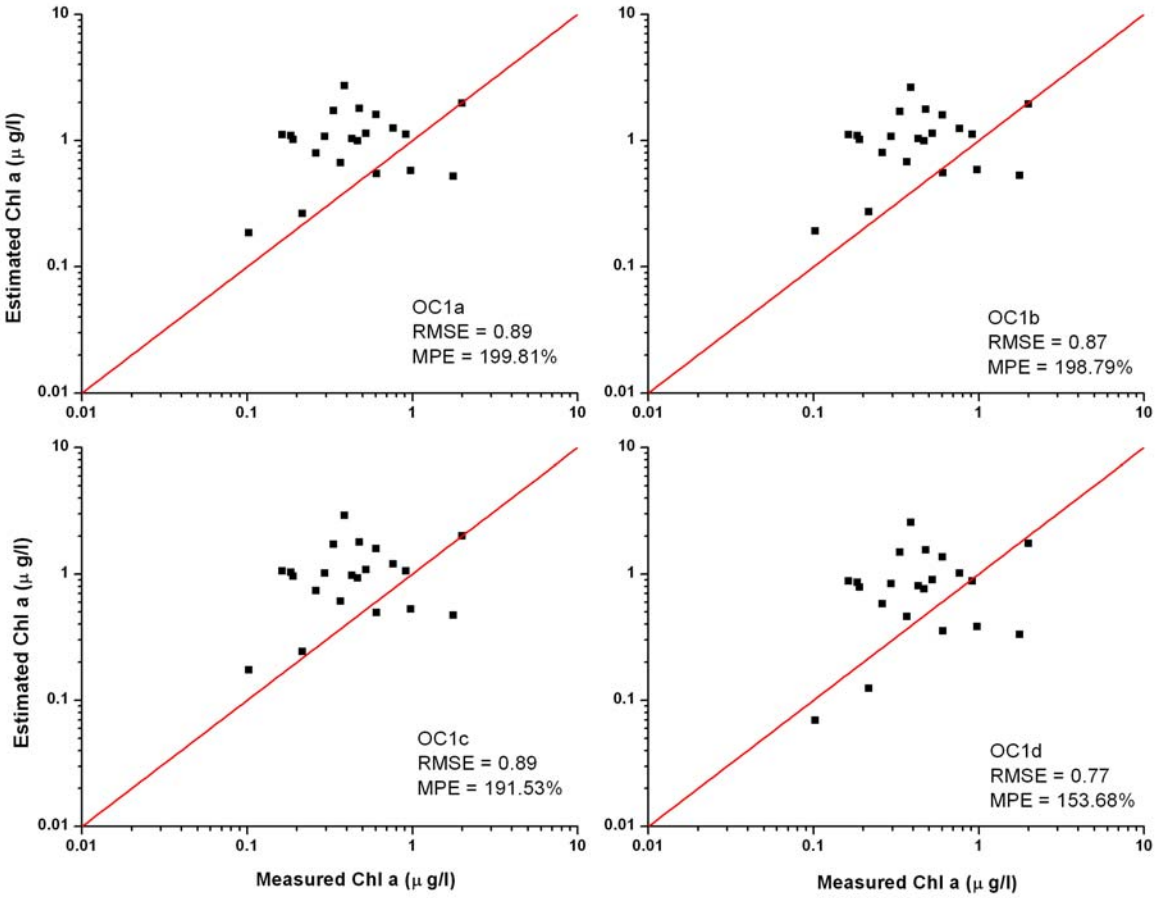

Figure 33. *Chl a estimated by OC1a, OC1b, OC1c and OC1d empirical algorithms versus measured Chl a for the data subset TSS < 5 mg/l (RMSE in* $\mu g\ l^{-1}$).

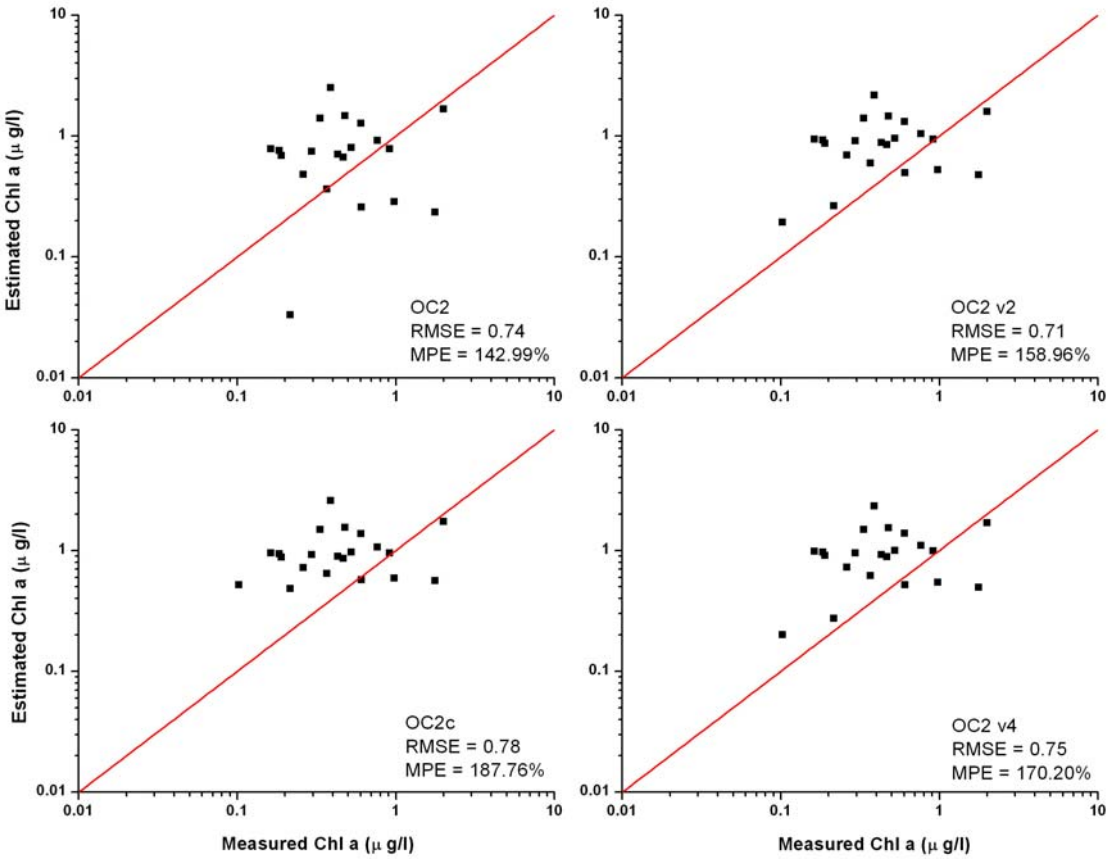

Figure 34. *Chl a estimated by OC2, OC2 v2, OC2c and OC2 v4 empirical algorithms versus measured Chl a for the data subset TSS < 5 mg/l (RMSE in* $\mu g\ l^{-1}$).

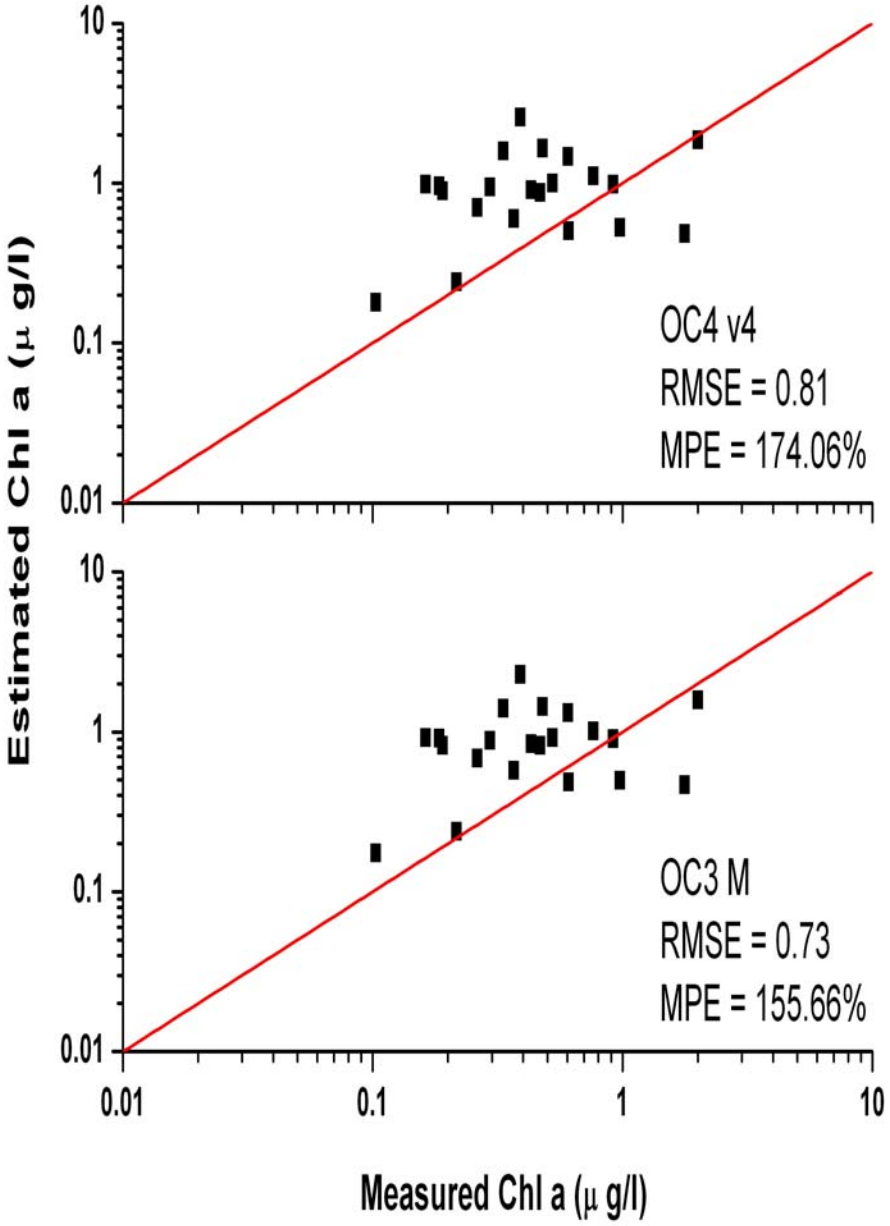

Figure 35. *Chl a estimated by OC4 v4, and OC3M empirical algorithms versus measured Chl a for the data subset TSS < 5 mg/l (RMSE in* μg l^{-1}).

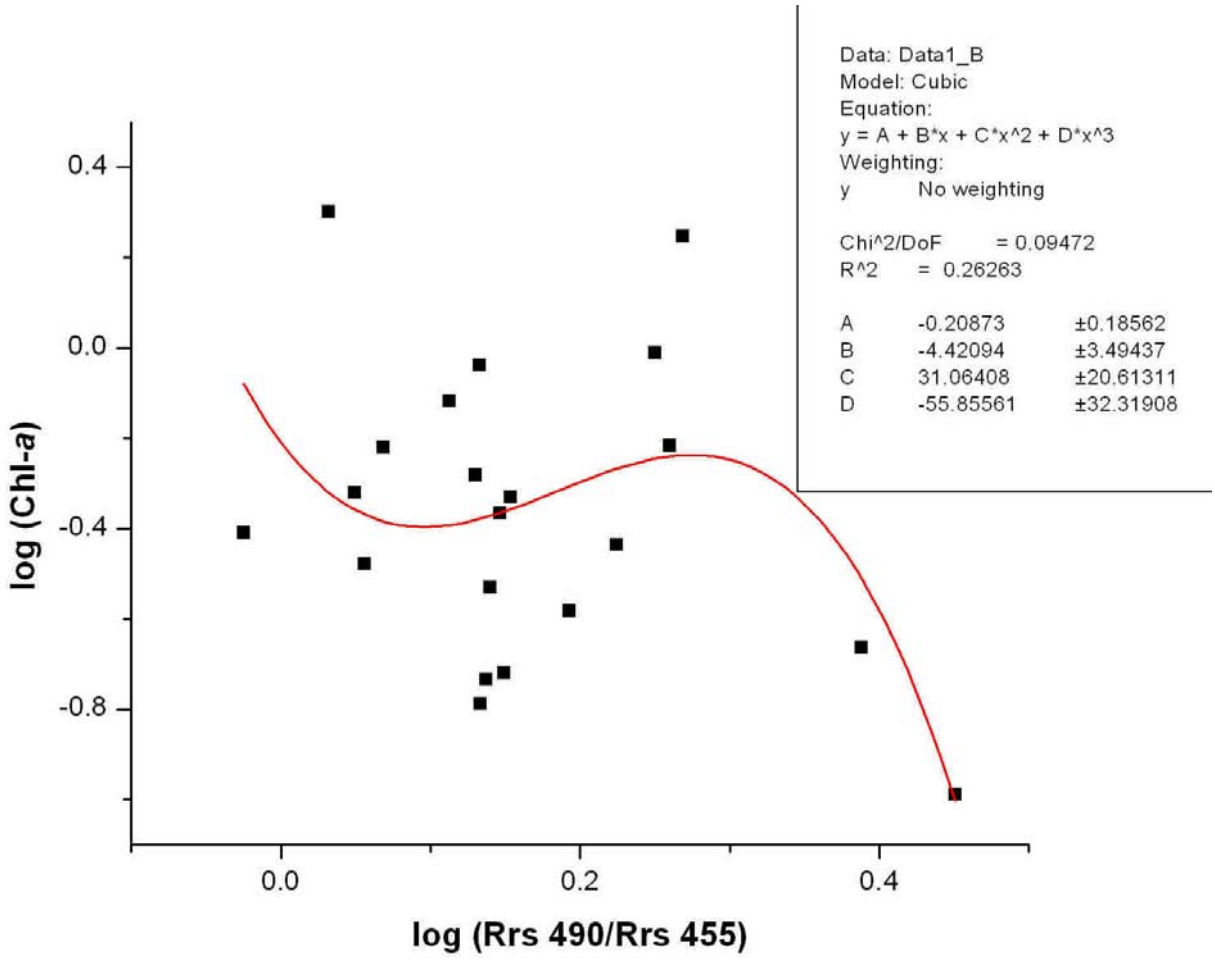

Figure 36. *Third order polynomial curve fitting of the log (Chl a) versus log (Rrs 490/Rrs 455). The regression equation is log(Chl a) = -0.20873 – 4.42094 log(Rrs 490/ Rrs 455) + 31.06408 log(Rrs 490/ Rrs 455)^2 – 55.85561 log(Rrs 490/ Rrs 455)^3.*

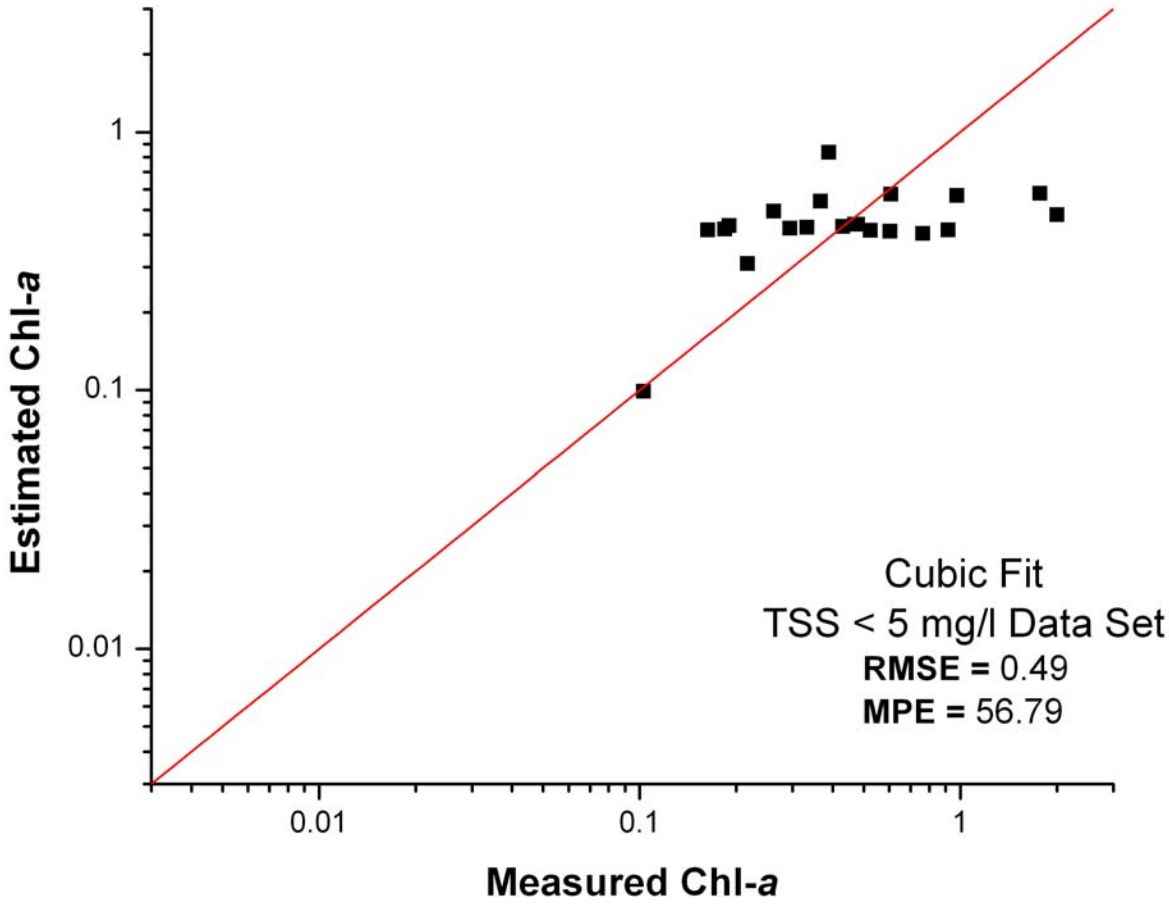

Figure 37. *Performance of the cubic fit algorithm developed with the TSS < 5 mg/l data set. Note that RMSE was reduced to 0.49* $\mu g\ l^{-1}$ *and MPE was reduced to 56.79% in comparison with the previously tested algorithms.*

The fourth order polynomial fit of log (Chl *a*) vs. log (Rrs 490/Rrs 555) resulted in an R^2 of 0.33 (Figure 38). This was an improvement over the cubic model but still considered a low R^2. The regression performance was slightly better. The RMSE was reduced to 0.46 µg l^{-1} and the MPE was reduced to 56.15% (Figure 39). A modified form of the fourth order polynomial is used by NASA in their latest empirical chlorophyll algorithms (e.g. OC3M).

The third approach for the development of an empirical algorithm for the estimation of Chl *a* in Mayagüez Bay was to use a Rrs 670/Rrs 680 ratio as suggested by Szekielda *et al*. (2003). In this case, a linear regression between log(Chl a) and log(Rrs 670/Rrs 680) was used. The R^2 for the regression had a value of 0.34 (Figure 40). This R^2 value is similar to that found for the fourth order polynomial algorithm. The performance of this algorithm is shown in Figure 41. Note that RMSE and MPE are slightly higher to those found with the fourth order polynomial algorithm.

The performance of the three algorithms developed were tested using an alternate set of Chl *a* and Rrs measurements collected in Mayaguez Bay from 2004 to 2006. This data set was limited to data where TSS concentration was less than 5 mg/l. The results are shown in Figure 42. Both the fourth order polynomial and the 670/680 red ratio algorithms performed better than the traditional blue/green ratio band algorithms tested (MPE of 79.00% and 120.15% respectively). The cubic algorithm overestimated Chl *a* by a vast margin (MPE = 8231.80%) for this data set.

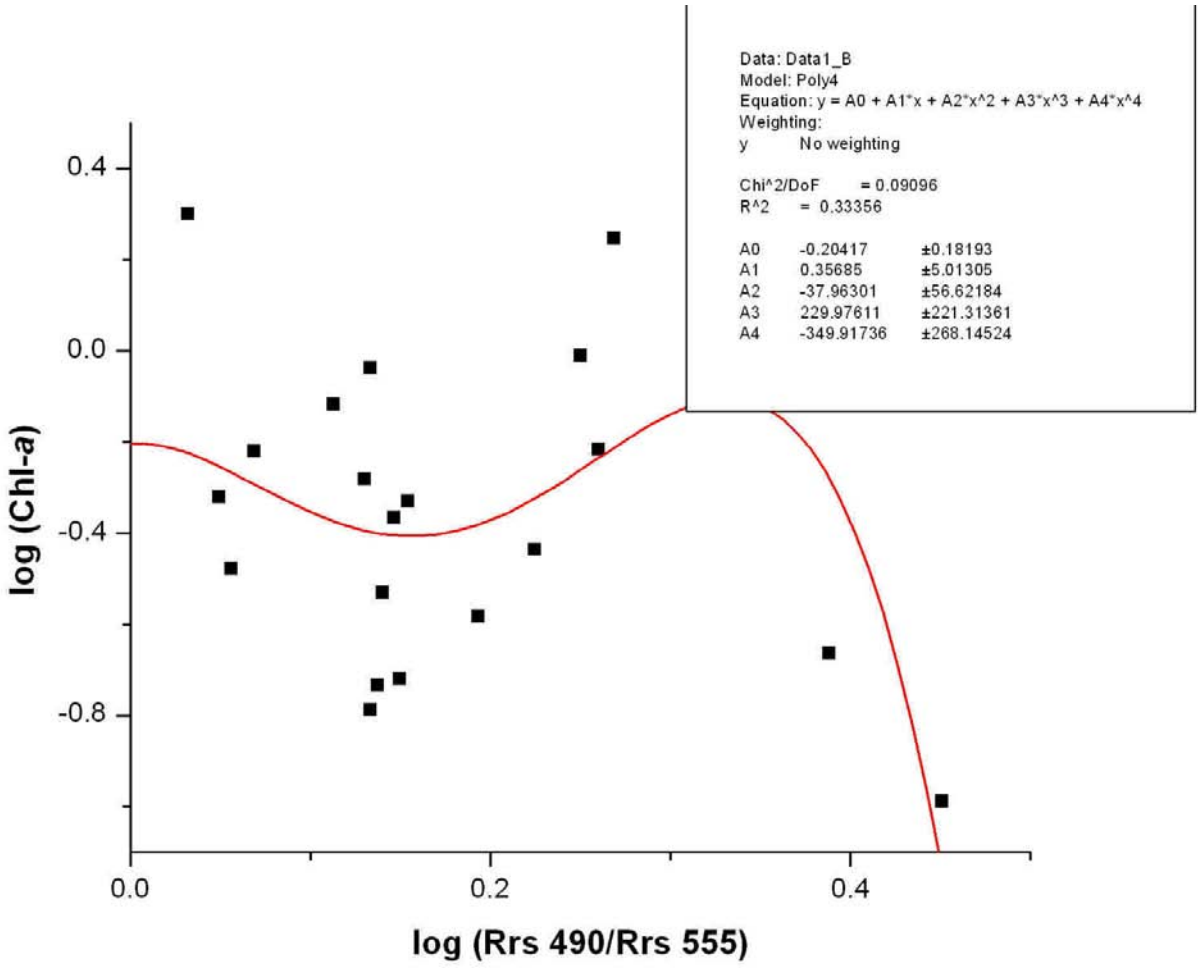

Figure 38. *Fourth order polynomial curve fitting of the log (Chl a) versus log (Rrs 490/Rrs 455). The regression equation is log(Chl a) = -0.20417 + 0.35685 log(Rrs 490/ Rrs 455) – 37.96301 log(Rrs 490/ Rrs 455)^2 + 229.97611 log(Rrs 490/ Rrs 455)^3 - 349.91736 log(Rrs 490/ Rrs 455)^4.*

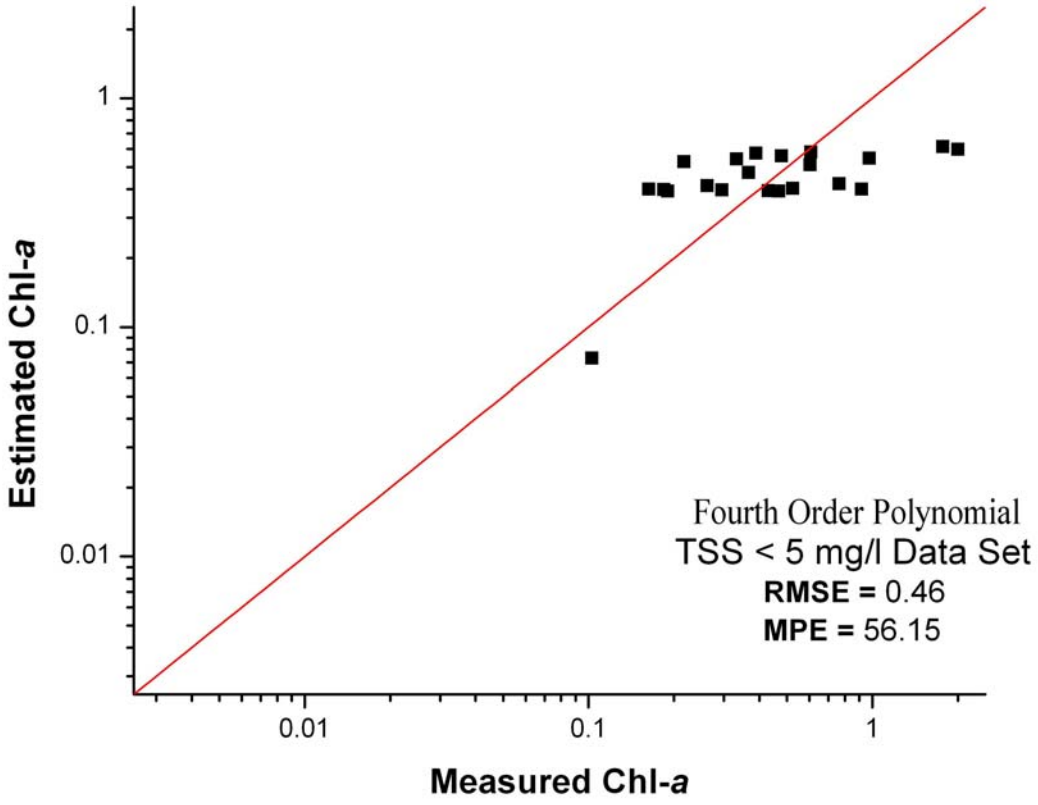

Figure 39. *Performance of the fourth order polynomial fit algorithm developed with the TSS < 5 mg/l data set. RMSE was reduced to 0.46* $\mu g\ l^{-1}$ *and MPE was reduced to 56.15% in comparison with the previously tested algorithms.*

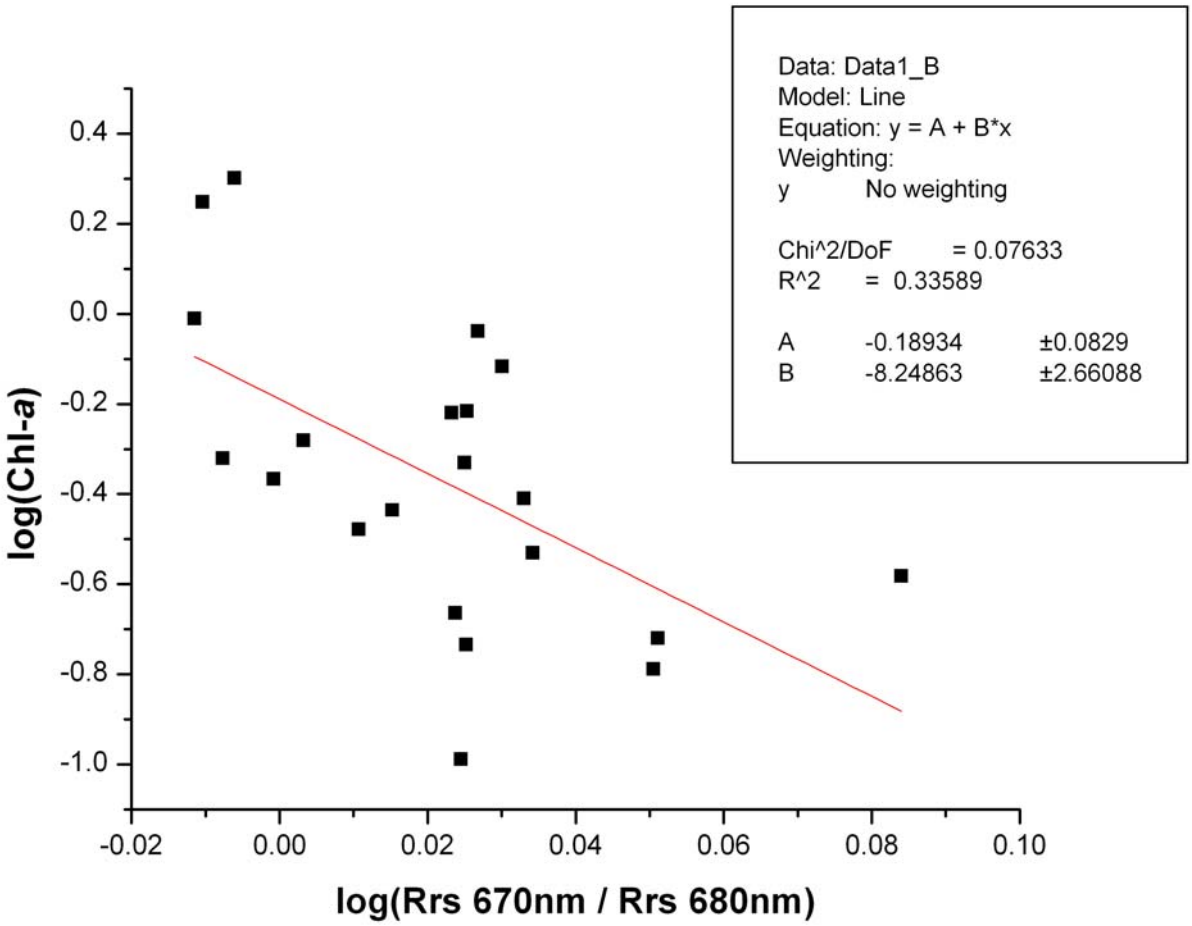

Figure 40. *Results of the linear regression between log(Chl a) and log(Rrs 670/Rrs 680). The regression equation was log(Chl a) = -0.18934 – 8.24863 log(Rrs 670/Rrs 680).*

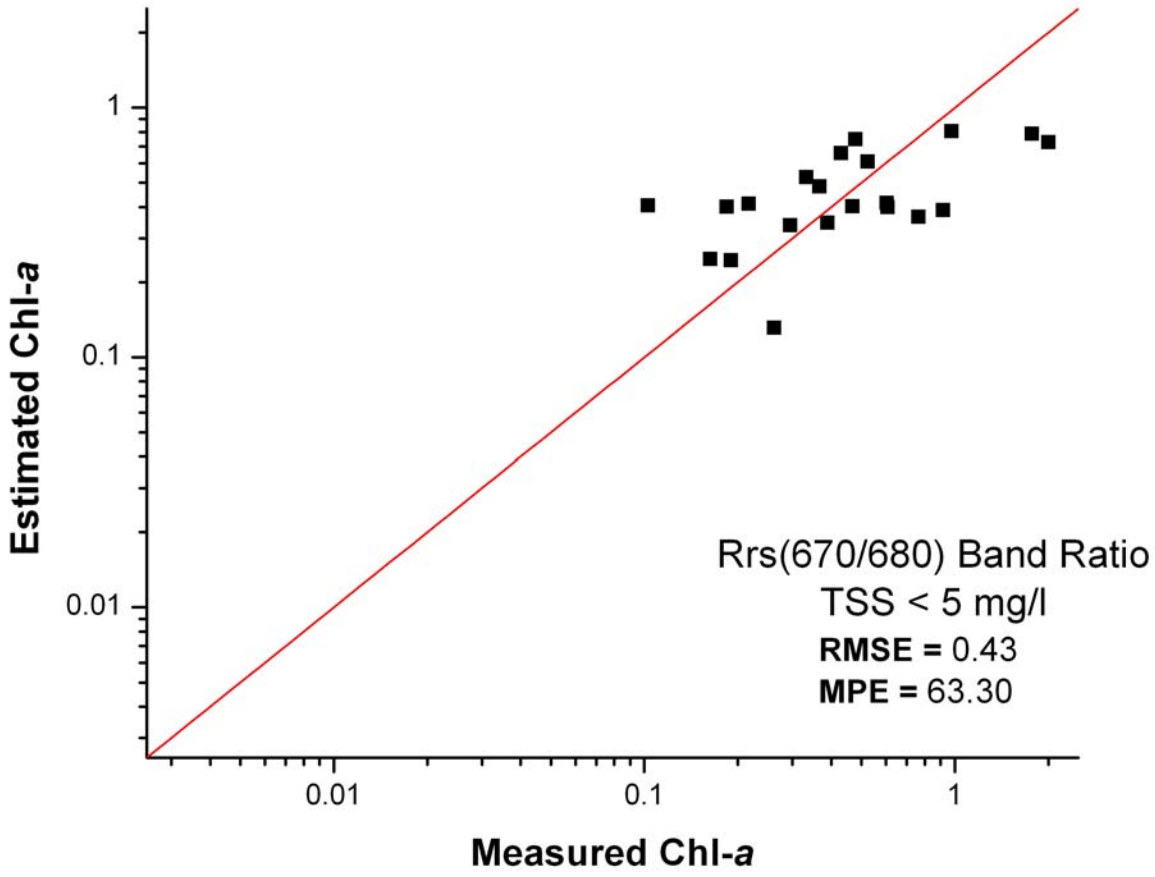

Figure 41. *Performance of the Rrs 670/Rrs 680 band ratio algorithm for the TSS < 5 mg/l data set. RMSE and MPE are slightly higher than that those obtained with the cubic and fourth order polynomial fits.*

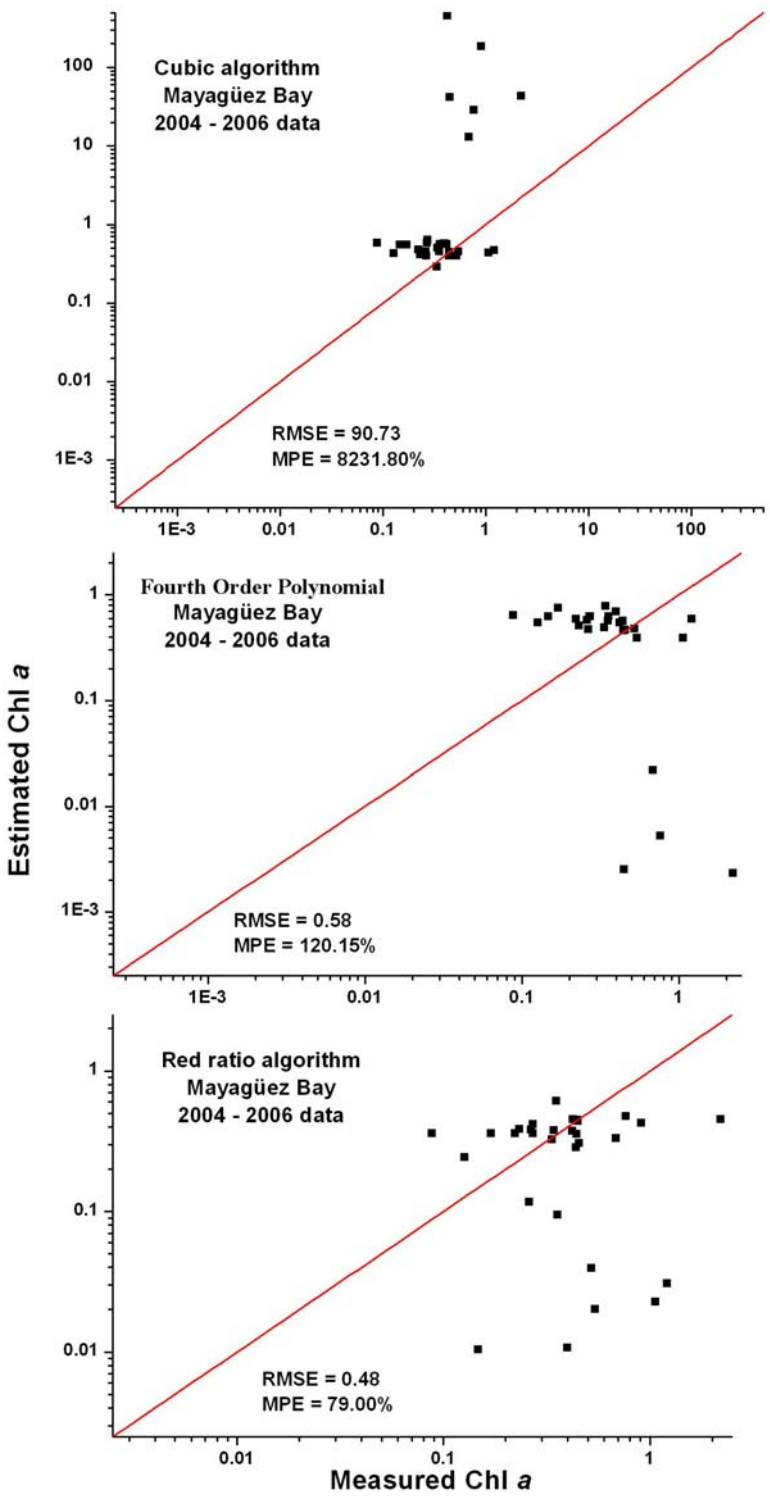

Figure 42. *Performance of the cubic, fourth order polynomial and 670/680 (red) ratio algorithms assessed with 2004-2006 Mayagüez Bay data (TSS<5mg/l). The red ratio algorithm performed best with this particular data set.*

Quasi-analytical algorithm

In order to optimize the quasi-analytical algorithm for implementation in Mayagüez Bay both the $a_{dg}(410/440)$ and the $a_{\varphi}(410/440)$ was calculated from the measured data. The results of the calculation of the $a_{dg}(410/440)$ for quasi-analytical algorithm (Lee *et al*., 2002) are shown in Figure 43. Data from July 1998 and October 1999 was used in the calculation (n = 17). The mean and 95% confidence intervals for the a_{dg} (410/440) were 1.30 ± 0.02. The mean spectral slope from 412 to 440 of the a_{dg} curves (S_{dg}) was found to be 8.90×10^{-3}. This value was used for the derivation of $a_{dg}(\lambda)$ from $a(\lambda)$.

The $a_{\varphi}(410/440)$ was calculated from data that spanned from June, 1997, to October, 1999 (n=57). The mean and 95% confidence intervals for the $a_{\varphi}(410/440)$ were 0.74 ± 0.04. Two distinct groups of points were identified from the plot. A group of 8 points, corresponding to the Acueductos and Manchas stations, had values around 0.40 while the rest of the data points were located around 0.80. Removing those data points from the analysis yields a mean of 0.80 ± 0.01. These results are shown in Figure 44.

Spectral particle backscattering coefficients [$b_{bp}(\lambda)$] obtained from the QAA are presented in Figure 45. The phase function and the magnitude of the $b_{bp}(\lambda)$ curves are in good agreement with those published in the literature (Bricaud *et al.*, 1981; Lee *et al*., 1996).

Spectral total absorption coefficients [$a(\lambda)$], produced by Lee's QAA for the TSS < 5 mg/l are shown in Figure 46. When compared with the examples of $a(\lambda)$ cuves presented in Figure 2 of Lee *et al.* (2002), the spectral shape agrees in the range of 400 to 600 nm. From 600 to 650 nm, a characteristic trough and noise is evident in the results derived from Mayagüez Bay Rrs spectra.

The combined detritus-CDOM spectral absorption [$a_{dg}(\lambda)$] curves derived from the QAA are in good agreement with those published by Lee *et al.* (2002). The curves showed the typical exponential shape and their values where within the expected for the bay (Figure 47).

The phytoplankton spectral absorption [$a_{\varphi}(\lambda)$] coefficients are shown in Figure 48. Note the absence of an absorption peak near 440 nm and the noise in the 600 to 700 nm region. The QAA derived $a_{\varphi}(\lambda)$ curves do not represent the typical curves measured from Mayagüez Bay from *in situ* samples (Rosado-Torres, 2001) and those reported in the literature (Kirk, 1994).

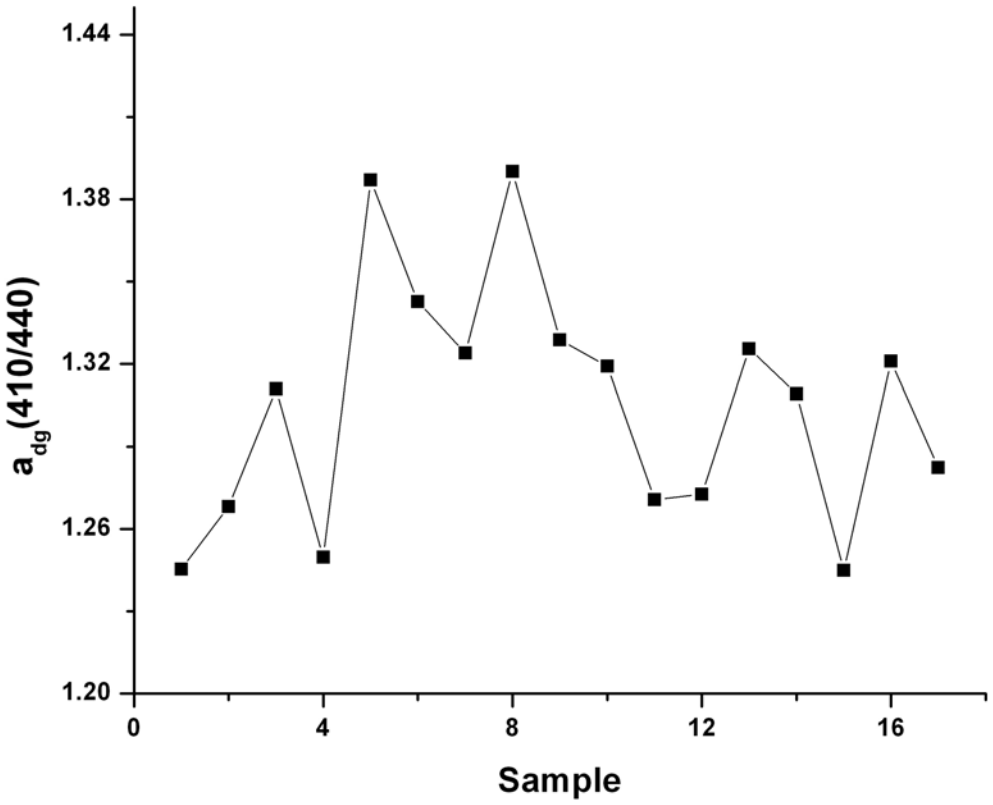

Figure 43. *Results of the a_{dg}(410/440) for the July 1998 and October 1999 data (n=17).*

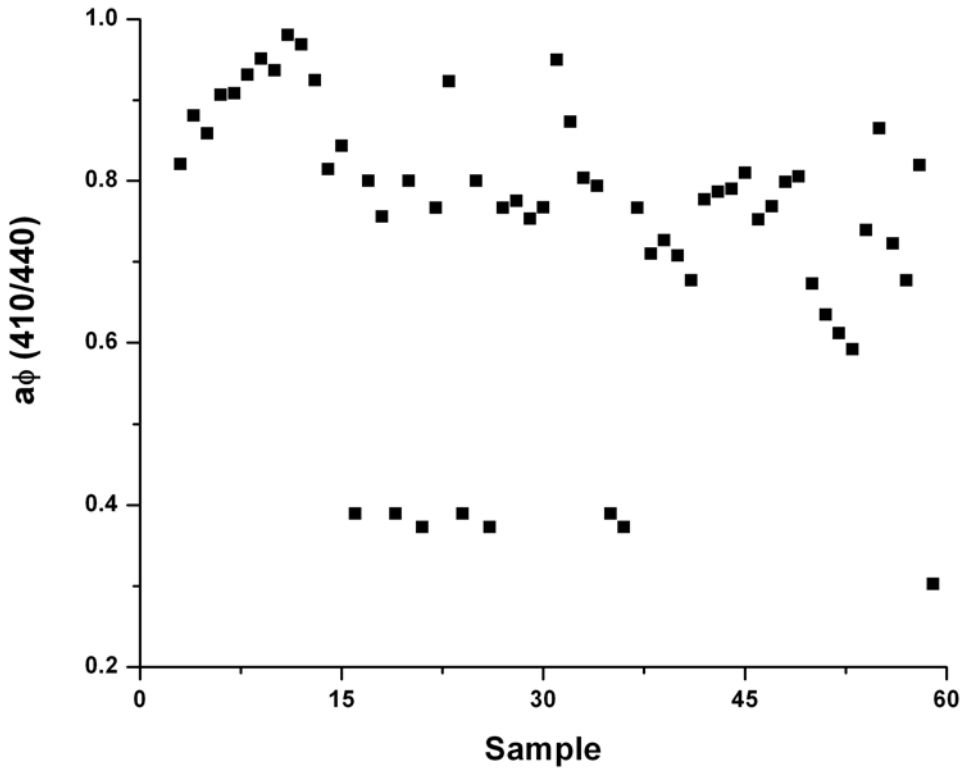

Figure 44. *Results for the $a_{\varphi}(410/440)$ calculations for Mayaguez Bay data from June, 1997 to October, 1998. Note that the data points form two distinct groups. The points with values around 0.40 are from Acueductos and Manchas stations.*

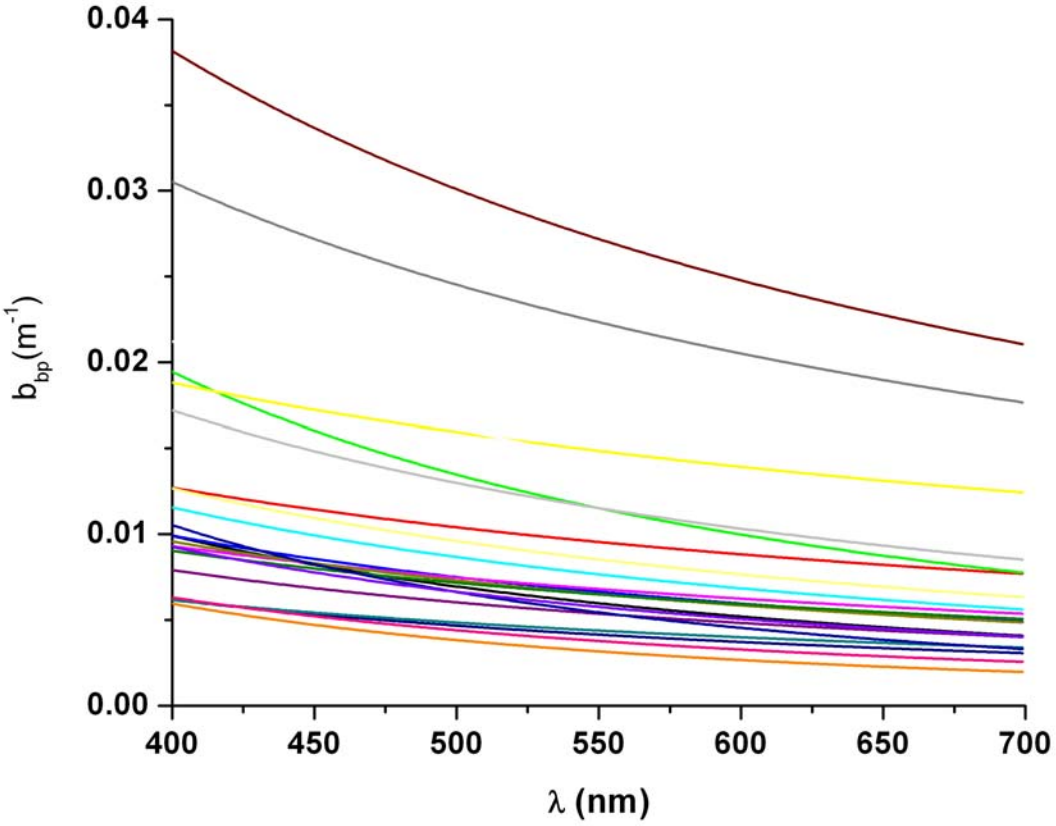

Figure 45. *Spectral particle backscattering coefficients [$b_{bp}(\lambda)$] obtained from the QAA for the TSS < 5 mg/l data set in Mayagüez Bay.*

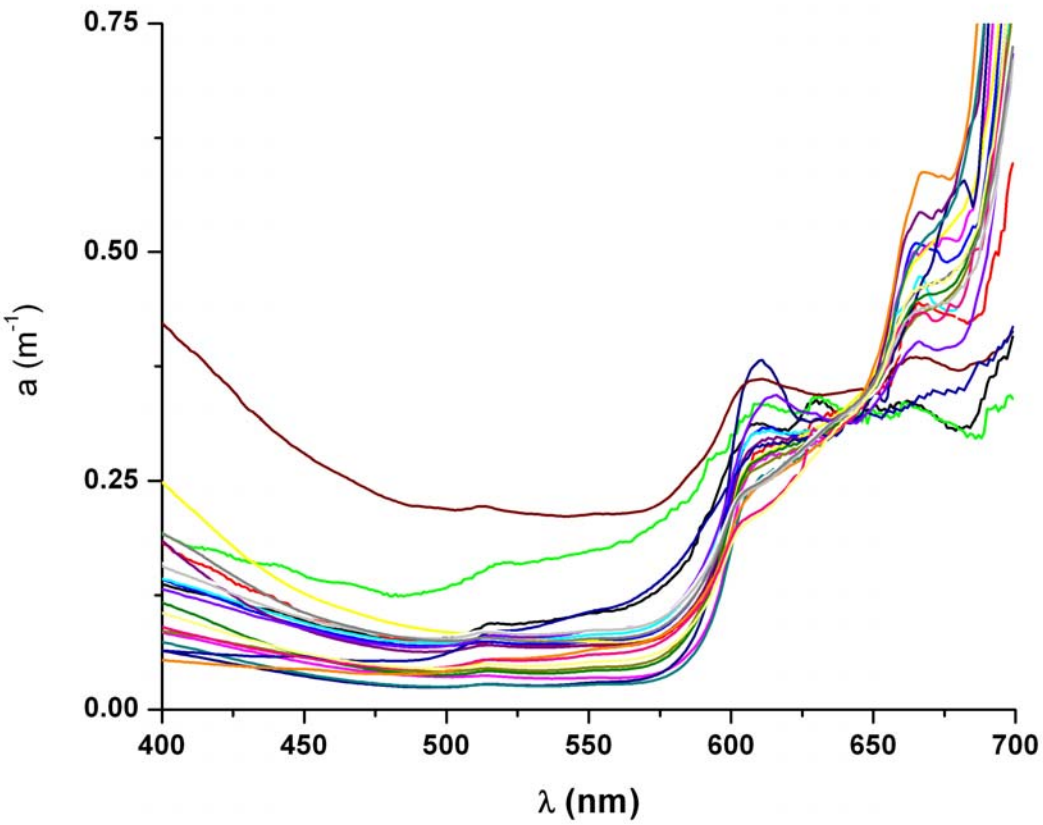

Figure 46. *Spectral total absorption coefficients [a(λ)], produced by Lee's QAA for the TSS < 5 mg/l data set in Mayagüez Bay. Note the noise apparent in the a(λ) curves from 600 to 700 nm.*

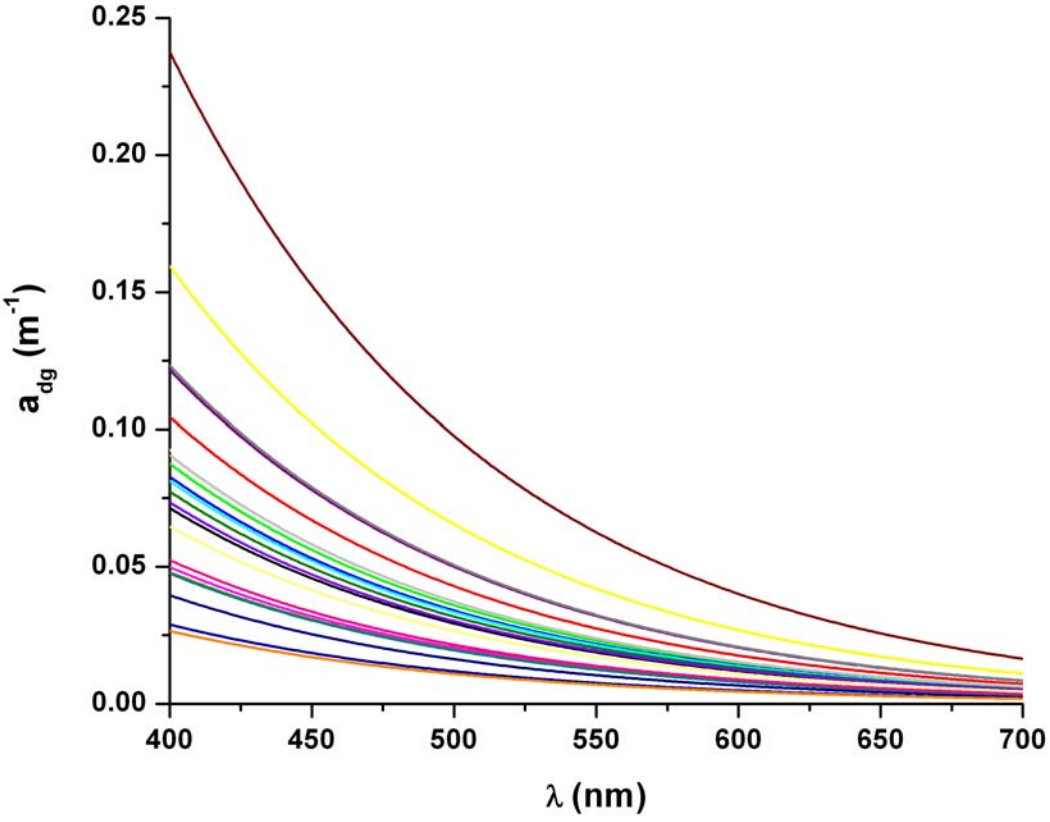

Figure 47. *Spectral combined detritus and CDOM absorption curves [$a_{dg}(\lambda)$] obtained from the QAA for the TSS < 5 mg/l data set in Mayagüez Bay.*

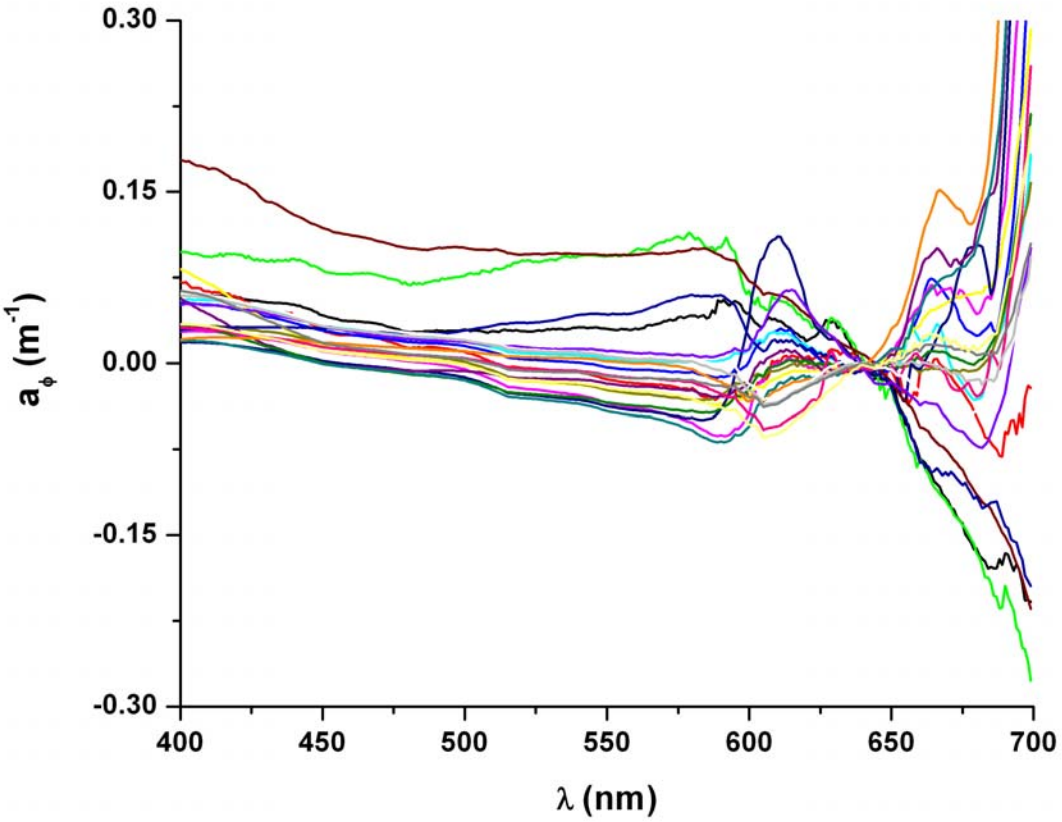

Figure 48. *Spectral phytoplankton absorption coefficients [a_φ (λ)] obtained from the QAA for the TSS < 5 mg/l data set in Mayagüez Bay.*

Due to the fact that all of the $a_\varphi(\lambda)$ curves derived from the QAA had abnormal spectral shapes and approximately half of $a_\varphi(675)$ values obtained were negative, Chl *a* values were not calculated. An attempt to calculate Chl *a* using some of the curves that had positive $a_\varphi(675)$ resulted in extremely high concentrations, well out of the range observed in Mayagüez Bay.

Discussion

Empirical algorithms

Algorithm performance in Mayagüez Bay is strongly affected by the spatial and temporal variability of bio-optical properties in the area (Rosado-Torres, 2000). The Mayagüez Bay data set includes both case 1 and case 2 stations and the seasonality of precipitation peaks in Western Puerto Rico makes it difficult to clearly distinguish among those groups through the year. Due to the strong variability in bio-optical parameters observed in the bay, it is almost certain that most ocean color algorithms tested in this work were developed in waters with less dispersion in the band ratios considered.

Mayagüez Bay is characterized by low Chl *a* concentrations and moderate to high TSS and CDOM concentrations. This is a worst case scenario for the remote estimation of Chl *a* since the signal is comparatively small in relation to the noise.

Of all the optically active constituents present in Mayagüez Bay, the inorganic suspended sediments seem to be the dominant optical parameter as suggested by the Hydrolight simulations. Mineral particles have been suggested to be the most significant optical component on energetic shelves and estuaries (Wosniak and Stramski, 2004; Bowers and Binding, 2006).

The effect of mineral particles on the Rrs curve can be relentless. Wosniak and Stramski (2004) reported that mineral concentrations in the order of 100 g m^{-3} modify the reflectance spectra in such manner that the standard remote sensing algorithms are rendered useless. Moreover, they found that even low and medium concentrations of the order of 0.1 g m^{-3} to 1 g m^{-3} should be considered a potential source of significant error in the chlorophyll estimation. For comparison, the mean TSS concentration measured in the bay in this study was 8.15 mg l^{-1} while the mean Chl *a* value was 0.65 µg l^{-1}. The dominance of inorganic mineral particles in the bio-optics of Mayagüez Bay is supported by the fact that the mean b_{bp} ratio calculated for both the rainy and dry season is ~ 0.025 (Rodríguez, unpublished data). Even in the offshore stations the b_{bp} ratio was found to be greater that 0.10. In phytoplankton dominated waters this ratio is in the range of 0.004 to 0.006 (Kirk, 1994).

This observation is supported by the fact that applying the empirical algorithms to the TSS < 5 mg/l decreased the mean percent error in half for most algorithms. It is well known that suspended particles and dissolved substances associated with river plumes have a strong influence in the reflectance ratios used for Chl *a* estimation (Ouillon and Petrenko, 2005). An

example of this phenomenon is that reflectance near the 550 nm band is used to quantify suspended particles in moderately turbid waters (Ahn *et al.*, 2001). This problem may be especially important in waters with high mineral and low Chl *a* concentrations such as Mayagüez Bay.

When the complete data set was considered, the empirical algorithms tended to overestimate Chl *a*. Similar findings has been reported in other coastal studies. Dareckia and Stramski (2004) reported a systematic and large overestimation of chlorophyll products for the MODIS and SeaWiFS algorithms for the coastal waters of the Baltic Sea.

It is important to note that the three regression curves fitted to the TSS < 5 mg/l data set resulted in an R^2 of approximately 0.30. The low R^2 suggest that about 70% of the variability between the Rrs ratios and Chl *a* values was unaccounted for. This result could be explained by the presence of optically active substances other than Chl *a* influencing the Rrs band ratios in Mayagüez Bay. For example, Wosniak and Stramski (2004) reported that a mineral concentration as low as 0.1 g m^{-3} has the potential of causing overestimation of 100% in waters with Chl *a* concentration of 0.5 mg m^{-3} or less.

Of the three algorithms developed in this study, the red ratio algorithm [Rrs (670/680)] produced the lowest MPE values (79.0 %) when challenged with a new data set. The magnitude of this error is still considerable but when compared with the values obtained with the published algorithms considered in this work (142.99 to 1249.07 % error), it shows a vast improvement in performance. Taking into account that the largest errors in Chl *a* prediction are found in waters where Chl *a* concentration values are below 10 mg m^{-3} (Dall'Olmo and Gitelson, 2005) and that mineral particles are still a source of error even in concentrations below 5 mg l^{-1}, the red ratio approach is worth investigating in more detail.

In order to implement these bio-optical algorithms, the data set must be limited to water parcels with low concentrations of suspended minerals. Minerals, especially the red clays found in Mayagüez Bay, are highly efficient scattering red light (Wosniak and Stramski, 2004), thus negatively affecting Rrs band ratios in the red part of the visible spectrum. Based on the results obtained in this work, it is strongly suggested to study in detail the absorption and scattering properties of mineral particles found in Mayagüez Bay. Only by a meticulous analysis of the optical properties and their variability will be possible to use optical algorithms for an accurate estimation of Chl *a*.

Quasi-analytical algorithm

Semi-analytical algorithms can be applied to a variety of water types and generally offer much better retrieval accuracy than empirical algorithms (Lee *et al.*, 2002). However, their performance is dependent on accurate spectral models of each optical constituent present in the water (Lee *et al.*, 2002). This implies that semi-analytical algorithms perform better in water types with bio-optical properties similar to the data set used for their development. D'Sa *et al*. (2006) suggested the complexity of using semi-analytical algorithms in river-dominated coastal waters due to short term and seasonal variability in the bio-optical properties. It has been reported that semi-analytical algorithms do not perform adequately in some coastal waters (Chang *et al.*, 2006). Their poor performance has been attributed primarily to inadequacy in modeling the spectral shape of the IOPs in complex turbid environments.

Lee *et al*. (2002) suggested that in order to improve the QAA performance a fine tuning with regional parameters must be done. In the case of Mayagüez Bay, the QAA did not perform satisfactorily even after the $a_{dg}(410/440)$, the $a_{\varphi}(410/440)$ and the S_{dg} where optimized with *in situ* data. This fact implies that in its present form, the model itself may be inadequate for retrieving the IOPs of Mayagüez Bay.

It is recommended in Lee *et al*. (2002) to shift the reference wavelength to longer wavelengths (from 550 nm to 640 nm) near river plumes. The reason for the shift in reference wavelength is because pure water absorption is still dominant at longer wavelengths. However, red clays scatter light very efficiently at those wavelengths and possibly dominate the $Rrs(\lambda)$ at longer wavelengths in water bodies with high concentrations of these minerals (Wosniak and Stramski, 2004). Indirect evidence of this happening in Mayagüez Bay is apparent by studying both the measured and modeled $Rrs(\lambda)$ from the bay. Although in most waters Rrs values approach zero near the red/near infrared portion of the spectrum (Kirk, 1994), in Mayagüez Bay the corrected Rrs curves are seldom near zero at these wavelengths.

A case study may be used to better understand the performance of the QAA in Mayagüez Bay. A sample from Rodríguez station taken in July 1998 cruise to Mayagüez Bay was used for this purpose. Figure 49 presents the $a(\lambda)$ curves obtained with the QAA for Rodríguez station using the two different reference wavelengths (555 and 640 nm) described in Lee *et al.* (2002). Note that the spectral shape of both curves was identical. This exercise was repeated with the rest

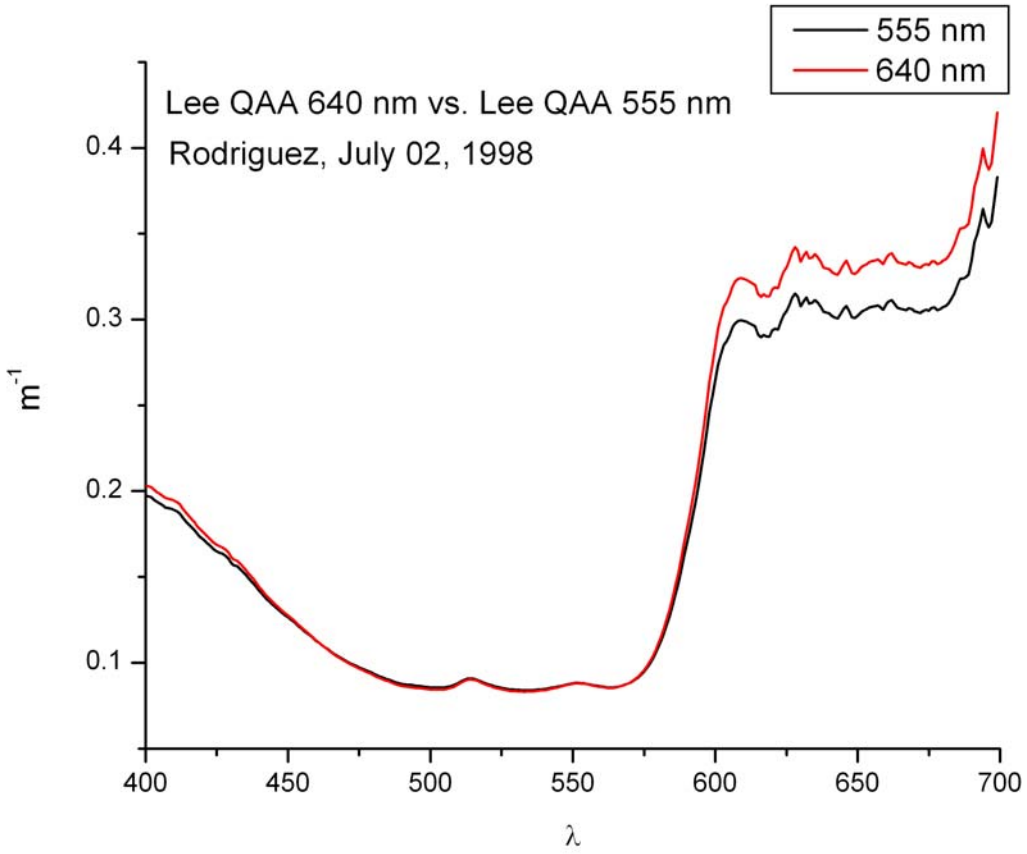

Figure 49. *Spectral total absorption curves for Rodríguez station (July, 1998) obtained with the QAA using two different reference wavelengths (555 and 640 nm) as described in Lee et al. (2002). Note that the spectral shape of both curves is identical.*

of the samples in the TSS < 5 mg l^{-1} data set with similar results. The modifications to the QAA suggested in Lee *et al.* (2007) were also tested but the results were still very similar.
The abnormal shape and noise in the QAA derived a(λ) observed in the red part of the spectrum was a typical finding in the data set studied. The presence of these features in the QAA derived a(λ) curves suggests that the Rrs(λ) is been affected by a reflecting component in the 600 to 650 nm spectral range. This spectral range agrees with the inorganic sediment peak in reflectance found by Gin *et al*. (2003). Since the $a_{dg}(\lambda)$ and the aφ(λ) are derived from a(λ), it was expected that the modeling error would be transferred to these curves. The QAA derived $a_{dg}(\lambda)$ overestimates the measured $a_{dg}(\lambda)$ about 50% at 412 nm (Figure 50).

The aφ(λ) derived from the QAA overestimated absorption near the blue and produced an abnormal curve with a displaced absorption peak in the red and negative values near 550 nm and from 640 nm toward the red end of the visible spectrum when compared to the aφ(λ) measured *in situ* (Figure 51). Since the aφ(675) value was negative, Chl *a* could not be retrieved.

The main reason for the poor performance of the QAA algorithm in Mayagüez Bay appears to be its failure in modeling the $b_{bp}(\lambda)$ curve. This step is of first order of importance in the derivation of the optical properties from the QAA (Lee *et al.*, 2002). When the derived b_{bp} (λ) curves are compared with measured b_{bp} (λ) curves, a large discrepancy in spectral shape is noted (Figure 52). The characteristic phase function of the $b_{bp}(\lambda)$ measured in Mayagüez Bay is very similar to those reported by other investigators (Whitmire, 2008). Since the a(λ) is function of the $b_{bp}(\lambda)$ it is crucial to accurately model the $b_{bp}(\lambda)$ phase function before attempting to retrieve total absorption from the Rrs curve using the QAA.

Although semi-analytical algorithms offer an improvement over empirical algorithms in determining biogeochemical quantities in many waters, there are still some problems associated with their implementation. Defoin-Platel and Chami (2007) pointed out that the major difficulty related to the inversion of ocean color was the non uniqueness or ambiguity of the problem. These investigators argued that most semi-analytical algorithms are based on the following relationship:

$$Rrs = b_b / a$$

where b_b is the total backscattering coefficient and a is the total absorption coefficient. Because of the mathematical nature of the relationship, many different combinations of b_b and a could theoretically produce similar Rrs values. They found a rate of ambiguity of around 90% for

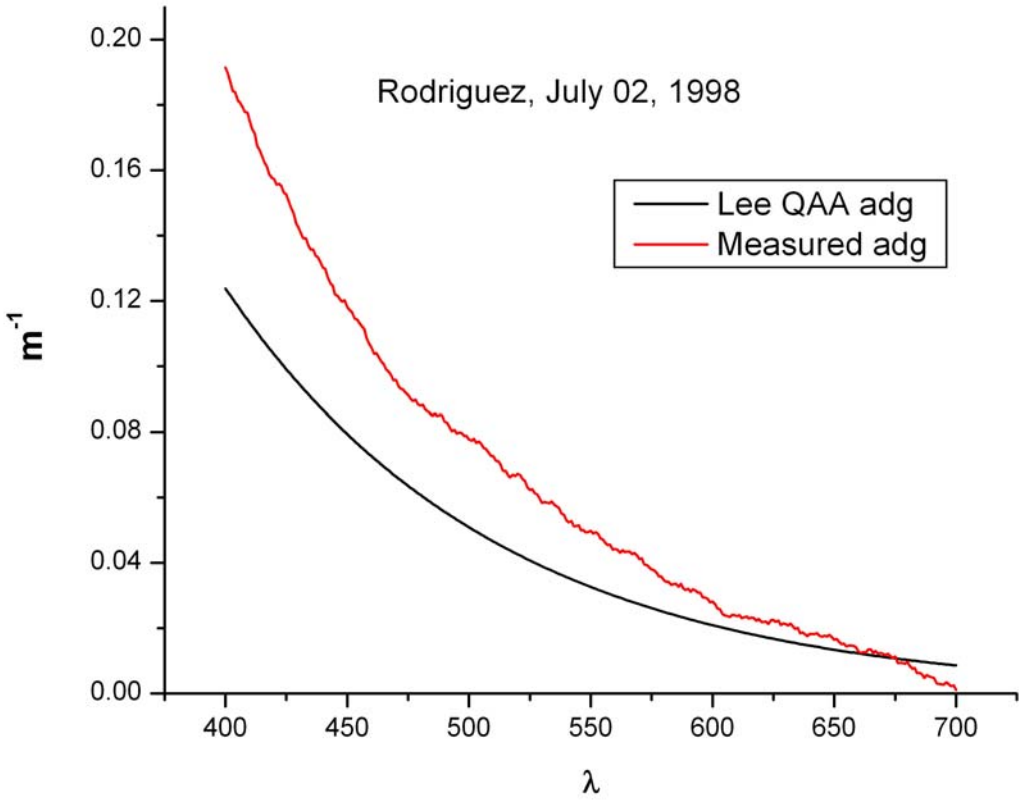

Figure 50. *Comparison of spectral a_{dg} curves derived from the QAA (Lee et al., 2002) and measured in situ for Rodríguez station in July, 1998.*

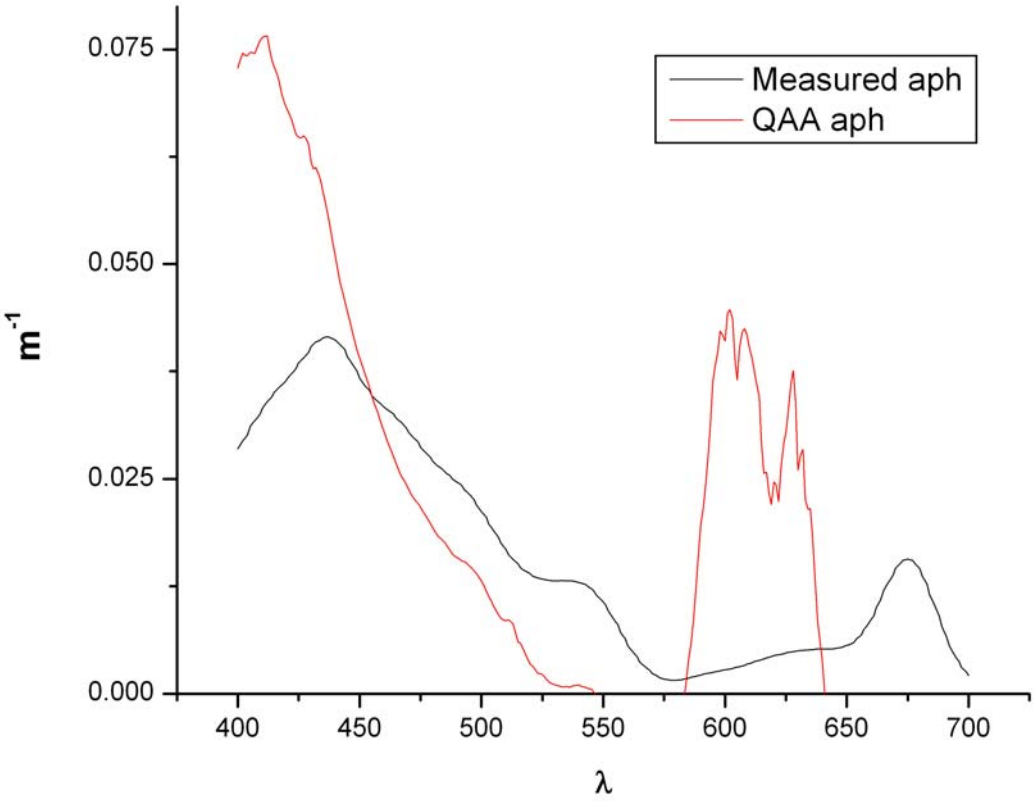

Figure 51. *Comparison of spectral a_{φ} curves derived from the QAA (Lee et al., 2002) and measured in situ for Rodríguez station in July, 1998.*

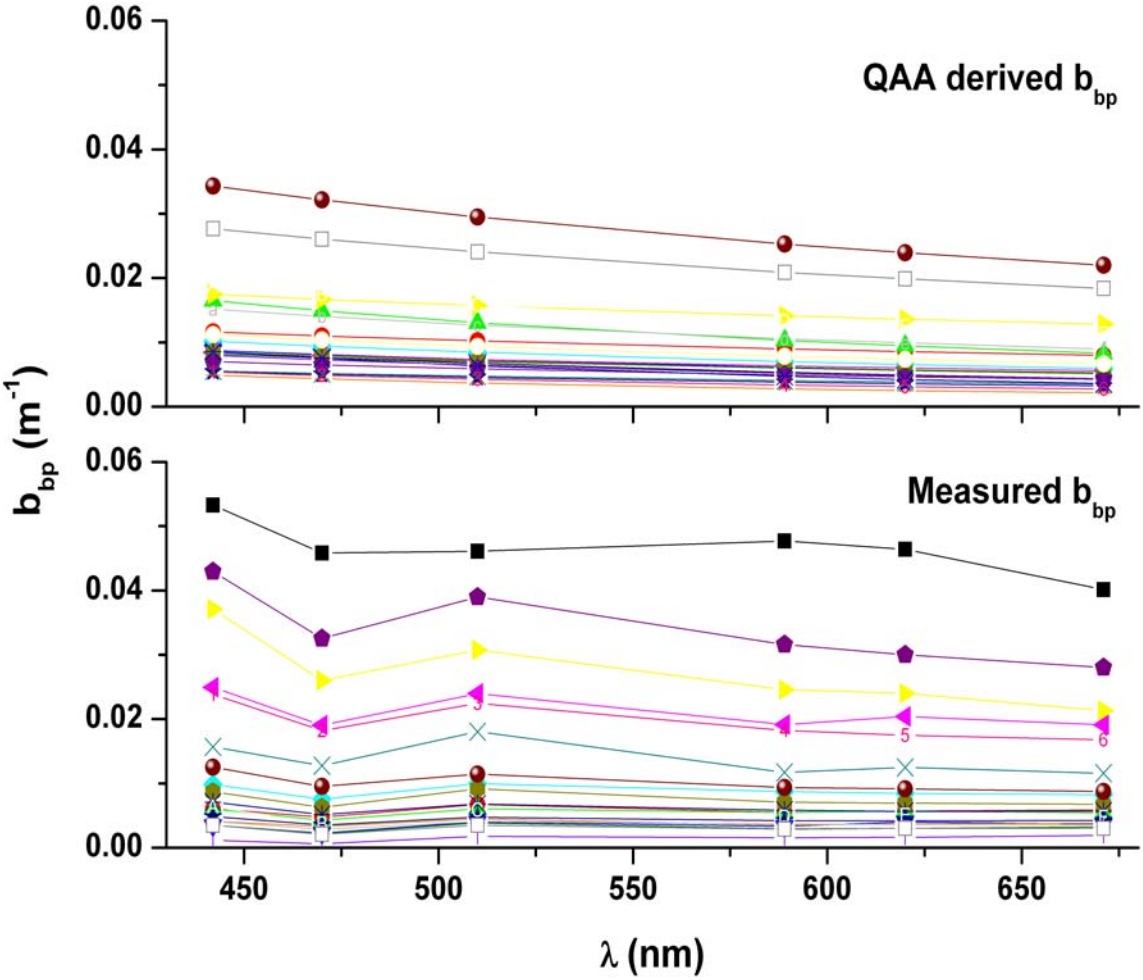

Figure 52. *A comparison of $b_{bp}(\lambda)$ curves measured in Mayagüez Bay in August, 2002 with $b_{bp}(\lambda)$ curves derived from the QAA (Lee et al., 2002).*

simulated coastal data. Furthermore, they found that the error in the estimation of total absorption was highest when reflectance in the blue was weak. This is typically the case in case-2 waters. The semi-analytical algorithms are based on three important assumptions (Wang *et al.*, 2005). First, the relationship between Rrs, b_b and a is known. Second, the absorption and backscattering coefficients are known. Third, the spectral shapes of the absorption and backscattering coefficients are known. Of these three assumptions, the third is the more critical in terms of applicability of a semi-analytical model to regional waters. It appears that the assumptions of the QAA do not hold in waters with high concentration of inorganic particles and low Chl *a* concentrations such as Mayagüez Bay. Lumping inorganic minerals with CDOM and detritus as a single optical constituent may not necessarily be correct as these parameters have different optical properties (Wosniak and Stramski, 2004).

It is necessary to better understand the importance of mineral particles in the bio-optics of Mayagüez Bay in order to perform the inversion of IOPs from Rrs accurately. Inversion algorithms, as the empirical algorithms, ultimately depend on the signal (phytoplankton) to noise (all the other optical components) ratio present in the Rrs curve.

CONCLUSION

The underlying causes of the optical variability observed in Mayagüez Bay are thought to be: a) the coastal nature of the area, b) the abundance of rivers and smaller water bodies discharging into the bay, c) the industrialized and agricultural nature of Mayagüez city, and d) the seasonal changes in precipitation and wave action observed in the region. This work provides direct and indirect evidence supporting the variable bio-optical nature of the bay and confirms the bio-optical complexity of Mayagüez Bay reported in previous works.

Mayagüez Bay appears to be relatively stable in terms of phytoplankton dynamics. The fourth derivative analyses of $a_\varphi^*(\lambda)$ spectra suggest that diatoms are the dominant group in the local waters. This information is not only relevant from an ecological viewpoint, but must be taken into account when selecting Rrs bands for the retrieval of ocean color products. Another important finding was indirect evidence of the presence of photosynthetic pigments signatures in the $a_d(\lambda)$ spectra. Since the hot methanol extraction method is used for *in situ* measurement of Chl *a* concentration, this finding suggests an important source of error that should be investigated in more detail.

Despite our best efforts, remote sensing of chlorophyll *a* remains a challenging endeavor in Mayagüez Bay. Hydrolight simulations suggest that inorganic suspended sediments play a very important role in defining the bio-optics of Mayagüez Bay. An important contribution of this work is suggesting the notion of a preliminary mineral threshold value in Mayagüez Bay over which the Chl *a* concentration cannot be estimated from the Rrs curve. The chemical nature, optical properties, spatial and temporal variability of mineral particles needs to be studied in order to ascertain a more precise threshold value.

The standard ocean color algorithms evaluated in this work performed poorly in Mayagüez Bay. Empirical algorithms tend to overestimate Chl *a* concentration, especially in stations with higher suspended sediment values. The QAA derivation of the IOPs was inadequate also, failing to model the spectral shape of $b_{bp}(\lambda)$ and $a(\lambda)$. This is not to say that the QAA is not capable of Chl *a* estimation in the coastal waters of Mayagüez, but it points out the fact that the local bio-optical relationships must be studied in more detail and the development of a regional version of the QAA is needed.

Limiting the application of ocean color algorithms to waters with mineral concentrations under the suggested threshold value is an essential element of any strategy for the remote sensing

of Chl *a* in Mayagüez Bay and similar environments. The development of regional algorithms, fine tuning of existing algorithms designed for coastal waters and the use of novel algorithms are all recommended for minimizing error in remotely sensed Chl *a* estimates.

Two approaches are suggested for future studies attempting to quantify Chl *a* concentration using remote sensing reflectance. Both of these strategies rely on the use of Hydrolight as a research tool. The first approach is to create an extensive lookup table with a Hydrolight generated Rrs database using field measurements collected in Mayagüez Bay. The data must be collected keeping in mind the requirements of Hydrolight in order to minimize the use of models when defining the optical characteristics of each optically active constituent. The data set must include above surface Rrs measurements, in water radiometric data, chlorophyll mass specific absorption and scattering coefficients, chlorophyll bearing particles scattering phase functions, chlorophyll concentration profiles, CDOM concentration profiles, mineral concentration profiles and minerals mass specific absorption and scattering data. Other ancillary data should be collected as needed. The above surface Rrs database generated by Hydrolight could then be used for the construction of a lookup table. The concept is that by measuring some carefully selected bands, CDOM absorption and chlorophyll and mineral concentrations can be retrieved.

The second approach is to use Hydrolight to create a large ($n > 1000$) synthetic data set that could be used for the design and training of artificial neural networks. The neural network algorithms are capable of modeling complex non linear relationships more precisely than the standard algorithms used for ocean color remote sensing. Because neural networks are sensitive to noise not encountered during their training, the variability of the extensive data set described above should be examined and incorporated into the database.

This hypothesis that minerals dominate the Rrs signal when present in high enough concentration should be tested. If experimental data support the hypothesis, a threshold concentration must be established. If mineral concentrations are known precisely, it is possible to apply masks to remote sensing data when the noise produced by mineral particles makes the retrieval of the chlorophyll signal difficult. From the remote sensing viewpoint this could be accomplished by applying an algorithm capable of accurately estimating mineral concentrations before applying the Chl *a* algorithms to the reflectance data. Once the relationship between TSS and inorganic suspended sediments for Mayagüez Bay is known, one of the various TSS

algorithms being developed at the Geological and Environmental Remote Sensing Laboratory at UPR-Mayagüez could be used for such purpose.

LITERATURE CITED

Adhikari, C., A. Proctor and G. D. Blyholder (1997). "An Infrared Spectroscopy Study of Lipid Adsorption from Hexane onto an Acid-Activated Bleaching Clay." Journal Americal Oil Chemists' Society **74**(10): 1265 - 1268.

Aguirre-Goméz, R., A. R. Weeks and S. R. Boxall (2001). "The identification of phytoplankton pigments from absorption spectra." International Journal of Remote Sensing **22**(2 & 3): 315 - 338.

Ahn, Y.-H. (1990). Proprietes optiques des particules biologiques et minerales presentes dans l'ocean; Application: Inversion de la reflectance [Optical properties of biogenous and numerical particles in the ocean : application: inversion of reflectance]. Universite Pierre et Marie Curie. Ph.D. Thesis. 214p.

Ahn, Y. H., J. E. Moon and S. Gallegos (2001). "Development of Suspended Particulate Matter Algorithms for Ocean Color Remote Sensing." Korean Journal of Remote Sensing **17**(4): 285 - 295.

Albert, A. and C. D. Mobley (2003). "An analytical model for subsurface irradiance and remote sensing reflectance in deep and shallow case-2 waters." Optics Express **11**(22): 2873 - 2890.

Alfaro, M. (2002). Oceanographic features and zooplankton community structure at Mayagüez Bay, Puerto Rico. University of Puerto Rico at Mayagüez. Department of Marine Sciences. Ph. D. Thesis. 151p.

Ansotegui, A., J. M. Trigueros and E. Orive (2001). "The use of pigment signatures to assess phytoplankton assemblage structure in estuarine waters." Estuarine, Coastal and Shelf Science **52**: 689 – 703.

Babin, M. and D. Stramski (2004). "Variations in the mass-specific absorption coefficient of mineral particles suspended in water." Limnology and Oceanography **49**(3): 756 - 767.

Bigidare, R. R., J. H. Morrow and D. A. Kiefer (1989). "Derivative analysis of spectral absorption by photosynthetic pigments in the western Sargasso Sea." Journal of Marine Research **47**: 323 - 341.

Bowers, D. G. and C. E. Binding (2006). "The optical properties of mineral suspended particles: a review and synthesis." Estuarine, Coastal and Shelf Science **67**(2006): 219 - 230.

Bowers, D. G., D. Evans, D. N. Thomas, K. Ellis and P. J. le B. Williams (2004). "Interpreting the colour of an estuary." Estuarine, Coastal and Shelf Science **59**(2004): 13 - 20.

Bricaud, A., A. Morel and L. Prieur (1981). "Absorption by dissolved organic matter of the sea (yellow substance) in UV and visible domains." Limnology and Oceanography **26**: 43 - 53.

Bricaud, A. and D. Stramski (1990). "Spectral absorption coefficients of living phytoplankton and nonalgal biogenous matter: A comparison between the Peru upwelling and the Sargasso Sea." Limnology and Oceanography **35**(3): 562 - 582.

Campbell, N. A., J. B. Reece, L. A. Urry, M. L. Cain, S. A. Wasswerman, P. V. Minorski and R. B. Jackson (2008). Biology. San Francisco, CA, Pearson.

Carder, K. L., F. R. Chen, Z. Lee, S. K. Hawes and J. P. Cannizzaro (2003). Algorithm Theoretical Basis Document 19 - Case 2 Chlorophyll a. MODIS Ocean Science Team Algorithm Theoretical Basis Document**:** 65p.

Carder, K. L., F. R. Chen, Z. Lee, S. K. Hawes and D. Kamykowski (1999). "Semianalytic Moderate-Resolution Imaging Spectrometer algorithms for chlorophyll a and absorption

with bio-optical domains based on nitrate-depletion temperatures." Journal of Geophysical Research **104**(C3): 5403 – 5421.
Carder, K. L., S. K. Hawes, K. A. Baker, R. C. Smith, R. G. Steward and B. G. Mitchell (1991). "Reflectance model for quantifying chlorophyll a in the presence of productivity degradation products." Journal of Geophysical Research **96**: 20,599 – 20,611.
Carder, K. L., R. G. Steward, G. Harvey and P. Ortner (1989). "Marine humic and fulvic acids: Their effects on remote sensing of ocean chlorophyll." Limnology and Oceanography **34**(1): 68 - 81.
Chami, M. and D. Robilliard (2002). "Inversion of oceanic constituents in case I and case II waters with genetic programming algorithms." Applied Optics **41**(30): 6260 - 6275.
Chang, G. C., A. H. Barnard, S. McLean, P. J. Egli, C. Moore, J. R. V. Zaneveld, T. D. Dickey and A. Hanson (2006). "*In situ* optical variability and relationships in the Santa Barbara Channel: implications for remote sensing." Applied Optics **45**(15): 3593 - 3604.
Dall'Olmo, G. and A. A. Gitelson (2005). "Effect of bio-optical parameter variability on the remote estimation of chlorophyll-a concentration in turbid productive waters: experimental results." Applied Optics **44**(3): 412 - 422.
Dareckia, M. and D. Stramski (2004). "An evaluation of MODIS and SeaWiFS bio-optical algorithms in the Baltic Sea." Remote Sensing of Environment **89**: 326 - 350.
Defoin-Platel, M. and M. Chami (2007). "How ambiguous is the inverse problem of ocean color in coastal waters?" Journal of Geophysical Research **112**(C03004): 16 pp.
Del Castillo, C. (2005). Remote sensing of organic matter in coastal waters. Remote sensing of coastal aquatic environments: technologies, techniques and applications. R. L. Miller, *et al*. Dordrecht, Springer**:** 157 - 180.
D'Sa, E. J. and R. L. Miller (2005). Bio-optical properties of coastal waters. Remote sensing of coastal aquatic environments: technologies, techniques and applications. R. L. Miller, *et al*. Dordrecht, Springer**:** 129 - 155.
D'Sa, E. J., R. L. Miller and C. Del Castillo (2006). "Bio-optical properties and ocean color algorithms for coastal waters influenced by the Mississippi River during a cold front." Applied Optics **45**(28): 7410 - 7428.
Falkowski, P. G., R. T. Barber and V. Smetacek (1998). "Biogeochemical controls and feedbacks on ocean primary production." Science **281**: 200 - 206.
Faust, M. A. and K. H. Norris (1985). "In vivo spectrophotometric analysis of photosynthetic pigments in natural populations of phytoplankton." Limnology and Oceanography **30**(6): 1316 -1322.
Gilbes, F., J. M. López and P. M. Yoshioka (1996). "Spatial and temporal variations of phytoplankton chlorophyll a and suspended particulate matter in Mayagüez Bay, Puerto Rico." Journal of Plankton Research **18**(1): 29 - 43.
Gin, K. Y.-H., S. T. Koh and I.-I. Lin (2003). "Spectral irradiance profiles of suspended marine clay for the estimation of suspended sediment concentration in tropical waters." International Journal of Remote Sensing **24**(16): 3235 - 3245.
Gordon, H. R., D. K. Clark, J. W. Brown, O. B. Brown, R. H. Evans and W. W. Broenkow (1983). "Phytoplankton pigment concentrations in the Middle Atlantic Bight: comparison of ship determinations and CZCS estimates." Applied Optics **22**(1): 20 - 36.
Gordon, H. R. and A. Morel (1983). Remote Assessment of Ocean Color for Interpretation of Satellite Visible Imagery: A Review. New York, Springer-Verlag.

Gross, L., S. Thiria, R. Frouin and B. Greg Mitchell (2000). "Artificial neural networks for modeling the transfer function between marine reflectance and phytoplankton pigment concentration." Journal of Geophysical Research **105**(C2): 3483 - 3495.

Güller, C. and F. Tunc (1992). "Chlorophyll Adsorption on Acid-Activated Clay." Journal Americal Oil Chemists' Society **69**(9): 948 - 950.

Hinrichsen, D. (1998). Coastal Waters of the World: Trends,Threats, and Strategies. Washington, D.C., Island Press.

Hochman, H. T., F. E. Muller-Karger and J. J. Walsh (1994). "Interpretation of the coastal zone color scanner signature of the Orinoco River plume." Journal of Geophysical Research **99**: 7443 - 7455.

Hsiu-Ping, L., G. Gwo-Ching and H. Tung-Ming (2002). "Phytoplankton pigment analysis by HPLC and its application in algal community investigations." Botanical Bulletin of Academia Sinica **43**: 283 - 290.

Karabulut, M. and N. Ceylan (2005). "The spectral reflectance responses of water with different levels of suspended sediment in the presence of algae." Turkish Journal of Engineering and Environmental Science **29**: 351 - 360.

Kirk, J. T. O. (1994). Light & Photosynthesis in Aquatic Ecosystems. Cambridge, Great Britain, Cambridge University Press.

Kishino, M., N. Okami and S. Ichimura (1985). "Estimation of the spectral absorption coefficients of phytoplankton in the sea." Bulletin of Marine Science **37**(634 - 642).

Lange, R. and C. Balny (2002). "UV-visible derivative spectroscopy under high pressure." Biochimica et Biophysica Acta **1595**: 80 - 93.

Laza-Martínez, A., S. Seaone, M. Zapata and E. Orive (2007). "Phytoplankton pigment patterns in a temperate estuary: from unialgal cultures to natural assemblages." Journal of Plankton Research **29**(11): 913 - 929.

Lee, Z. and K. L. Carder (2004). "Absorption spectrum of phytoplankton pigments derived from hyperspectral remote-sensing reflectance." Remote Sensing of Environment **89**: 361 - 368.

Lee, Z., K. L. Carder and R. A. Arnone (2002). "Deriving inherent optical properties from water color: a multiband quasi-analytical algorithm for optically deep waters." Applied Optics **41**(27): 5755 - 5772.

Lee, Z., K. L. Carder, R. G. Steward, T. G. Peacock, C. Davis and J. L. Mueller (1996). Remote-sensing reflectance and inherent optical properties of oceanic waters derived from above-water measurements. Ocean Optics XIII.

Lee, Z., K. L. Carder, R. G. Steward, T. G. Peacock, C. O. Davis and J. L. Mueller (1997). Remote sensing reflectance and inherent optical properties of oceanic waters derived from above-water measurements. Ocean Optics XIII, Halifax, Nova Scotia, Canada.

Lee, Z., A. Weidemann, J. Kindle, R. Arnone, K. L. Carder and C. Davis (2007). "Euphotic zone depth: Its derivation and implication to ocean-color remote sensing." Journal of Geophysical Research **112**(C03009): 11 pp.

Lee, Z., A. Weidemann, J. Kindle, R. A. Arnone, K. L. Carder and C. Davis (2007). "Euphotic zone depth: Its derivation and implication to ocean-color remote sensing." Journal of Geophysical Research **112**(C03009): 11 pp.

Lee-Borges, J. (2003). Contribution of picoplankton to phytoplankton dynamics and bio-optics of the eastern Caribbean Sea. University of Puerto Rico at Mayagüez. Department of Marine Sciences. Ph. D. Thesis. 133p.

Legates, D. R. and G. J. McCabe (1999). "Evaluating the use of "goodness of fit" measures in hydrologic and hydroclimatic model validation." Water Resources Research **35**: 233 - 241.

Linton, D. M. and G. F. Warner (2003). "Biological indicators in the Caribbean coastal zone and their role in integrated coastal management." Ocean & Coastal Management **46**: 261 - 276.

Loisel, H. and A. Morel (1998). "Light scattering and chlorophyll concentration in case 1 waters: A reexamination." Limnology and Oceanography **43**(5): 847 - 858.

Louchard, E. M., R. P. Reid, C. F. Stephens, C. O. Davis, R. A. Leathers, T. V. Downes and R. Maffione (2002). "Derivative analysis of absorption features in hyperspectral remote sensing data of carbonate sediments." Optics Express **10**(26): 1573 - 1584.

Ludeña, Y. (2007). Cianobacterias en la Bahía de Mayagüez: abundancia,distribución y su relación con las propiedades bio-ópticas. University of Puerto Rico at Mayagüez. Department of Biology. M.S. Thesis. 120p.

Miller, R. L., J. F. Cruise and J. M. López (1994). "Monitoring suspended sediment particulate matter in Puerto Rico: field measurements and remote sensing." Water Resources Bulletin **30**(2): 271 - 282.

Millero, F. J. (2006). Chemical Oceanography. Miami, Fl, CRC Press.

Millie, D. F., G. J. Kirkpatrick and B. T. Vinyard (1995). "Relating photosynthetic pigments and *in vivo* optical density spectra to irradiance for the Florida red-tide dinoflagellate Gymnodinium breve." Marine Ecology Progress Series **120**: 65 - 75.

Mitchell, B. G. and M. Kahru (1998). SeaWiFS algorithms developed with CalCOFI bio-optical data. CalCOFI Report.

Mitchell, B. G. and D. A. Kiefer (1984). Determination of absorption and fluorescence excitation spectra of phytoplankton. Berlin, Springer-Verlag.

Mobley, C. D. (1994). Light and water: radiative transfer in natural waters. San Diego, Academic Press.

Mobley, C. D. and L. K. Sundman (2001). Hydrolight 4.2 User's Guide. Redmond, WA, Sequoia Scienrific Inc.**:** 88p.

Morel, A. (1988). "Optical modeling of the upper ocean in relation to its biogenous matter content (Case 1 water)." Journal of Geophysical Research **93**(10): 749 - 768.

Morel, A. and L. Prieur (1977). "Analysis of variations in ocean color." Limnology and Oceanography **22**(4): 709 -722.

Morelock, J., W. R. Ramírez, A. W. Bruckner and M. Carlo (2001). "Status of coral reefs in southwest Puerto Rico." Caribbean Journal of Science **Special Publication V. 4.**

Muller-Karger, F. E., C. Hu, S. Andréfouet, R. Varela and R. Thunell (2005). The color of the coastal ocean and applications in the solution of research and management problems. Remote sensing of coastal aquatic environments: technologies, techniques and applications. R. L. Miller, *et al*. Netherlands, Springer**:** 101 - 127.

O'Reilly, J. E. and Coauthors (2000). SeaWiFS Postlaunch Calibration and Validation Analyses. NASA Tech. Memo. 2000-206892. S. B. Hooker, *et al*. NASA Goddard Space Flight Center**:** 49p.

O'Reilly, J. E., S. Maritorena, B. G. Mitchell, K. L. Siegel, S. A. Garver, M. Kahru and C. McClain (1998). "Ocean color chlorophyll algorithms for SeaWiFS." Journal of Geophysical Research **103**(11): 24937 - 24953.

Oubelkheir, K., L. A. Clementson, I. T. Webster, P. W. Ford, A. G. Dekker, L. C. Radke and P. Daniel (2006). "Using inherent optical properties to investigate biogeochemical dynamics in a tropical macrotidal coastal system." Journal of Geophysical Research **111**(C07021): 15p.

Ouillon, S. and A. A. Petrenko (2005). "Above-water measurements of reflectance and chlorophyll-a algorithms in the Gulf of Lyons, NW Mediterranean sea." Optics Express **13**(7): 2531 - 2548.

Pérez, L. R., G. Suárez, D. Sotomayor and G. Martínez (2005). Hydrologic analysis for nutrient and sediment loading determinations. Proceedings of the third conference on watershed management to meet water quality standards and emerging TMDL (Total Maximum Daily Load), Atlanta, Georgia.

Pope, R. M. and E. S. Fry (1997). "Absorption spectrum (380-700 nm) of pure water. II. Integrating cavity measurements." Applied Optics **36**: 8710 - 8723.

Prieur, L. and S. Sathyentranath (1981). "An optical classification of coastal and oceanic waters based on the specific spectral absorption curves of phytoplankton pigments, dissolved organic matter, and other particulate material." Limnology and Oceanography **26**(4): 671 - 689.

PUTPR (2006). Plan de uso de terreno de Puerto Rico -Perfil regional, Región Oeste. San Juan, PR

Rodríguez, I. E. (2004). Characterization of temporal and stratigraphic changes in texture, composition, nutrients, and organic content of bottom sediments in the Mayagüez Bay, Puerto Rico. University of Puerto Rico at Mayagüez. Department of Geology. M.S. Thesis. 82p.

Rosado-Torres, M. A. (2000). Variability in the bio-optical properties of Mayagüez Bay. University of Puerto Rico at Mayagüez. Department of Marine Sciences. M.S. Thesis. 61p.

Ruddick, K. G., H. J. Gons, M. Rijkerboer and G. Tilstone (2001). "Optical remote sensing of chlorophyll a in case 2 waters by use of an adaptive two-band algorithm with optimal error properties." Applied Optics **40**(21): 3575 - 3584.

Ruiz-Suárez, J. Y. (2004). Arenicolous filamentous fungi in Mayagüez Bay shoreline, western Puerto Rico. University of Puerto Rico at Mayagüez. Department of Biology. M.S. Thesis. 58 p.

Salinas, S. V., C. W. Chang and S. C. Liew (2007). "Multiparameter retrieval of water optical properties from above-water remote-sensing reflectance using the simulated annealing algorithm." Applied Optics **46**(14): 2727 - 2742.

Savitzky, A. and M. J. E. Golay (1964). "Smoothing and differentiation of data by simplified least squares procedures." Analytical Chemistry **36**: 1627 - 1639.

Schiller, H. and R. Doerffer (1998). "Neural network fofr emulation of an inverse model-operational derivation of case II properties from MERIS data." International Journal of Remote Sensing **20**: 1735 - 1746.

Smith, R. C. and K. A. Baker (1981). "Optical properties of the clearest natural waters (200–800 nm)." Applied Optics **20**: 177 - 184.

Suzuki, K., N. Handa, H. Kiyosawa and J. Ishizaka (1997). "Temporal and spatial distribution of phytoplankton pigments in the central Pacific Ocean along 175°E during the boreal summers of 1992 and 1993." Journal of Oceanography **53**: 386 - 393.

Sydor, M., R. W. Gould, R. A. Arnone, V. I. Haltrin and W. Goode (2004). "Uniqueness in remote sensing of the inherent optical properties of ocean water." Applied Optics **43**(10): 2156 - 2161.

Szekielda, K.-H., C. Gobler, B. Gross, F. Moshary and S. Ahmed (2003). "Spectral reflectance measurements of estuarine waters." Ocean Dynamics **53**(98 - 102).

Tapia-Larios, C. (2007). Variación espacial y temporal del fitoplancton en la Bahía de Mayagüez, Puerto Rico. UPR-Mayagüez. Department of Biology. M.S. Thesis. 143 p.

Tietjen, T., A. V. Vahatalo and R. G. Wetzel (2005). "Effects of clay turbidity on dissolved organic carbon and bacterial production." Aquatic Science **67**: 51-60.

Wang, P., E. S. Boss and C. Roesler (2005). "Uncertainties of inherent optical properties obtained from semianalytical inversions of ocean color." Applied Optics **44**(19): 4074 - 4085.

Warne, A. G., R. M. T. Webb and M. C. Larsen (2005). Water, sediment, and nutrient discharge characteristics of rivers in Puerto Rico, and their potential influence on coral reefs. Scientific Investigations Report 2005-5206, U.S. Geological Survey**:** 58 pp.

Welschmeyer, N. A. (1994). "Fluorometric analysis of chlorophyll a in the presence of chlorophyll b and pheopigments." Limnology and Oceanography **39**(8): 1985 - 1992.

Whitmire, A. L. (2008). The Spectral Backscattering Properties of Marine Particles. Oregon State University. Ph. D. Thesis. 136.

Wollast, R. (1998). Evaluation and comparison of the global carbon cycle in the coastal zone and in the open ocean. The sea: Ideas and observations on progress in the study of the seas. Hoboken, N. J., John Wiley. **10:** 213 - 252.

Wozniak, S. B. and D. Stramski (2004). "Modeling the optical properties of mineral particles suspended in seawater and their influence on ocean reflectance and chlorophyll estimation from remote sensing algorithms." Applied Optics **43**(17): 3489 - 3503.

Wright, S. W. and S. W. Jeffrey (1987). "Fucoxanthin pigment markers of marine phytoplankton analysed by HPLC and HPTLC." Marine Ecology Progress Series **38**: 259 - 266.

Zibordi, G., F. Mélin, S. B. Hooker, D. D'Alimonte and B. Holben (2004). "An autonomous above-water system for the validation of ocean color radiance data." IEEE Transactions on Geoscience and Remote Sensing **42**(2): 401 - 415.